Response to reviews

We would like to thank the referees for their detailed and constructive comments (marked blue in the following text). Our answers are in black and the changes to the manuscript are marked in italic.

Answers to the comments of Anonymous Referee #1

1) Section 2.3: The authors should present a table in which all the emitted and simulated PM species will be presented in detail for each model. The existing Table 2 cannot explain how sea salt is speciated in model simulations (is it simulated explicitly as Na and Cl?). Similar is the comment for fire PM species. Usually, fire PM emissions are simulated as OC and EC emissions and I would expect these emissions to have a contribution to OC and EC levels. How is this issue addressed in the different models? If fire PM emissions were speciated as OC and EC then how was it possible to distinguish between anthropogenic OC/EC and fire-related OC/EC? The models simulate OC or OA? Also in Table 2, the PM size is not presented (PM10 versus PM2.5).

 - LOTOS-EUROS and CMAQ calculate the sea salt components separately, in SILAM and EMEP sea salt is not speciated and is emitted and transported as whole. Standard sea salt composition is assumed when comparing the total sea salt concentration with Na observations with 30.8% sodium content by dry mass.

 - The fire PM originated from IS4FIRES (Sofiev et al., 2009), which provides unspeciated PM_{10} and $PM_{2.5}$ emissions. In SILAM, EMEP and LOTOS-EUROS the emitted PM was transported as a separate field of unspeciated particulates, in CMAQ the fine fraction was included in primary OA and the coarse fraction in coarse primary PM. The fire OA in CMAQ cannot be distinguished from the anthropogenic OA and fire EC was not included in that model. In the other models the fire PM can be further speciated as post-processing following Akagi et al., (2011) or Andreae and Merlet, (2001). On average these papers suggest roughly 5% EC and 50% OC content for fire emitted aerosol, the rest mainly consisting of non-carbon atoms in the organic compounds and some inorganics (up to 5%).

 - CMAQ provided total organic aerosol mass; EMEP model calculates both OC and OA.

Table 2 in the paper has been changed to include the speciation and sizes of the aerosol components computed by each model. Clarifications have been added to Section 2.5 (Model measurement comparison). Wild-land fire emitted contributions to OC and EC have been added to comparisons and discussion of them has been extended.

2) Section 2.4: Please present in Table 3 the size of the PM measured (PM10 versus PM2.5).

The inorganic species were measured mostly in total aerosol without size limits; concentration in PM_{10} was used where available. In 2005 EC and OC were measured in both $PM_{2.5}$ and PM_{10}. The 2002-2003 campaign observed EC and OC in PM_{10}.

Table 3 has been updated to include this information.

3) Section 2.5: The method for the estimation of nss-Ca levels from the model results is not clear. Are the simulated nss-Ca concentrations estimated as the sum of the 10% of dust concentrations plus 3.5% of the unspeciated other primary PM concentrations? The authors should also make clear in the whole manuscript (e.g. in Table 6) that it is not the mineral dust model results that are evaluated but the nss-Ca values (including both the desert dust and the anthropogenic contribution).

The simulated nss-Ca concentrations are indeed estimated as the sum of the 10% of dust concentrations plus 3.5% of the unspeciated other primary PM concentrations. *Clarifications were added.*

4) Section 3.1, page 9, lines 7-18: The authors explained the bad model performance in Schauinsland Mountain station as the result of model spatial resolution and high station altitude. The position and altitude of the stations should be provided in the supplement. Are there other stations of similar altitude in which the models performance is not as bad in the Schauinsland Mountain station?

There are other high altitude stations, located in Alps and in Spain. The Schauinsland station was pointed out in the paper, because it was the only station where the models consistently overestimated the PM concentration. Also the temporal correlations between the models and observations are the lowest there for both PM_{10} and $PM_{2.5}$. The models' performance does degrade also in the other high stations - there is a strong negative correlation between the station altitude and the models' temporal correlation coefficients for both PM_{10} and $PM_{2.5}$. However, the bad model performance is caused not only by the altitude difference between the station and the model grid cell average, but also other inhomogeneities, such as strong emission sources in the area. The Schauinsland station, for instance, is located about 10 km from Freiburg city, and about 1 km above it. In the models both the city and the station are covered with one uniformly mixed grid cell, while in reality the winter time low boundary layer traps the pollution below the station altitude. Indications of wintertime overestimation are also visible for some of the other high stations, though with smaller magnitude, as not all the high stations are located at extreme points of the terrain, such as mountain summits, and not all of them have strong emission sources in the immediate vicinity. Opposite problems arise for sites located in narrow valleys, where the models cell-mean altitude is higher than the station and the models overspread the pollution that in reality can be trapped in the valley.

The stations' locations have been be added to the supplement. The discussion about the station representativity has been extended.
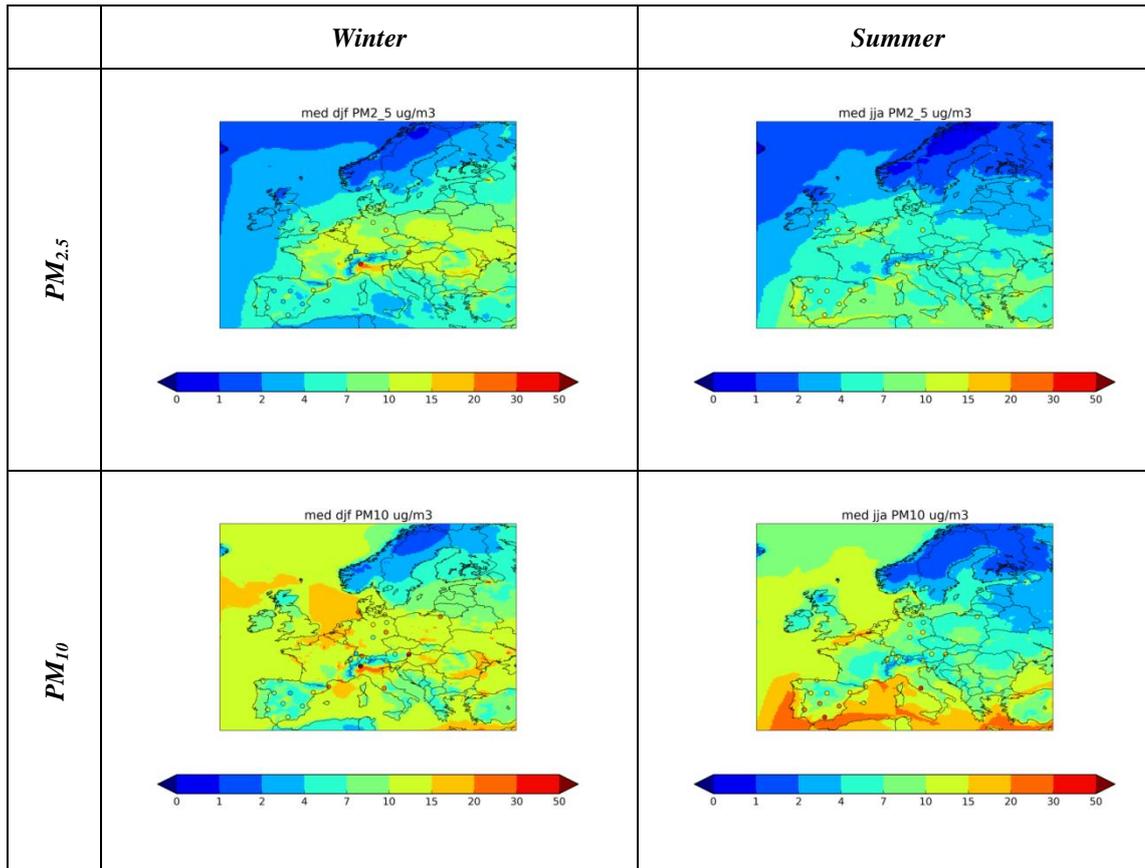
5) Section 3.1, page 10, lines 2-4: Explain the reasons for models' different ability in simulating PM2.5 and PM10 in summer and winter.

For most of the models, temporal correlations and factor-two agreements are better in winter than in summer for both PM fractions, and the spatial correlation of $PM_{2.5}$ is also better in winter. The only score with opposite behaviour is the spatial correlation for PM_{10}. The summertime worse scores are probably due to the highly uncertain components that dominate the

summer aerosol - wind-blown dust, wild-land fires, and biogenic secondary organic aerosols. In summer the PM_{10} pattern over Europe is formed by the inflow of Saharan dust and wild-land fires in Portugal and Spain creating a strong south to north gradient. This gradient is reproduced by the models, although with smaller magnitude (Figure A1.1, lower right panel). As LOTOS-EUROS misses the dust and fire contribution, it does not reproduce this pattern. As the species contributing to

5 this summer time south-north gradient are desert dust and wild-land fires, which by nature are episodic and hard to model, the temporal correlation and factor-two agreement are still generally lower and bias is larger in summer. In winter the particulate matter is dominated by the anthropogenic emissions, forming a more complex pattern (Figure A1.1, left panels), and thus the spatial correlation is worse.

Explanations have been added to the section.

10

	Winter	Summer
$PM_{2.5}$	med djf PM2_5 ug/m3	med jja PM2_5 ug/m3
PM_{10}	med djf PM10 ug/m3	med jja PM10 ug/m3

Figure A1.1. Seasonal average observed and ensemble median PM concentrations for winter and summer.

6) Section 3.1, page 10, line 11: The authors state: "The medianComp fully includes SOA, desert dust and fire-induced PM." This is not true since according to Table 2, SOA are not included in LOTOS-EUROS and in SILAM. Also BCs dust

15 *is not included in LOTOS-EUROS.*

3

MedianComp is the sum of the ensemble medians of all the individual PM components. Although not all components are provided by all four models, when computing the median field for every component only those models are used which provided a valid field for that component. Thus, medianComp will include the median SOA of EMEP and CMAQ and median dust of SILAM and EMEP. As these models have provided valid fields for these components, the medianComp PM also includes valid fields of SOA and dust.

The description of MedianComp model has been extended

7) Section 3.1, page 10, lines 16-18: The authors explain that the differences between median and medianComp are due to desert dust. However, according to Table 2, it is only the fire originated PM that were not included in total PM while BCs dust was included all CMAQ, EMEP and SILAM.

That is correct. However, in CMAQ the dust and fire contributions are very low and LOTOS-EUROS does not have them at all, so the median total PM is based on half of the models with zero or very low dust concentration. MedianComp is based only on the valid dust fields of SILAM and EMEP and thus includes noticeably higher dust contribution.

Explanations have been added.

8) Section 3.2, Table 6: Which are the size bins of the PM species validated (comment mostly for sea salt and mineral dust). The words "mineral dust" should be replaces with "nss-Ca".

- The Ca and Na observations in EMEP network are made mostly in whole aerosol without size limits.

- Dust in the EMAC model is emitted in two log-normal modes with the size distribution parameters from (Dentener et al., 2006): accumulation mode with 0.42 µm median diameter and standard deviation 1.59, and coarse mode with 1.30 µm median diameter and standard deviation 2.00. These modes are selected to cover the whole dust distribution relevant for atmospheric transport (Ginoux et al., 2004, 2001). When the EMAC boundary conditions are projected to the model size bins in EMEP and SILAM, both of the size modes are assumed to be fully inside PM10, which agrees reasonably well with the observations of (Dubovik et al., 2002). The sum of these two modelled modes is used when comparing with the nss-Ca observations.

- For all models the Na concentration for model-measurement comparison was computed from sea salt in PM10. As the models already overestimate Na concentration, if taking into account also the particles larger than 10 µm the real overestimation would be even larger than what is shown. However, comparing Na in PM10 with Na in whole sea salt in SILAM (size range 0.01 to 30 µm), the changes are minor for majority of the EMEP stations that observed Na in 2005: below 5% for 65% of the stations, below 10% for 77%, and below 20% for all stations. The concentration changed more than 10% only in the stations located directly at seaside.

Table 3 has been updated to include the aerosol sizes for the observations. Reference to the dust size distribution has been added to EMAC model description. Explanations have been added to the results section about the sea salt size distributions.

Why evaluation is presented explicitly only for SO2 and not for other PM precursor gas compounds like NH3 or NOx?

- Observations of NH3 and HNO3 are more prone to artefacts(e.g. Chang et al., 2002; Schaap et al., 2011), thus the less uncertain NH3+NH4 and HNO3+NO3 observations were originally chosen for model evaluation. Those were also available from larger number of stations. The contribution of HNO3 and NH3 to the sum is shown on Figure 4 of the resubmitted manuscript with dark shading. On annual average level the gas phase fraction is in both cases relatively well reproduced by most of the models, only SILAM underestimates HNO3 and overestimates NH3 contributions. However, the models do not reproduce well the seasonal variations in HNO3 and NH3 concentrations – EMEP and LOTOS-EUROS overestimate the seasonal variability of HNO3, CMAQ strongly overestimates the autumn NH3 concentrations and so does with smaller magnitude also SILAM. Temporal correlation coefficients and factor-2 agreements are noticeably worse for NH3 and HNO3 compared with NH4 and NO3 aerosols or the gas-aerosol sums (Table 7 of the resubmitted manuscript). In addition to the uncertainties in the observations, there are other reasons for model errors in these species. Especially for NH3 the timing of the emissions as used in the models (fixed temporal profiles) can deviate substantially from real world emission timing which is largely controlled by meteorology (Backes et al., 2016; Hamaoui-Laguel et al., 2014; Hendriks et al., 2016). Meteorology also influences the total amount of emitted NH3 but the strongest influence is on the timing. The timing of agricultural activities, such as manure spreading has also a strong impact on the emissions (Hendriks et al., 2016). This mismatch may translate into episodes where the models predict high concentrations but due to unfavorable meteorology very little was emitted and vice versa, partly explaining why the models do not properly reproduce the seasonal fluctuations but on annual average are quite OK.
- Regarding NOx, NO was measured by only one EMEP station and thus no thorough evaluation is possible. The model scores and seasonal developments of NO2 concentration are shown on Table A1.1 and Figure A1.2. The seasonal variations of NO2 are well reproduced, but all models apart from CMAQ overestimate NO2 all the seasons. This can be one of the reasons for the overestimation of the sum of NO3- and HNO3.

NH_3 and HNO_3 have been added to Figure 4 of the manuscript, model scores for those species have been added to Table 7. Section on the comparison results has been extended. A figure with seasonal variations of NO_2 and a table with model scores for it have been added to the supplementary material.

Table A1.1. Model skill scores for the gas phase precursors of NO_3 and NH_4, average over the EMEP stations that observed these species.

Species	Model	Scaled bias	tCor	Fac2
NH₃	CMAQ	0.04	0.18	0.25
Ave obs:	EMEP	-0.07	0.30	0.36
0.75 µg N/m³	LOTOS-EUROS	0.19	0.22	0.38
	SILAM	0.32	0.30	0.40
	median	0.05	0.31	0.39
HNO₃	CMAQ	0.21	0.34	0.43
Ave obs:	EMEP	-0.11	0.38	0.39
0.19 µg N/m³	LOTOS-EUROS	0.00	0.38	0.40
	SILAM	-0.53	0.32	0.32
	median	-0.16	0.41	0.44
NO₂	CMAQ	-0.06	0.57	0.59
Ave obs:	EMEP	0.19	0.52	0.60
1.76 µg N/m³	LOTOS-EUROS	0.26	0.45	0.58
	SILAM	0.39	0.54	0.57
	median	0.16	0.56	0.61
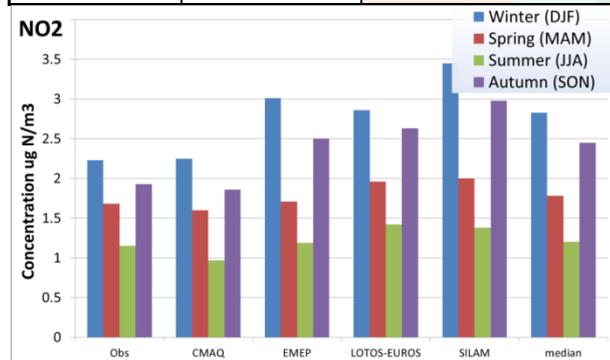
Figure A1.2 Observed and predicted seasonal concentrations of NO_2.

5

9) Section 3.2.3: The performance of CMAQ, can it be explained by the fact that fire emissions are included in other PM?

CMAQ has the largest negative bias and lowest correlation for the carbonaceous aerosols. For EC EMEP is as biased as CMAQ, while being closer to the observations for OC. In CMAQ the fine mode fire emissions were actually included in the primary OA, although not to EC; only the coarse mode fire PM was included in the unspeciated coarse primary PM. For all other models the fire contribution was excluded from comparison with EC and OC. Thus, the missing fire contribution cannot explain the bias in CMAQ and other explanations are needed for the negative bias found for the carbonaceous aerosols.

The fire PM concentrations modelled by EMEP, LOTOS-EUROS and SILAM can be speciated as post-processing following Akagi et al., (2011) or Andreae and Merlet, (2001). On average these papers suggest roughly 5% EC and 50% OC content

for fire emitted aerosol. The fire contribution to EC and OC calculated following this composition is shown on Figure 4 of the resubmitted manuscript with darker shading. SILAM only shows a small fire contribution to EC in spring and summer, while in EMEP and LOTOS-EUROS the contribution is larger and visible all year round. EMEP also predicts a noticeable fire contribution to OC for all seasons. For EMEP and LOTOS-EUROS, the fire contribution reduces the model bias for the carbonaceous species, while at the same time reducing the correlation with the measurements (Table A1.2). The SILAM EC prediction quality does not noticeably change.

Table 2 has been corrected to show that the fine particles from fires were included in CMAQ as OA. Fire contributions have been added to Figure 6 in the paper. For CMAQ the fire emitted OC is mixed with the primary anthropogenic part and cannot be shown separately and the fire emissions are excluded for EC. The section has been updated so that the carbonaceous aerosols of the other models include the fire contribution.

Table A1.2 Comparison of model scores for the carbonaceous species with and without the wildfire contribution

Species	Model	Without firePM			With firePM		
		Scaled bias	tCor	Fac2	Scaled bias	tCor	Fac2
EC in PM$_{2.5}$	CMAQ	-0.61	0.51	0.35	-0.61	0.51	0.35
Ave obs:	EMEP	-0.60	0.56	0.43	-0.56	0.53	0.4
1.08 µg C/m^3	LOTOS-EUROS	-0.42	0.58	0.45	-0.34	0.51	0.44
	SILAM	-0.17	0.61	0.41	-0.17	0.61	0.4
	median	-0.51	0.61	0.37	-0.45	0.6	0.38
OC in PM$_{2.5}$	CMAQ	-0.80	0.52	0.26	-0.80	0.52	0.26
Ave obs:	EMEP	-0.38	0.58	0.64	-0.25	0.54	0.6
3.61 µg C/m^3	median	-0.59	0.60	0.58	-0.52	0.54	0.61
EC in PM$_{10}$	CMAQ	-0.69	0.42	0.32	-0.69	0.42	0.32
Ave obs:	EMEP	-0.70	0.43	0.37	-0.66	0.46	0.35
1.32 µg C/m^3	LOTOS-EUROS	-0.53	0.43	0.45	-0.48	0.39	0.44
	SILAM	-0.36	0.43	0.37	-0.35	0.45	0.38
	median	-0.61	0.46	0.38	-0.58	0.49	0.37
OC in PM$_{10}$	CMAQ	-0.85	0.36	0.18	-0.85	0.36	0.18
Ave obs:	EMEP	-0.51	0.38	0.52	-0.37	0.46	0.52
4.78 µg C/m^3	median	-0.67	0.40	0.45	-0.61	0.46	0.48

10) Section 3.2.5: Any comments on OA comparison with observations should be based on CMAQ and EMEP results since the other models include OC in other PM. Similar remark for dust straightforwardly included only in EMEP and SILAM.

The text has been changed according to the reviewer's suggestion

11) Section 3.2.5., page 15, line 7: Correct OA with OC.

Done

Done

5

10 a) As total OC is measured the observations on Figure 8 are shown as total OA. The modelled OA has been shown as POA and SOA separately, to demonstrate how the contribution of these varies between the models and the stations.

b) Apart from CMAQ that included the fire emissions in OA, the fire emissions were modelled as unspeciated particulates. The concentration can be speciated following the average composition from Akagi et al., (2011) and Andreae and Merlet, (2001), giving ~90% OM, ~5% EC and ~5% non-carbonaceous compounds.

15 *Figure 8 has been updated to show the fire contribution to OC and EC. The legend has been fixed.*

20

As the models did not include any other dust sources than the inflow from the boundaries, underestimation of dust concentration is expected and comparison with nss-Ca confirms it, while not providing its exact magnitude. Various sources
25 give Saharan dust Ca content from <5% to >15% and for the anthropogenic emissions the variations are even larger, depending on the source sector and local soil, so the uncertainty in aerosol Ca content can be expected to be a few times. However, with the 10 and 3.5% Ca content, the EMEP model underestimated the nss-Ca by 75% and SILAM by 58%, so even assuming twice the calcium content, the nss-calcium concentrations would still be underestimated by the models. This uncertainty does not influence the accuracy of the predictions and evaluation of PM_{10} and $PM_{2.5,}$ as primary PM and dust
30 were modelled as totals and the 3.5% and 10% factors were only applied when comparing with the nss-Ca observations.

In EMEP and LOTOS-EUROS, using the IS4FIRES v1 emissions resulted in degradation of model scores for $PM_{2.5}$ and PM_{10} and thus these models excluded the fire PM from their total $PM_{2.5}$ and PM_{10} fields, while still providing it as a separate field. In SILAM, a newer version of the emission data was used (IS4FIRES v2, (Soares et al., 2015), together with dynamic emission vertical profiles of (Sofiev et al., 2012), while in other models, the IS4FIRES v1 emission data was spread evenly

to the first 1000m. Mainly due to the vertical profiles that release most of the smoke high aloft, the ground level concentrations of fire PM were substantially lower in SILAM and thus the fire PM does not significantly affect the model performance for PM, demonstrating that the quality of the fire emission data is essential for simulating the particulate matter concentrations.

5   *Clarifications have been added.*

15) Section 4.3: It is a very interesting section. The authors should present results on the models' improved performance when water is accounted for (even in the four stations providing a complete set of PM measurements; after all section 3.2.5 was based on the measurements in these few stations).

Based on the dry PM mass and speciation provided by the models, aerosol thermodynamic model ISORROPIA2 (Fountoukis
10 and Nenes, 2007) was applied to evaluate the equilibrium water content at the conditions where the filters were weighted (20°C, 50% relative humidity). ISORROPIA2 was run in the reverse mode, where the input quantities were the soluble inorganic components (SIA, sea salt, Ca) in the aerosol phase. The aerosols were assumed to be internally mixed. Both stable and metastable states were computed, corresponding to the lower and upper branches of the deliquescence hysteresis loop, the latter one describing the case when the aerosol has been exposed to more humid environment and crystallization has not
15 occurred. In this way lower and upper limits of the aerosol bound water amount can be estimated.

ISORROPIA2 was applied to estimate the water contribution at all the EMEP sites that measured $PM_{2.5}$ or PM_{10}. In the stable case, the annual mean $PM_{2.5}$ water content, average over all EMEP stations, stayed between 4 and 9% depending on the model, and between 11 and 17% for PM_{10}. For $PM_{2.5}$, the models predicted annual average water content above 10% for only a few stations. For PM_{10}, CMAQ and EMEP predict majority of the stations to have less than 10% of water content, while
20 LOTOS-EUROS and SILAM predict the majority to be between 10 and 20%; annual average water contents of more than 25% were predicted for some stations. The water content of PM_{10} computed in the metastable mode was on average about twice higher (~25%); ~20% water content was predicted for $PM_{2.5}$.

As seen from Table 6 of the resubmitted manuscript, adding the aerosol-bound water reduces noticeably the model bias for both PM_{10} and $PM_{2.5}$. For $PM_{2.5}$ the correlation coefficients are not much affected, while for PM_{10}, they are noticeably
25 reduced. The factor-2 agreements improve due to the bias reduction. The worse correlations could be related to the models overestimating the sea salt concentrations that can lead to overestimation of the water content in PM_{10}, as it is the most hydrophilic of the considered aerosol components.

Also other uncertainties exist estimating of the PM water content. Firstly, ISORROPIA2 computes the water content based on the inorganic part of aerosol – SIA, sea salt, calcium; it does not take into account the water related to the hydrophilic part
30 of the organic aerosol. Secondly, the aerosols were assumed fully internally mixed, which lowers the deliquescence humidity compared to external mixtures and might lead to overestimation of water uptake.

The water contribution for the four stations with most complete aerosol composition observations can be seen on Figure 8 of the resubmitted manuscript. Adding the aerosol bound water in metastable state closes the gap between the observed total PM_{10} and the sum of the individual components in all stations (in Montseny the PM_{10} estimate based on nearby stations can

be inaccurate). In Ispra and Birkenes the observed PM is exceeded, which could indicate that the aerosol on the filters is in crystallized state or be due to inaccuracies in other observed species. In Ispra, errors were suspected in the observations of the carbonaceous components, while in Birkenes, the sea salt observations are taken from all aerosol, not PM_{10}. The models predict very high aerosol water content for Birkenes and noticeably overestimate the PM_{10} there, as the overestimated sea salt concentration leads to very high water uptake of the aerosol.

The water contribution has been added to figures 3 and 8 and Table 6 has been divided to two parts, the first of those comparing the model scores for the dry PM to the water equilibrated PM. The discussion regarding the aerosol-bound water has been extended according to the reviewers suggestion.

16) Figure 6: Correct in the lower-right plot the OC to EC.
Done

17) Figure S6: Was CMAQ excluded from the average since dust in CMAQ was included in other PM?
Yes, the figures are based only on the models that included the shown component explicitly.

The figure captions have been updated to include this information.

18) Figure S7: Was LOTOS-EUROS and SILAM excluded from OA mean values since OA in these modes were included in other PM? The Figure is not commented in the text of the manuscript.

The OA figure is now based on EMEP model only, as SILAM and LOTOS-EUROS included primary OA in PM and CMAQ included in its OA the fire emissions.

The figure caption has been updated to include this information.

19) Figure S8: Please check comment 1. How fire emissions were simulated and consequently presented in the Figure for PM? If speciated to OC and EC emissions, how fire-related OC and EC concentrations were distinguished from anthropogenic OC and EC concentrations?

CMAQ emitted OC, which cannot be distinguished from the anthropogenic OC. EMEP, LOTOS-EUROS and SILAM emitted unspeciated $PM_{2.5}$ and PM_{10} and transported them as separate fields. Figure S8 shows the median of those fields.

The caption of Figure S8 has been updated

References

Akagi, S.K., Yokelson, R.J., Wiedinmyer, C., Alvarado, M.J., Reid, J.S., Karl, T., Crounse, J.D., Wennberg, P.O., 2011. Emission factors for open and domestic biomass burning for use in atmospheric models. Atmos. Chem. Phys. Discuss. 11, 4039–4072. doi:10.5194/acp-11-4039-2011

Andreae, M.O., Merlet, P., 2001. Emission of trace gases and aerosols from biomass burning. Global Biogeochem. Cycles 15, 955–966.

Backes, A.M., Aulinger, A., Bieser, J., Matthias, V., Quante, M., 2016. Ammonia emissions in Europe, part II: How ammonia emission abatement strategies affect secondary aerosols. Atmos. Environ. 126, 153–161. doi:10.1016/j.atmosenv.2015.11.039

Chang, K., Lu, C., Bai, H., Fang, G.C., 2002. A theoretical evaluation on the HNO3 artifact of the annular denuder system due to evaporation and diffusional deposition of NH4NO3-containing aerosols. Atmos. Environ. 36, 4357–4366. doi:10.1016/S1352-2310(02)00352-7

Dentener, F., Kinne, S., Bond, T., Boucher, O., Cofala, J., Generoso, S., Ginoux, P., Gong, S., Hoelzemann, J.J., Ito, A., Marelli, L., Penner, J.E., Putaud, J.-P., Textor, C., Schultz, M.G., van der Werf, G.R., Wilson, J., 2006. Emissions of primary aerosol and precursor gases in the years 2000 and 1750 prescribed data-sets for AeroCom. Atmos. Chem. Phys. 6, 4321–4344.

Dubovik, O., Holben, B., Eck, T.F., Smirnov, A., Kaufman, Y.J., King, M.D., Tanré, D., Slutsker, I., 2002. Variability of Absorption and Optical Properties of Key Aerosol Types Observed in Worldwide Locations. J. Atmos. Sci. 59, 590–608. doi:10.1175/1520-0469(2002)059<0590:VOAAOP>2.0.CO;2

Fountoukis, C., Nenes, A., 2007. ISORROPIA II : a computationally efficient thermodynamic equilibrium model for K+-Ca2+-Mg2+-NH4+-Na+-SO42--NO3--Cl--H2O aerosols. Atmos. Chem. Phys. 7, 4639–4659.

Ginoux, P., Chin, M., Tegen, I., Prospero, J.M., Holben, B., Dubovik, O., Lin, S.-J., 2001. Sources and distributions of dust aerosols simulated with the GOCART model. J. Geophys. Res. 106, 20255. doi:10.1029/2000JD000053

Ginoux, P., Prospero, J.M., Torres, O., Chin, M., 2004. Long-term simulation of global dust distribution with the GOCART model: Correlation with North Atlantic Oscillation. Environ. Model. Softw. 19, 113–128. doi:10.1016/S1364-8152(03)00114-2

Hamaoui-Laguel, L., Meleux, F., Beekmann, M., Bessagnet, B., Génermont, S., Cellier, P., Létinois, L., 2014. Improving ammonia emissions in air quality modelling for France. Atmos. Environ. 92, 584–595. doi:10.1016/j.atmosenv.2012.08.002

Hendriks, C., Kranenburg, R., Kuenen, J.J.P., Van den Bril, B., Verguts, V., Schaap, M., 2016. Ammonia emission time profiles based on manure transport data improve ammonia modelling across north western Europe. Atmos. Environ. 131, 83–96. doi:10.1016/j.atmosenv.2016.01.043

Schaap, M., Otjes, R.P., Weijers, E.P., 2011. Illustrating the benefit of using hourly monitoring data on secondary inorganic aerosol and its precursors for model evaluation. Atmos. Chem. Phys. 11, 11041–11053. doi:10.5194/acp-11-11041-2011

Soares, J., Sofiev, M., Hakkarainen, J., 2015. Uncertainties of wild-land fi res emission in AQMEII phase 2 case study. Atmos. Environ. doi:10.1016/j.atmosenv.2015.01.068

Sofiev, M., Ermakova, T., Vankevich, R., 2012. Evaluation of the smoke-injection height from wild-land fires using remote-sensing data. Atmos. Chem. Phys. 12, 1995–2006. doi:10.5194/acp-12-1995-2012

Sofiev, M., Vankevich, R., Lotjonen, M., Prank, M., Petukhov, V., Ermakova, T., Koskinen, J., Kukkonen, J., 2009. An operational system for the assimilation of the satellite information on wild-land fires for the needs of air quality modelling and forecasting. Atmos. Chem. Phys. 9, 6833–6847. doi:10.5194/acpd-9-6483-2009

Answer to the comments of Anonymous Referee #2

- please double check the reference list: I checked the first three citations, and they are all missing in the list at the end of the manuscript.

Thanks to the reviewer for noticing this, all references from the first few paragraphs had indeed disappeared from the reference list. *The reference list has been fixed.*

- I find too much overlap and redundancy in the introductory part on model-to-obs uncertainties (page 2-4) and the discussion (section 4). My impression is that a quite long list of possible reasons for model-to-obs disagreement is presented in both parts, but never really demonstrate them for the specific simulations presented here. I thus suggest to shorten both the introduction and the discussion, and possibly move all the model-to-obs issue directly into the discussion section.

Majority of the model-observation comparison issues have been moved to discussion, the uncertainties related to the aerosol-bound water have been evaluated for the simulations.

- page 4, lines 7-10: I do not completely agree with this final statement. From my understanding, the "main reasons behind model-measurements" are not clearly identified in the study. I would better state that the model error regarding the PM simulation is characterized against available measurements.

The sentence has been restated according to the reviewer's suggestion.

- Figure S4: please define PPMr in the caption.

Done

- page 8, lines 9-13: there seems to be some inconsistency between the major components illustrated in figures S5-S8 and values given in Table 6. In particular, from Table 6 one would say that carbonaceous aerosol are the major fraction of PM, not secondary organic aerosol. Please clarify.

There are several reasons for the noticed discrepancies. Firstly, the concentrations are given in different units. Table 6 reports the annual mean concentrations observed by the EMEP network, averaged over all the stations. They are given in the units the observations are provided – micrograms of nitrogen, sulphur, sodium, calcium or carbon. The model median maps on the figures S5-S8 follow the speciation in the models and are in the total mass of the component (NO_3, NH_4, SO_4, sea salt, mineral dust, organic aerosol, fire-emitted PM). Converting the observed values to the total mass of the components, we get the sum of the secondary inorganic species very close to the carbonaceous ones in $PM_{2.5}$. Taking into account that the models underestimate substantially the carbonaceous part, the model maps probably overestimate the SIA fraction in PM. Additional differences are introduced by sampling the map only at the station locations. For the SIA species the station network is well covering and representative, while the carbonaceous components were measured in only four stations.

Clarifications have been added.

- page 8, line 31: could a poor correlation coefficient for NO3- be related to a pulsed behaviour of the aerosol nitrate production in the PBL, as recently described in this paper: Curci, G., Ferrero, L., Tuccella, P., Barnaba, F., Angelini, F.,

Bolzacchini, E., Carbone, C., Denier van der Gon, H. A. C., Facchini, M. C., Gobbi, G. P., Kuenen, J. P. P., Landi, T. C., Perrino, C., Perrone, M. G., Sangiorgi, G., and Stocchi, P.: How much is particulate matter near the ground influenced by upper-level processes within and above the PBL? A summertime case study in Milan (Italy) evidences the distinctive role of nitrate, Atmos. Chem. Phys., 15, 2629-2649, doi:10.5194/acp-15-2629-2015, 2015.

5   The paper of Curci et al presents a detailed study on nitrate formation in Po Valley and how its concentration is influenced by the boundary layer processes and temperature and humidity vertical profiles. It is indeed an interesting question, how well these effects are taken into account in the regional models. The models use a range of different algorithms for SIA creation, such as thermodynamic equilibrium model ISORROPIA2 in LOTOS-EUROS or separate equilibrium computations for NH_4NO_3 and a parameterization for coarse NO_3 production on sea salt particles in SILAM and EMEP. Generally these

10   should be capable of simulating the profile of NO_3 creation and brake up, provided that the model vertical resolves the temperature and relative humidity profiles. However, this can easily not be the case - for instance LOTOS-EUROS has a single layer representing the whole boundary layer and SILAM layers at boundary layer top can easily be 500-1000 meters thick.

    While the low vertical resolution of the gathered model data does not allow for a detailed analysis of this effect in the whole

15   dataset, elevated plumes of NH_4NO_3 are clearly visible in SILAM model output (**Error! Reference source not found.**), mainly because the efficient dry deposition of HNO_3 depletes its concentration in the near-surface layers making NH_4NO_3 break to the gaseous compounds. Thus, the formation of the residual layers and mixing them down in the morning and the ability of the models to reproduce these effects can have an impact on the simulation quality. However, as the EMEP aerosol composition observations have daily resolution, it's hard to tell, how much these processes influence the model-

20   measurement correlation compared with all the other uncertainties related to NH_4NO_3 formation, such as the temperature dependence of NH_3 emission.

The discussion of the uncertainties in NO_3 modelling has been extended and the reference added to the manuscript.
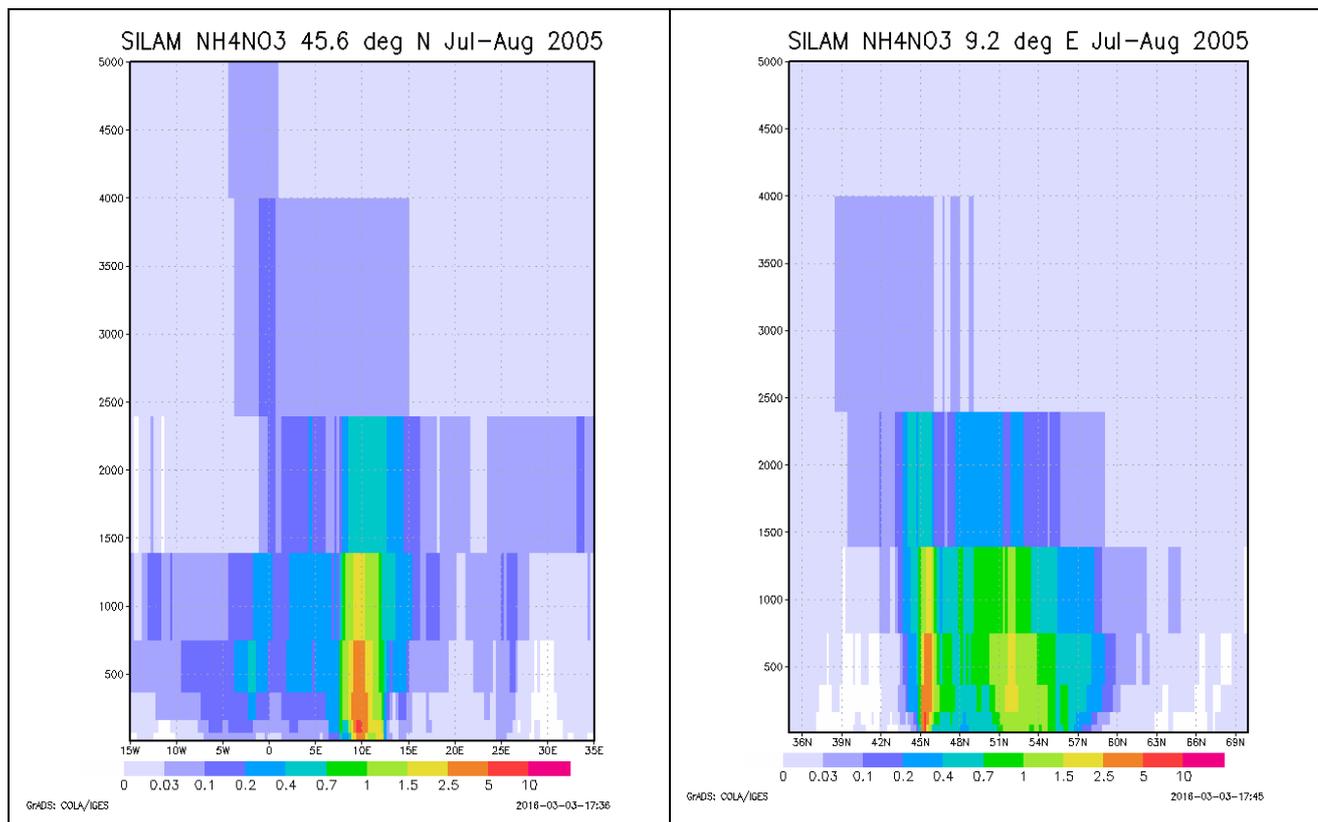
Figure A2.1 Summer time concentration profiles of NH4NO3 from SILAM model, west-east and south-north cross-sections of Europe, selected to cut through Po Valley.

- page 9, lines 7-8: the discussion on HNO3 bias is made difficult by the fact that HNO3 is not shown alone in the figure. Could this be shown, or the results commented on the NO3+HNO3 concentration that the reader may actually directly see in the plots?

The reason for selecting HNO_3+NO_3 as the presented variable was, that there are more stations in EMEP network that measure the sum than there are those that measure HNO_3 alone, also the sum is measured with higher accuracy, while the HNO3 concentration is more prone to observation artefacts .

Figure 4 in the resubmitted manuscript shows HNO_3+NO_3 together with the contribution from HNO_3 (shaded). On annual average level all models overestimate the sum by 5-35 %. EMEP and LOTOS-EUROS accurately predict the HNO_3 fraction in the sum, while SILAM underestimates and CMAQ overestimates it by 10%. However, the models do not reproduce well the seasonal variations in HNO_3 concentration.

Figure 4 and related discussion has been updated in the paper.

14

The sentence has been restated.

5

Done

10

Of the natural aerosols considered (Figure 5 in the manuscript), sea salt exhibits no spring peak - elevated Na^+ concentrations are observed only in winter and the models reproduce this behaviour. Dust, on the other hand, seems to be contributing – observed nss-Ca concentrations peak in spring and so do the modelled Saharan dust concentrations. Previous studies about Saharan dust have found the emissions peaking at spring (Fiedler et al., 2013; Laurent et al., 2008). Additionally to desert
15 dust there are other possible reasons for elevated crustal aerosol concentration in spring, such as agricultural activities and vehicle caused erosion of roads - in colder regions where winter tires are used and the roads are sanded against slipperiness high dust emissions occur when the road conditions get dry in spring.

Considering the biogenic primary particles, pollens are abundant in air in spring - maximum concentrations can reach a few tens of thousands of pollen/m^3, equivalent to tens of $\mu g/m^3$. However, their size is mostly too large to make them relevant for
20 PM_{10} (~20 μm for abundant early spring flowering species like birch). Evidence exist, that pollen grains can break in atmosphere and produce particles in size range relevant for even $PM_{2.5}$, however, such particles are unlikely to be abundant enough to be noticeable in the PM budget. Also the fungal spores become abundant only in summer – high concentrations can be observed from June to October.

Regarding the anthropogenic contribution, all observed secondary inorganic species show spring maxima.

25

30 The paper of Wang et al reports shorter EC lifetimes to be more consistent with observations and a similar conclusion was reached by Samset et al., (2014) - both studies found that shorter lifetime was necessary for reproducing the EC vertical profiles and low concentrations in remote regions. This result somewhat contradicts with the current model intercomparison, where SILAM was found to best reproduce the observed EC concentrations, and longer EC lifetime due to slower deposition in that model was assumed as the main reason for the model-to-model differences. Also the temporal correlation with 2005

observations and spatial correlation between the models 2005 average EC and EC observed during the 2002-2003 EMEP campaign is no worse for SILAM than it is for the other models, so there is no clear indication that the slower deposition would not be consistent with the surface EC observations in European scale. However, as indications were found of strong underestimation of EC emission, the slower deposition in SILAM is likely to be compensating for the missing emissions. Observations of vertical profiles and concentrations in more remote locations would be necessary for investigating this issue; unfortunately such were not available in Europe in 2005.

Discussion of EC lifetimes has been added to the manuscript.

References

Fiedler, S., Schepanski, K., Heinold, B., Knippertz, P., Tegen, I., 2013. Climatology of nocturnal low-level jets over North Africa and implications for modeling mineral dust emission. J. Geophys. Res. Atmos. 118, 6100–6121. doi:10.1002/jgrd.50394

Laurent, B., Marticorena, B., Bergametti, G., Leon, J.F., Mahowald, N.M., 2008. Modeling mineral dust emissions from the Sahara desert using new surface properties and soil database. J. Geophys. Res. Atmos. 113, 1–20. doi:10.1029/2007JD009484

Samset, B.H., Myhre, G., Herber, A., Kondo, Y., Li, S.M., Moteki, N., Koike, M., Oshima, N., Schwarz, J.P., Balkanski, Y., Bauer, S.E., Bellouin, N., Berntsen, T.K., Bian, H., Chin, M., Diehl, T., Easter, R.C., Ghan, S.J., Iversen, T., Kirkevag, A., Lamarque, J.F., Lin, G., Liu, X., Penner, J.E., Schulz, M., Seland, Skeie, R.B., Stier, P., Takemura, T., Tsigaridis, K., Zhang, K., 2014. Modelled black carbon radiative forcing and atmospheric lifetime in AeroCom Phase II constrained by aircraft observations. Atmos. Chem. Phys. 14, 12465–12477. doi:10.5194/acp-14-12465-2014

Evaluation of the performance of four chemical transport models in predicting the aerosol chemical composition in Europe in 2005

M. Prank[1], M. Sofiev[1], S. Tsyro[2], C. Hendriks[3], V.S. Semeena[2], X. Vazhappilly Francis[4], T. Butler[5], H. Denier van der Gon[3], R. Friedrich[6], J. Hendricks[7], X. Kong[4], M. Lawrence[5], M. Righi[7], Z. Samaras[8], R. Sausen[7], J. Kukkonen[1], R. Sokhi[4]

[1] Finnish Meteorological Institute, Helsinki, 00560, Finland
[2] met.no, Norwegian Meteorological Institute, Oslo, Norway
[3] TNO, Netherlands Organization for Applied Research, Utrecht, The Netherlands
[4] Centre for Atmospheric and Instrumentation Research (CAIR), University of Hertfordshire, Hatfield, UK
[5] Institute for Advanced Sustainability Studies, Potsdam, Germany
[6] IER, University of Stuttgart, Stuttgart, Germany
[7] Deutsches Zentrum für Luft- und Raumfahrt (DLR), Institut für Physik der Atmosphäre, Oberpfaffenhofen, Germany
[8] Aristotle University of Thessaloniki, Thessaloniki, Greece

Correspondence to: M. Prank (marje.prank@fmi.fi)

Abstract. Four regional chemistry transport models were applied to simulate the concentration and composition of particulate matter (PM) in Europe for 2005 with horizontal resolution ~20 km. The modelled concentrations were compared with the measurements of PM chemical composition by the EMEP monitoring network. All models systematically underestimated PM_{10} and $PM_{2.5}$ by 10-60%, depending on the model and the season of the year, when the calculated dry PM mass was compared with the measurements. The average water content at laboratory conditions was estimated between 5 and 20% for $PM_{2.5}$ and between 10 and 25% for PM_{10}. For majority of the PM chemical components, the relative underestimation was smaller than that, exceptions being the carbonaceous particles and mineral dust. Some species, such as sea-salt and NO_3^-, were overpredicted by the models. There were notable differences between the models' predictions of the seasonal variations of PM, mainly attributable to different treatments or omission of some source categories and aerosol processes. Benzo(a)pyrene concentrations were overestimated by all the models over the whole year. The study stresses the importance of improving the models' skill in simulating mineral dust and carbonaceous compounds, necessity for high-quality emissions from wildland fires, as well as the need for an more explicit consideration of aerosol water content in model-measurement comparison.

Keywords. particulate matter, aerosol chemical composition, chemical transport model, model evaluation, CMAQ, EMEP, LOTOS-EUROS, SILAM

1 Introduction

Exposure to particulate air pollution has been estimated to be among the ten most significant risk factors for public health globally, and among the 15 most relevant for Europe (Lim et al., 2012), substantially increasing the risks of respiratory and

heart diseases. Recently air pollution and especially the particulate matter were classified as carcinogenic by WHO (Loomis et al., 2013). Substantial research efforts have been dedicated to assess the health relevance of specific aerosol chemical components, although results are still largely inconclusive (Stanek et al., 2011). Particulate matter has also been recognized as a strong climate forcer that influences the Earth's energy balance through direct radiative effects and cloud processes.

5   Clouds and aerosols contribute the largest uncertainty to the radiative budget estimates (IPCC, 2013). Both aerosol radiative properties and its ability to serve as a cloud condensation nuclei depend critically on its composition. The above-mentioned aerosol effects make it important for the atmospheric chemistry and transport models to accurately assess not only the total PM amount but also the particle chemical composition, size spectra and other physical and chemical features.

A systematic underestimation of total PM (also called PM deficit) has been frequently reported in chemical transport
10   modelling studies (Bessagnet et al., 2016; Im et al., 2014; Solazzo et al., 2012a; Stern et al., 2008)~~(Im et al., 2014; Solazzo et al., 2012a; Stern et al., 2008)~~. In many cases such underestimation is to be expected: owing to the high complexity and uncertainty of associated emission and formation processes, models often omit some components of atmospheric aerosols and therefore fail to reproduce the total PM budget (Kukkonen et al., 2012). Among the most uncertain components are secondary organic aerosols (SOA) and natural emissions (forest fire smoke and wind-blown or re-suspended dust), which are
15   often omitted or reproduced with large uncertainties by the models. Numerous studies have stressed the importance of these components. Perez et al., (2008, 2012); Putaud et al., (2004b, 2010) and Querol et al., (2004) reported that the coarse fraction ($PM_{2.5-10}$) includes large contributions from mineral dust, particularly in southern Europe, while the fine fraction ($PM_{2.5}$) is dominated by carbonaceous particles and secondary inorganic aerosol (SIA) (Putaud et al., 2010). According to Belis et al. (2013), SOA makes up most of the organic carbon, especially in rural areas and during warm periods, whereas a noticeable
20   contribution from biomass burning is visible during cold season indicating the impact of domestic heating. The modelling quality of these compounds suffers from the relatively small amount of available observational data for the carbonaceous and crustal compounds. Several dedicated efforts have recently been made in order to understand and quantify the errors in modelling of these components and adequately represent them in the total PM budget, e.g. the studies of Denier van der Gon et al., (2015) for residential combustion, Soares et al. (2015) for wildfire emission, Kim et al. (2014) for wind-blown dust,
25   Arneth et al. (2008) for biogenic VOC emissions. Modelling studies of SOA formation include those by Bergström et al., (2012); Ots et al., (2016).; and Shrivastava et al., (2011). and others for modelling SOA formation.

A specific challenge of the model-measurement comparison for individual PM ~~individual~~ components is the difference in how PM composition is represented in the models and observations. The observations are available for specific molecules or ions (Na^+, SO_4^{2-}, NH_4^+, NO_3^-, Ca^{2+}, Al, Fe, etc.) and elemental and organic carbon (EC, OC), while in the models, the
30   speciation of primary aerosols rather follows the emission categories, such as anthropogenic sources, wildland fires, sea salt or wind-blown dust, which all can include several of the measured components (see e.g. Kuenen et al. (2014) for anthropogenic emissions, Akagi et al. (2011) and Andreae and Merlet, (2001) for wildland fire smoke, Avila et al. (1998) for wind-blown dust). ~~Due to such differences in the speciation of PM between the models and observations, conversions are necessary for model-measurement comparison, which in turn introduce further uncertainties to the results.~~ For instance, for

2

~~converting organic carbon to total organic aerosol (OA), OM/OC (organic matter to organic carbon) ratios ranging from 1.2 to 2.4 have been reported for different organic aerosol types (Aiken et al., 2008; Turpin and Lim, 2001). Various options exist for deriving the total mineral dust concentration from observations of e.g. aluminium or non sea salt fraction of calcium (nss-Ca^{2+}) (Marconi et al., 2014; Putaud et al., 2004b), but fractions of these vary among different minerals and dust source areas (Avila et al., 1998; Formenti et al., 2011).~~

A~~s a further complication, n~~ ~~additional complication is introduced by the fact that~~ the PM speciation measurements do not resolve the whole PM mass. Observational studies of the PM mass closure (Putaud et al., 2004b; Sillanpää et al., 2006) have reported an unidentified fraction of fine PM reaching up to 20-30% of the gravimetrically determined aerosol mass, while it might be as large as 40% for coarse particles. The explanations for this deficiency include possible artefacts in observations of semivolatile organic and inorganic components, unaccounted non-carbon atoms (e.g. O, H) in organic matter, uncertainties in estimating the concentration of the crustal particles, and most importantly aerosol-bound water. A~~In gravimetric sampling, which is the reference method for PM observations defined by the European Committee of Standardization, the filters are weighted in laboratory conditions of 20°C and 50% relative humidity. While the deliquescence relative humidity of most pure inorganic salts present in aerosol is higher than 50% (Martin, 2000), it can be lower for mixed particles (Seinfeld and Pandis, 2006, chapter 10.2). Apart from that, hysteresis exists in the particle deliquescence crystallization cycle, and for some common aerosol components, such as ammonium sulphate and sodium chloride, the efflorescence humidity, at which the particle crystallizes and loses its water content, is below 50% (Martin, 2000). Therefore, if the particle has been exposed to a more humid outdoor environment, crystallization might not occur in the standard laboratory conditions, leaving some amount of water bound to the particles on the filter. In addition to the particle bound water, the filters themselves can accumulate humidity and influence the measurement results (Brown et al., 2006). Hence, the observed concentrations will depend on the outdoor humidity as well as the filter transportation and storage conditions. Due to this complexity, a~~lthough some model-measurement comparison studies (e.g. Tsyro, 2005) have stressed the importance for the models to take the aerosol water content into account, it is still not considered in the majority of the studies. ~~The spatial features of the compared data can also lead to uncertainties in model measurement comparison. Regional models with grid cell sizes of a few tens of kilometres are not designed to reproduce the concentration patterns with smaller spatial scales, e.g. in the vicinity of strong sources, in urban conditions or mountainous areas. For instance, the study by (Im et al., 2014) found a stronger underestimation of PM in urban stations than in rural ones, which, apart from emission underestimation, could also be explained by the limited representative area of these stations. Also (Vautard et al., 2007) found larger PM underestimation in the urban stations by the large scale models than by those with higher resolution. Even for stations of the EMEP network, which locations have been carefully selected to represent the regional background (EMEP, 2001), the effects of local topography and sources may still be noticeable.~~

Within the TRANSPHORM project (www.transphorm.eu), four state-of-art chemical transport models (CTMs) – CMAQ, EMEP/MSC-W, LOTOS-EUROS and SILAM - were applied to predict PM concentrations in Europe for 2005. In this paper we evaluate the ability of these models to reproduce the chemical composition and the total mass of PM_{10} and $PM_{2.5}$ by

comparing the model predictions with the measurements at the EMEP network (www.emep.int). The effect of the omission of certain PM components by the models is investigated. Attention is paid to the role of the most uncertain components, such as carbonaceous aerosols, mineral dust and wild-land fire emissions, as well as the role of aerosol-bound water in the PM observations. In addition to the individual models, the median of the 4-member multi-model ensemble is ~~also~~ compared with the observations.

Majority of the multi-model inter-comparison studies for particulate matter have considered either only the total PM mass or just a few PM components (Hass et al., 2003; Im et al., 2014; Solazzo et al., 2012a), and some of them have been~~also being~~ concentrated only on specific environmental conditions (e.g. Stern et al., 2008) or limited areas (Vautard et al., 2007). In the current study the model error regarding the PM simulation is characterized against available measurements of PM mass and composition in whole Europe ~~The current study aims to clarify the main reasons behind the model measurement discrepancies and especially the PM deficit by evaluating the ability of the models to reproduce the complete PM_{10} and $PM_{2.5}$ mass budget~~ during the different seasons. ~~in whole Europe, and at identifying T~~the most prominent areas for model improvement are identified.

2 Input data and participating models

2.1 European Emissions in 2005

A new anthropogenic emission inventory was compiled within the TRANSPHORM project, with substantial updates regarding the EU-wide transport activities. The baseline emission data contains the following substances: NOx, SO_2, NMVOC, CH_4, NH_3, CO, PM_{10}, $PM_{2.5}$, EC, B[a]P (benzo[a]pyrene), and particle number (Denier van der Gon et al., 2014). The natural emissions of biogenic VOCs and sea salt were calculated online by each model. The wild-land fire emissions were provided by the Integrated System for wild-land fires IS4FIRES v.1 (Sofiev et al., 2009)~~(Sofiev et al., 2009a)~~ and were injected as primary particles to a homogeneous layer up to 1km above the surface. An exception was the SILAM model that calculates the wildfire emissions online, based on the IS4FIRES v.2 calibration (Soares et al., 2015) and vertical profiles of (Sofiev et al., 2012)~~(Sofiev et al., 2012a)~~. Desert dust was included only through the lateral boundary conditions; no wind-blown dust was emitted inside the modelling domain.

2.2 Global boundary conditions

The inflow of PM and gases through the lateral boundaries was prescribed according to global simulations by two different models. The aerosol boundary conditions were generated by the EMAC (ECHAM/MESSy Atmospheric Chemistry, Jöckel et al., (2006)) global model including the aerosol sub-model MADE (Modal Aerosol Dynamics model for Europe, adapted for global applications, Lauer et al., (2005, 2007)). Boundary conditions for gas phase chemical species were provided by the global chemical transport model MATCH-MPIC (Model for Atmospheric CHemistry and Transport, Max Planck Institute

for Chemistry version, Lawrence et al. (1999) and von Kuhlmann et al. (2003), Butler et al. (2012)). A detailed description of the models and the simulation setups can be found in Appendix A.

2.3 The regional models

The setups of the four participating models are summarized in Table 1. The detailed model descriptions ~~can be found~~are given in Appendix B.

The collected model output consists of hourly concentrations of ~~the individual~~each PM component~~s~~, separately for ~~coarse~~ fine (PM$_{2.5}$) and ~~fine~~ coarse (PM$_{2.5-10}$) fractions: SO$_4^{2-}$, NO$_3^-$, NH$_4^+$, EC, OC, SOA, sea salt, mineral dust, wild-land fire originated particulate matter, unspeciated other primary PM, and additionally also total PM$_{2.5}$ and PM$_{10}$ fields. While the primary anthropogenic PM, EC, secondary inorganic species and sea salt were computed by all models, other components were not always available (Table 2). For instance, OC was provided as a separate species only by EMEP and CMAQ models that included the secondary organic aerosol formation, while in the case of SILAM and LOTOS-EUROS primary OC was lumped with the rest of the anthropogenic primary PM. Due to very high uncertainties in the forest fire emission inventory, this component was left out of the total PM output of EMEP and LOTOS-EUROS, but was still provided as a separate field. In CMAQ the fine fraction of fire emitted PM was included in primary OA and the coarse fraction in unspeciated coarse primary PM.

Models also computed the concentration of benzo[a]pyrene (BaP), which was assumed to be an inert fine aerosol not participating in any chemical transformations and not affecting the total-PM budget due to its very low concentrations.

The ensemble median fields for total PM and each separate chemical component listed in Table 2 were computed from the hourly model data from the CTMs (hereinafter, median model). To reduce the influence of the components omitted in some of the models to the total PM, the median fields of the PM components were added up to form another dataset of total PM (hereinafter, medianComp model). When computing the median field for every component only those models are used which provided a valid field for that component, and thus the medianComp PM includes valid fields for all species computed by at least one model.

2.4 Observational data

The PM observations of the EMEP network were used for the model evaluation (Table 3). A detailed description of EMEP observations of PM and its components for 2005 is available in (Yttri et al., 2007). Table S1 shows the location and altitude of all stations together with a list of observed species.

EC/OC observations were available at four stations ~~(Table 4)~~, which, along with data for a wide range of other species at these sites (Table 4) allowed ~~for~~ a detailed evaluation of the PM composition ~~along~~evaluation at a transect from northern to southern Europe formed by these stations (Birkenes in Norway, Melpitz in Germany, Ispra in Italy and Montseny in Spain, Fig. S1).

5

In addition to the regular monitoring data, the EMEP 2002-2003 EC/OC campaign data are used for evaluation of the seasonality of the carbonaceous aerosols. The data were collected at 12 stations, one day per week from July 2002 to June 2003. One station in Portugal (Braganca, PTR0001R) was excluded from the comparison due extremely high modelled wild-land fire contribution which made that station not representative of average conditions – 2005 and 2003 were both record high wild-land fire years in Portugal, while being closer to average in rest of Europe. However, the 2002-2003 EMEP intensive campaign ends in the beginning of July 2003 and thus does not cover the 2003 Portuguese fires which mostly took place in August.

2.5 Model measurement comparison

For the model-measurement comparison, the hourly model results were extracted at the station locations and averaged to the temporal resolution of the observations. The model data were converted to the observed quantities. The observed Na^+ was assumed to originate only from sea salt, sea salt consisting 30.8% of sodium by dry weight. The part of the Ca^{2+} observations not related to sea salt (nss-Ca^{2+}) was used to evaluate the modelled mineral aerosol. The sea salt related calcium was subtracted from the observations proportionally to observed Na^+ concentrations, sea salt including 1.2% of calcium by dry weight. Widely varying calcium contents have been reported for Saharan dust from different origin areas ranging from <5% to >15% (Avila et al., 1998; Formenti et al., 2011; Marconi et al., 2014; Putaud et al., 2004a). The calcium content of anthropogenic emissions also varies between the sources, ranging from less than a percent for biomass burning (Akagi et al., 2011; Larson and Koenig, 1993) to ~30% for cement and lime production (Lee and Pacyna, 1999; van Loon et al., 2005). In the current study the modelled dust originating from the boundary conditions was assumed to come mainly from Sahara and was attributed 10% Ca^{2+} content (Marconi et al., 2014). In addition, 3.5% Ca^{2+} content was attributed to the mineral part of primary anthropogenic emissions. This value was chosen as it maximizes the correlation between the observed nss-Ca^{2+} and the model results. It stays well within the reported range for the anthropogenic emissions. The simulated nss-Ca concentrations were estimated as the sum of the 10% of dust concentrations plus 3.5% of the unspeciated other primary PM concentrations.

The OC to OM ratios have been reported to range from 1.2 to 1.6 for fresh anthropogenic emissions, while factors around 2 have been found for aged, secondary and oxygenated aerosol and particles originating from biomass burning (Aiken et al., 2008; Turpin and Lim, 2001). Factor 1.6 was used in this study, analogously to (Bessagnet et al., 2014), however, this might be an underestimation for the EMEP stations, which are mostly located in rural areas and would thus be largely influenced by aged aerosols.

The aerosols emitted by wild-land fires also consist mainly of carbonaceous compounds. The fire emissions originated from IS4FIRES (Sofiev et al., 2009), which provides unspeciated PM_{10} and $PM_{2.5}$ emissions In SILAM, EMEP and LOTOS-EUROS the emitted PM was transported as a separate field of unspeciated particulates, while in CMAQ the fine fraction was included in primary OA and the coarse fraction in coarse primary PM. The fire OA in CMAQ cannot be distinguished from the anthropogenic OA, and fire EC was not included in that model. In the other models the fire PM has been further

6

speciated as post-processing following Akagi et al., (2011) and Andreae and Merlet, (2001). On average these papers suggest roughly 5% EC and 50% OC content for fire emitted aerosol, the rest mainly consisting of non-carbon atoms in the organic compounds and some inorganics (up to 5%). The fire contribution to EC and OC has been calculated following this composition and added to the modelled EC and OC.

The models provided dry PM concentrations, which exclude the aerosol-bound water. In gravimetric sampling, which is the reference method for PM observations defined by the European Committee of Standardization, the filters are weighted in laboratory conditions of 20˚C and 50% relative humidity. While the deliquescence relative humidity of most pure inorganic salts present in aerosol is higher than 50% (Martin, 2000), it can be lower for mixed particles (Seinfeld and Pandis, 2006, chapter 10.2). Apart from that, hysteresis exists in the particle deliquescence-crystallization cycle. F, and for some common aerosol components, such as ammonium sulphate and sodium chloride, the efflorescence humidity, at which the particle crystallizes and loses its water content, is below 50% (Martin, 2000). Therefore, if the particle has been exposed to a more humid outdoor environment, crystallization might not occur in the standard laboratory conditions, leaving some amount of water bound to the particles on the filter. Based on the dry PM mass and speciation provided by the models, the aerosol thermodynamic model ISORROPIA2 (Fountoukis and Nenes, 2007) was applied to estimate the water content of the aerosol at the conditions where the filters were weighted (20°C, 50% relative humidity). ISORROPIA2 was run in the reverse mode, where the input quantities were the soluble inorganic components (SIA and sea salt, Ca) in the aerosol phase. Both stable and metastable states were computed, corresponding to the lower and upper branches of the deliquescence hysteresis loop, providing the lower and upper limits of the aerosol bound water amount.

The model results were evaluated in terms of bias, temporal and spatial correlations and the fraction of model values that are within a factor of 2 of the observations (FAC2).

3 Results of the model simulations

3.1 $PM_{2.5}$ and PM_{10} concentrations in 2005

The annual mean $PM_{2.5}$ and PM_{10} fields are presented in Figure 1 and Figure 2, for the individual models and the ensemble median. All models predict generally similar patterns of the near-surface concentrations for both $PM_{2.5}$ and PM_{10} although there are significant quantitative differences between the models' predictions. For $PM_{2.5}$, the highest concentrations are in densely populated areas such as Benelux and Po Valley, which reflects the large contribution of anthropogenic sources. The $PM_{2.5}$ concentrations are lower over the open sea, whereas all models agree onpredict high PM_{10} concentrations at marine areas due to coarse sea salt contribution. However, large differences are visible in absolute PM_{10} concentrations over sea, reflecting the differences between the sea salt emission algorithms. For example, the PM_{10} level predicted by the EMEP model over sea is up to 4 times higher than that of LOTOS-EUROS, whereas SILAM predicts a considerable south to north decrease in the marine PM_{10} concentrations due to the strong temperature dependence of its sea salt emissions. The LOTOS-

EUROS predictions did not include desert dust and wildland fire smoke, which explains the low values of both PM fractions ~~in the vicinity of~~close to the southern border of the domain.

The MedianComp model that sums up the ensemble medians of all the PM components and thus fully includes the wildfire emissions, desert dust and secondary organics, shows higher PM concentrations than the median model in various areas. The difference between the MedianComp and median models in the Central Europe is mainly due to SOA. PM_{10} in the southern part of the domain is influenced by the dust inflow from Sahara, while the fire impact is visible in Portugal. ~~The difference between the MedianComp and median models in the Central Europe is mainly due to SOA.~~ In CMAQ the dust and fire contributions are very low, and LOTOS-EUROS does not have them at all, so the median total PM is based on half of the models with zero or very low dust concentration. MedianComp is based only on the valid dust fields of SILAM and EMEP and thus includes noticeably higher dust contribution.

Figures S2 and S3 show the spatial patterns of model bias for $PM_{2.5}$ and PM_{10} with regard to the EMEP network. The individual models and the ensemble median underestimate both $PM_{2.5}$ and PM_{10} concentrations quite homogeneously in space. The only station, where the models noticeably overestimate the PM concentrations, is located on the Schauinsland Mountain in the Black Forest, with an elevation above 1200 m. About 10 km from the station and about 1 km below it is Freiburg city. ~~The models with horizontal resolutions of 20 to 30km cannot be expected to resolve topographic features with smaller spatial scales, making such stations located on mountain summits not representative for the model grid scale.~~ The overestimation ~~at the Schauinsland station~~ occurs in winter (see the monthly average timeseries on Fig. S4), when the site is actually in the clear air above the low winter time boundary layer, while ~~–~~in the models, both the city and the station are covered with one uniformly mixed grid cell. ~~The cell-average orography height in the model is lower than the site height and thus the model output is provided for the more polluted boundary layer.~~ In summer, when the site is located within the boundary layer, the PM concentration there is mostly underestimated.

As seen from Figure 3, all models report stronger seasonal variations in total PM than is observed. The models report highest concentrations in autumn or winter, while the observations peak in spring. There are also noticeable differences between the models. In SILAM and LOTOS-EUROS the $PM_{2.5}$ concentration is noticeably lower in summer, while in CMAQ the autumn concentrations are substantially higher than during the other seasons. EMEP predictions show very small seasonal variations for both $PM_{2.5}$ and PM_{10}. The different anthropogenic emission seasonalities applied in the models (Table 1) explain part of the differences in Figure 3. However, omitting the secondary organic aerosol (SOA) is probably the main explanation for the exaggerated $PM_{2.5}$ summer minimums calculated by the LOTOS-EUROS and SILAM models. SOA is present in larger quantities in summer due to biogenic emissions of semivolatile organic compounds.

The model skill scores for PM_{10} and $PM_{2.5}$ in winter and summer are presented in Table 5. The fraction of model values that are within a factor of 2 from the observations is larger in winter than in summer for all models, except EMEP. The temporal correlation of daily concentrations tends to be higher in winter, with the exception of CMAQ that has the lowest winter time correlations among the models. The models' ability to reproduce the average seasonal concentration patterns differs between finer and coarser particles – spatial correlation of PM_{10} is higher in summer, while $PM_{2.5}$ correlates better in winter for most

of the models. Low summer-time correlations of LOTOS-EUROS result from large underestimations in Spanish stations due to missing Saharan dust. The summertime worse scores are probably due to the highly uncertain components that dominate the summer aerosol - wind-blown dust, wild-land fires, and biogenic secondary organic aerosols. The only score that is better in summer then in winter is the spatial correlation for PM_{10}. In summer, the PM_{10} pattern over Europe is formed by the inflow of Saharan dust and wild-land fires in Portugal and Spain which creates a strong south to north gradient. This gradient is reproduced by the models, although with smaller magnitude. As the species contributing to this summertime south-north gradient are desert dust and wild-land fires, which by nature are episodic and hard to model, the temporal correlation and factor-two agreement are still generally lower and bias is larger in summer. In winter, the particulate matter is dominated by the anthropogenic emissions, forming a more complex pattern, and thus the spatial correlation is worse.

As seen from Table 5, while the bias of the ensemble median follows the mean bias of the models, the temporal and spatial correlations exhibit more complicated relations. In winter, the ensemble median shows the overall best temporal correlation for both $PM_{2.5}$ and PM_{10}, while in summer EMEP performs better. The spatial correlations of SILAM or EMEP models usually slightly exceed that of the median model.

The medianComp fully includes SOA, desert dust, and fire-induced PM. As the contributions of those components are more important in summer, the difference between the median and medianComp is largest in summer, ~~being~~ and small in winter (Table 5). MedianComp thus shows a noticeably smaller summer-time bias than the median model for both PM_{10} and $PM_{2.5}$. For PM_{10} the medianComp outperforms the median model in summer in all quality scores, while for $PM_{2.5}$ its spatial and temporal correlations are worse. This indicates that accounting for desert dust, which is an important component in PM_{10} and less so in $PM_{2.5}$, improves significantly the models' ability to reproduce the observed coarse PM patterns. It is worth pointing out, that the measurement network includes a large number of Spanish sites, where mineral dust is more important than for the rest of the modelling domain. The worsening of the summer time correlations of $PM_{2.5}$, on the other hand, indicates that improvements are necessary also for modelling the other components that were included only by few models, such as smoke from the vegetation fires and formation of secondary organic aerosols from the biogenic precursors.

The water contribution estimated with ISORROPIA2 based on the modelled aerosol composition is shown on Figure 3 with light blue. The solid part indicates the stable water content (lower branch of the hysteresis cycle) and the striped part the metastable phase (the upper branch of the hysteresis cycle). In the stable case, the annual mean $PM_{2.5}$ water content, average over all EMEP stations, stayed between 4 and 9% depending on the model, and between 11 and 17% for PM_{10}. For $PM_{2.5}$, the models predicted annual average water content above 10% for only a few stations. For PM_{10}, CMAQ and EMEP predict majority of the stations to have less than 10% of water content, while LOTOS-EUROS and SILAM predict the majority to be between 10 and 20%. Annual average water contents of more than 25% were predicted for some stations. The water content of PM_{10} computed in the metastable mode was on average about twice higher (~25%); ~20% water content was predicted for $PM_{2.5}$.

As seen from Table 6, adding the aerosol-bound water reduces noticeably the model bias for both PM_{10} and $PM_{2.5}$. For $PM_{2.5}$ the correlation coefficients are not much affected, while for PM_{10}, they are noticeably reduced. The factor-2 agreements

9

improve due to the bias reduction. The worsening correlations could be related to the models overestimating the sea salt concentrations that can lead to overestimation of the water content in PM_{10}, as sea salt is the most hydrophilic of the considered aerosol components.

3.2 PM composition in 2005

The ensemble median maps of the PM components are shown in Figures S5, S6, S7 and S8. In the Continental Europe the models predict the highest contribution from the summed secondary inorganic species, nitrate being most important in Central Europe and sulphate contributing mostly in Southern and Eastern regions. Sea salt concentrations are high over the marine areas and shores but decrease rapidly inland. Desert dust and wild-land fires can be the main contributors to aerosol in some areas, but their impact is spatially limited.

The models' performance in comparison to the measurements of the PM chemical components is shown in Table 6Table 7 (note different units (µg N, S, C, Na, Ca / m³); the model maps (Figures S5-8) that are plotted in full modelled species mass).; Tthe right columns of Figures S5 and S6 show the spatial spread of the model bias. PM_{10} is underestimated slightly more than $PM_{2.5}$ by all models except EMEP, possibly due to the missing emissions of wind-blown dust, which mainly resides in the coarse fraction. Sodium and NO_3^- are on average overestimated, whereas NH_4^+ and SO_4^{2-} are underestimated but much less than total PM. The overestimation of NO_3^- is most noticeable in the Central and Eastern Europe, whereas the western areas are predicted accurately and the northern ones are underestimated (Fig. S5). The carbonaceous aerosols and the mineral dust are underestimated more than the total PM.

Temporal correlation of the daily timeseries is usually lower for the specific components than for the PM_{10} and $PM_{2.5}$, and same is true for FAC2. One possible reason for this is that summing up the non-correlated individual components smooths the gradients and reduces the penalty for slight mislocations of plumes. It cannot be ruled out, that the lower correlation can in some cases be also due to higher observation errors. In particular, higher uncertainties are present in observations of mineral dust and carbonaceous species (Putaud et al., 2010, Annex 5; Sillanpää et al., 2006), but observation artefacts also influence the species with dynamic-equilibrium partitioning between particulate and gaseous phases, such as NH_4NO_3 (EMEP, 2001; Putaud et al., 2010, Annex 5). It also has to be noted that different pollutants are observed by different sets of stations in EMEP network, which might induce some extra variations to the average model scores.

The temporal correlations of the modelled carbonaceous compounds with their observed concentrations in $PM_{2.5}$ are among the highest for the PM components, and substantially lower for the observations of the same compounds in PM_{10}. The correlation coefficients are lowest for dust, but also below-average for NO_3^-. One can also notice a better agreement for the sum of HNO_3 and NO_3^- than for HNO_3 or nitrates-only. Temporal correlation coefficients and factor-2 agreements are noticeably worse for NH_3 and HNO_3 compared with NH_4 and NO_3 aerosols or the gas-aerosol sums. The lower scores for nitrates reflect the complexity of the gas-particle equilibrium between the NH_4NO_3 and HNO_3 and NH_3. Another possible reason for higher scores for the summed gases and aerosols (NH_3+NH_4 and NO_3+HNO_3) than for NH_3, HNO_3 and nitrate

10

aerosol separately is the higher uncertainties in the observations of the latter (Chang et al., 2002; Schaap et al., 2011; EMEP, 2001; Putaud et al., 2010, Annex 5). Also the pulsed behaviour of the aerosol nitrate production in the PBL, recently described by (Curci et al., 2015), could be a reason for inaccuracies in modelling the nitrate aerosol. Conversely, for NH_3 + NH_4^+ the temporal correlation is lower than for NH_4^+ only, albeit the bias is smaller and FAC2 is better. Sulphate and NH_4^+ show very similar correlation values, as large fraction of NH_4^+ is present in the form of ammonium sulphate. The correlation for sulphates is higher than for SO_2, probably mainly due to the smoother features of the sulphate field – SO_4^{2-} as a secondary pollutant is less affected by the local sources.

3.3 Secondary inorganic aerosols

The evaluation of the secondary inorganic aerosols (Figure 4) shows that the models reproduce relatively well the observed seasonal variation of SIA and its precursors. Moderate deviations exist: somewhat exaggerated seasonal cycle of SO_2 is shown by EMEP; ~~HNO_3 winter levels are high in~~ CMAQ overestimates the autumn levels of both NO_3+HNO_3 and NH_3+NH_4,and predicts an autumn peak for all three SIA species~~and low in other models~~; high autumn NH_3+NH_4 and SO_4^{2-} ~~and low HNO_3~~are also predicted by SILAM and ~~very~~ high autumn levels of NO_3+HNO_3 ~~NH_3, NH_4^+ and NO_3^- are shown~~by ~~CMAQ~~EMEP. SILAM manifests strong over-estimation of sulphates in autumn – but ~~only a minor~~no over-statement of SO_2. While the models reproduce well the summertime drop in the concentrations of NH_4 and NO_3, they tend to overestimate the autumn concentrations and while ~~T~~the observations show the highest concentrations in spring for all three SIA species, ~~which~~this is not reproduced by the models. This could be one of the reasons for the errors in the seasonal cycle of total PM. The contribution of the gas phase HNO_3 and NH_3 to the sums of NO_3+HNO_3 and NH_3+NH_4, is shown on Figure 4 with dark shading. On annual average level the gas phase fraction is in both cases relatively well reproduced by most of the models, only SILAM underestimates HNO_3 and overestimates NH_3 contributions. However, the models do not reproduce well the seasonal variations in HNO_3 and NH_3 concentrations – EMEP and LOTOS-EUROS overestimate the seasonal variability of HNO_3, CMAQ strongly overestimates the autumn NH_3 concentrations and so does with smaller magnitude also SILAM. The seasonal variations of NO_2 are well reproduced, but all models apart from CMAQ overestimate NO_2 all the seasons Table S3 and Figure S9. This can be one of the reasons for the overestimation of the sum of NO_3^- and HNO_3 seen on Figure 4.

3.4 Natural primary aerosols

For the sea-salt concentrations, EMEP and CMAQ predict higher levels than the other models and are also higher than observations in all seasons (Figure 5, left-hand column). However, the seasonal cycle is reproduced well. Conversely, LOTOS-EUROS, while being closest to the average annual level, underestimates the seasonal variations. SILAM is also close to the observations but seems to ~~overestimate~~ have an exaggerated ~~the~~ temperature dependence of the sea salt emission as it overpredicts the summer and autumn concentrations while underestimating in winter. For all models the Na concentration for model-measurement comparison was computed from sea salt in PM_{10}, while the Na observations in EMEP network are made mostly in whole aerosol without size limits. As the models already overestimate Na concentration,

11

including also the particles larger than 10 µm would lead to overestimation even larger than what is shown. However, comparing Na in PM_{10} with Na in whole sea salt in SILAM (size range 0.01 to 30 µm), the changes are minor for majority of the EMEP stations that observed Na in 2005: below 5% for 65% of the stations, below 10% for 77%, and below 20% for all stations. The concentration changed more than 10% only in the stations located directly at seaside.

Only SILAM and EMEP modelled the transport of desert dust from the boundaries (mainly Sahara) as a separate tracer. A 10% Ca^{2+} content was assumed for it (right panel of Figure 5, shaded part of the bars) and in addition a 3.5% Ca^{2+} content was attributed to the mineral part of primary anthropogenic emissions (non-shaded part of the bars). The modelled contributions from these sources are about equal, except for winter when the models predict almost no dust from Sahara. The nss-Ca^{2+} concentrations are substantially underestimated by the models for the whole year (EMEP model underestimated the nss-Ca by 75% and SILAM by 58%). Considering that the models omitted the wind-blown dust emissions inside the European modelling domain, this underestimation is not surprising. The seasonal patterns of the models differ from the observations, where the autumn concentrations are noticeably lower than the summer ones and close to the winter levels - the models rather suggest similar dust levels for most of the year, except for winter when the predicted concentrations are lower.

3.5 Carbonaceous aerosols

Based on tThe available observations of the carbonaceous aerosols for 2005, one can point out a strong under-estimation of these components by the models (Figure 6, upper panels). The models underestimated the EC in $PM_{2.5}$ by ~20-60% and OC by 40-80% (Table 7Table 6). The models only provided the fine fraction of these compounds as separate tracers; the anthropogenic coarse mode emissions were included in the coarse unspeciated primary aerosol. The fire PM concentrations modelled by EMEP, LOTOS-EUROS and SILAM has been speciated as post-processing following Akagi et al., (2011) or Andreae and Merlet, (2001). On average these papers suggest roughly 5% EC and 50% OC content for fire emitted aerosol. The fire contribution to EC and OC calculated following this composition is shown on Figure 6 with darker shading.

The observations on the upper panels of Figure 6 are shown for OC and EC in both $PM_{2.5}$ (shaded part of the bars) and PM_{10} (whole bars). The observations in PM_{10} are about 20% higher than those in $PM_{2.5}$. The modelled fine EC and OC correlate substantially better with the observations in $PM_{2.5}$ than with those in PM_{10} (Table 7Table 6). This agrees quite well with the emission estimates of Kuenen et al., (2014), according to which the anthropogenic emissions of coarse EC and OC are about 5 times lower than their fine mode ($PM_{2.5}$) emissions and also originate mostly from different sectors than the fine mode – coarse EC from large scale combustion and coarse OC from agriculture, while the most contributing sources of fine carbonaceous aerosol are residential combustion and traffic. As large part of OC is secondary and that also resides in fine fraction, some extra sources are still necessary to explain the observed coarse OC. The contribution of the coarse mode to the OC concentrations is highest in summer and autumn and lowest in winter, consistent with origin from biological and agricultural sources.

SILAM only shows a small fire contribution to EC in spring and summer, while in EMEP and LOTOS-EUROS the contribution is larger and visible all year round. EMEP also predicts a noticeable fire contribution to OC for all seasons. For

12

EMEP and LOTOS-EUROS, the fire contribution reduces the model bias for the carbonaceous species, while at the same time reducing the correlation with the measurements of EC and OC in $PM_{2.5}$ (Table S2). The SILAM EC prediction quality does not noticeably change. The correlation with EC and OC observations in PM_{10} in some cases rises when including the fire emitted part.

5   The models reproduce the observed seasonal variation in EC concentration, but all underestimate with varying magnitude. As elemental carbon emission data were the same for all models and no chemical transformations affect its concentrations in the atmosphere, the large differences of the average EC concentrations between the models are rather surprising. SILAM predicted the highest concentrations, being more than twice higher than CMAQ and EMEP in winter, the difference being smaller for the other seasons. A possible explanation is the considerably lower dry deposition of fine aerosols in SILAM

10 (Kouznetsov and Sofiev, 2012). Different treatment of EC hygroscopicity and ageing, affecting the efficiency of its wet scavenging, could also contribute to differences in the model results. The relatively coarse vertical resolution near the surface is a plausible explanation of EMEP's underestimation of EC, especially in winter. Finally, the emissions of carbonaceous particles are likely to be underestimated during the cold seasons due to large uncertainties in the emission factors for the residential wood burning (Denier van der Gon et al., 2015).

15 For OC only CMAQ and EMEP results are included in the analyses, as OC was not available from LOTOS-EUROS and SILAM (these models did not calculate the secondary OC and lumped the primary anthropogenic OC into the primary PM emissions). The models did not reproduce the observed seasonal variations in OC concentration, which peak in winter and autumn - both models show quite flat seasonal profiles and if accounting for the wildfire emissions, EMEP even overestimates the summer concentrations.. The large underestimation in winter could be caused by missing emissions of

20 domestic heating (Denier van der Gon et al., 2015), but also the SOA formation from anthropogenic aromatics could be underestimated. A rather large portion of semi-volatile organics is believed to be missing in current anthropogenic emission inventories of $PM_{2.5}$ and NMVOCs (Denier van der Gon et al., 2015; Donahue et al., 2006; Ots et al., 2016; Robinson et al., 2007). Cooking emissions have been pointed out as another missing source of organic aerosols (Fountoukis et al., 2015; Young et al., 2015).

25 The above analysis was based on only four stations that measured the carbonaceous compounds during 2005, which makes it uncertain. To better understand the results for carbonaceous compounds, we used OC/EC observations from the EMEP campaign in 2002/2003 (Simpson et al., 2007; Tsyro et al., 2007), when the carbonaceous aerosols in PM_{10} were observed at 12 stations. Keeping in mind the inter-annual variability, some kind of indication of model biases can still be obtained from comparing the modelled seasonal average concentrations of EC and OC for 2005 with the seasonal averages of these

30 observations, especially as the PM_{10} concentrations observed during this campaign were underestimated by the models by about the same factor as the PM_{10} observations of 2005. The comparison supports the previous conclusion: the modelled OC concentrations, and also those of EC at many sites, are substantially lower than the observations (Figure 6, lower row) and models completely miss the observed OC winter maximum.

13

3.6 Benzo(a)pyrene

All models of this study overestimated the Benzo(a)pyrene concentrations all year round (Figure 7~~Figure 7~~) whereas the seasonal cycles are qualitatively similar to the observed. This is somewhat unexpected, as the models underestimate the concentrations of black carbon and the sources of these two pollutants significantly overlap. One possible reason for this can be a simplified approach taken by the models to simulate this species: BaP was assumed to be an inert fine aerosol not participating in chemical transformations and not partitioning to gas-phase. In more complex models the heterogeneous oxidation by ozone has been reported to efficiently reduce the BaP concentrations (Friedman and Selin, 2012; Matthias et al., 2009). It is also probable that some part of the over-estimation, especially in winter time when the oxidation is slower, may be attributed to the emissions.

3.7 PM composition in the four selected stations

The PM composition was evaluated at the four stations that provided more complete data on the chemical speciation of the PM concentrations (Fig. S1). All the modelled and observed species in Figure 8 are converted to total masses of the species in order to add up to total $PM_{2.5}$ or PM_{10}. O~~C~~A is converted to total organic aerosol mass by multiplying with 1.6 and nss-Ca^{2+} to mineral dust by multiplying with 10. Observed sea salt is taken as the sum of Na^+ and Cl. However, the modelled and observed species are not always directly comparable, e.g. some models include carbonaceous aerosol ~~also~~ in primary anthropogenic PM or ~~the~~ wildfire smoke and mineral dust in the primary unspeciated ~~anthropogenic~~ aerosol. OA comparison with observations is based on CMAQ and EMEP results only, since the other models include OC in other PM. Dust comparison is based on EMEP and SILAM.

As seen in Figure 8, for these stations the sum of measured PM components was up to ~20% lower than measured total $PM_{2.5}$ and PM_{10}. The water contribution estimated with ISORROPIA2 can be seen on Figure 8 in light blue. Adding the aerosol bound water in metastable state closes the gap between the observed total PM_{10} and the sum of the individual components in almost all cases (in Montseny the PM_{10} estimate based on nearby stations can be inaccurate). In Ispra and Birkenes the observed PM is exceeded, which could indicate that the aerosol on the filters is in crystallized state or be due to inaccuracies in other observed species.

At Melpitz the models are close to the observations for SIA~~, but underestimate the carbonaceous part~~ and overestimate the sea-salt contribution. Carbonaceous part is underestimated, though accounting also for the wild-fire emissions (striped orange on Figure 8) brings EMEP very close to the OC observations in $PM_{2.5}$. The mineral dust transported from the boundaries (separately only in EMEP and SILAM) shows lower values than the observed dust concentration. EMEP is the only model, where the unspeciated part of the primary PM (PPMr) consists solely of mineral components, while in the other models it is mixed with either the primary organic aerosol or wild fire smoke. The sum of EMEP PPMr and desert dust is very close to the observation. However, here the observed total mineral dust concentration is estimated assuming 10% Ca^{2+} fraction, which is an overestimation for majority of the anthropogenic emissions.

14

At Montseny all models overestimate NO_3^-, whereas NH_4^+ is overestimated by EMEP and LOTOS-EUROS and SO_4^{2-} by SILAM. Considering that forest fire emissions also have substantial organic aerosol content, EMEP model is even overestimating the observed OA, while EC is overestimated by all models. Due to over-predicted NO_3^-, $PM_{2.5}$ is overestimated by EMEP and LOTOS-EUROS at this station. The modelled desert dust values are again substantially lower than the observed dust, while adding the PPMr concentration brings EMEP very close to the observation in $PM_{2.5}$, although still underestimating the mineral part of PM_{10}.

At Ispra, the major contributor to the observed PM is organic aerosol, while the models show a few times lower values. Elemental carbon is also somewhat underestimated. However, Yttri et al. (2007) warn against possible errors in the observations of carbonaceous aerosols at that site for 2005, especially in the case of PM_{10}. CMAQ also underestimates all SIA in Ispra and all models miss some SO_4^{2-}, while fine NO_3^- is overestimated by LOTOS-EUROS and SILAM. Sea salt and dust cannot be evaluated in Ispra, as no Na^+ or Ca^{2+} observations were available in 2005. This also makes the estimation of water content in the observed PM inaccurate.

At Birkenes all models but LOTOS-EUROS overestimate the measured PM_{10}. $PM_{2.5}$ is not shown, as the SIA, Ca^{2+} and Na^+ observations were not available separately for fine and coarse aerosol. As these species were measured in total aerosol, they might partly also originate from larger particles than PM_{10}. Elemental carbon concentrations are somewhat overestimated by CMAQ and SILAM. EMEP overestimates the organic aerosol. All models overestimate the sea salt contribution in PM_{10} by factor of 2-3 times, leading to very high water uptake of the aerosol. Modelled desert dust alone is lower than the nss-Ca^{2+} based observation while its sum with PPMr brings EMEP again very close to the observation.

All-in-all, overestimations of some components can bring the models very close or even over the observed PM levels, while still underestimating other components. The sea-salt concentrations are usually overestimated by all models – up to a factor of 2-4 – and this becomes important at the sites with a significant sea salt fraction in the mass budget. Sulphates are reproduced comparatively well with limited regional differences, probably driven by emission data quality. NH_4^+ is quite well reproduced by all models, except for CMAQ, which under-estimates it. For nitrates, the models showed varying degree of agreement. OA is mostly underestimated, while EMEP can also sometimes overpredict its concentration. Models underestimate high observed EC observations, while low concentrations can be overestimated. Mineral dust, which was taken only from global boundary conditions, is not enough to explain the observed nss-Ca^{2+} concentrations. Adding it up with the mineral part of the anthropogenic PM brings EMEP model close to observations, at least for $PM_{2.5}$. However, EMEP still underestimates the mineral contribution to PM_{10} in Montseny, which is the station most influenced by Saharan dust. The underestimation of nss-Ca^{2+} is smaller in the north, further away from Sahara (Fig. S6, lowest right panel).

4 Discussion

In the following we consider the major reasons for discrepancies of the model-measurement comparisons described above.

4.1 Uncertainties in the model evaluation

The individual PM components are reproduced with about the same or lower quality as the total PM. The temporal correlation of the daily timeseries is usually lower for the specific components than for the total PM, and same is true for the FAC2 agreement. This could indicate compensating errors in the model parameterizations, but even without that the comparison for the sum of the non-correlating components would benefit from the averaging of the errors in the components. The considered models are found to underestimate the observed total $PM_{2.5}$ and PM_{10} concentrations. However, not all individual PM components are equally underestimated: secondary inorganic species are reproduced quite accurately and sea salt is usually overestimated. This suggests large underestimations for carbonaceous and mineral aerosols, which is supported by the few available observations. However, the mismatch between the modelled and observed quantities leaves large uncertainties in evaluating how much exactly these aerosol components are underestimated in this study.

Wind-blown crustal aerosols have been pointed out as a potentially underestimated fraction of PM (Im et al., 2014) and substantial underestimation is found also strongly indicated by this study. The fraction of calcium observations not related to sea salt was used to evaluate the mineral dust concentration in this study. However, the evaluation of the wind-blown dust against non-sea-salt calcium observations is highly uncertain. Various options exist for deriving the total mineral dust concentration from observations of e.g. aluminium or non-sea-salt fraction of calcium (nss-Ca^{2+}) (Marconi et al., 2014; Putaud et al., 2004b), but fractions of these vary among different minerals and dust source areas (Avila et al., 1998; Formenti et al., 2011). ~~The calcium fraction in minerals and soil varies widely.~~ Putaud et al. (2010) provided various formulas for estimating the mineral dust concentration from several related tracers, such as Si, Al and Fe and nss-Ca^{2+}. They estimated that the uncertainty of deriving mineral dust concentration from observations can reach ±150%. Observations of Si, Al and Fe were available only in Montseny station. The location of Montseny station about 30 km from the Mediterranean coast, at 700m height from sea level exposes it to Saharan dust episodes (the high dust contribution there is visible on Figure 8) and thus allows for evaluating the nss-Ca^{2+} as a desert dust tracer. The nss-Ca^{2+} concentrations there correlate well (correlation coefficient above 0.9) with the observations of the other mineral dust tracers, and the dust concentration obtained by assuming 10% Ca^{2+} content is not far from the estimates provided by the most detailed formulas presented in the Annex 5 of Putaud et al., (2010).

However, the wind-blown crustal emissions are not the only source of mineral aerosols. Generally, about half of primary fine anthropogenic aerosol emission consists of carbonaceous components (Kuenen et al., 2014), while the rest is mainly associated with mineral compounds. For coarse fractions, the carbon content is low; hence the bulk of mass consists of mineral components. Therefore, the unspeciated primary PM in the models has to also be included to the comparison with the ~~mineral dust~~nss-Ca observations. However, the variations of the calcium content are even wider there, ranging from less

16

than a percent for biomass burning (Akagi et al., 2011; Larson and Koenig, 1993) to ~30% for cement and lime production (Lee and Pacyna, 1999; van Loon et al., 2005). According to Lee and Pacyna, (1999), the emissions from coal combustion include 2% of Ca^{2+} and steel and iron production emissions 0.7-3.6%. The Ca^{2+} content in the top soil layer, influencing the dust emissions form agricultural activities, but also the dust suspended by wind and traffic, stays in Europe below 5% and

5   below 1% in the northern areas (van Loon et al., 2005). Although the 3.5% Ca^{2+} content used in this study for the anthropogenic mineral aerosol is well within these limits, good model-measurement agreement cannot be expected due to these large variations. The uncertainty in aerosol Ca content can be expected to be a few times. However, with the 10 and 3.5% Ca content, the EMEP model underestimated the nss-Ca by 75% and SILAM by 58%, so even assuming twice the calcium content, the nss-calcium concentrations would still be underestimated by the models.

10   In 2005, the wild-land fires took place in a comparatively small part of the domain and affected noticeably only a few stations in Spain and Portugal. However, the very strong emission within short time had a significant impact on PM concentrations even at annual level. Therefore, exclusion of this component from the computations results in strong under-estimation and poor correlation, both in space and in time. On the other hand, fire emission is arguably among the most uncertain input datasets (Soares et al., 2015) and requires careful treatment accounting for the strong diurnal variation of the

15   fluxes, as well as the vertical injection profile. The fires emit wide spectrum of pollutants and the observations rarely distinguish the fire-originated aerosol from the rest of atmospheric PM. Specific tracers of combustion of organic materials, such as levoglucosan, are occasionally measured, but their relation to the total emitted PM is not fixed. Also, wood burning is common in many other sources, such as domestic heating, which cannot be told apart from large scale fires. As a result, evaluating the modelled fire smoke becomes possible only for episodes with strong domination of fire-induced pollution –

20   and these were not common in Europe in 2005.On the other hand, Iinaccurate representation of the fire emissions and their temporal and vertical profiles can result in a very poor correlation with the measured concentrations. In EMEP and LOTOS-EUROS, using the IS4FIRES v1 emissions resulted in degradation of model scores for $PM_{2.5}$ and PM_{10} and thus these models excluded the fire PM from their total $PM_{2.5}$ and PM_{10} fields, the correlations for EC and OC also reduced when fire contribution was added (Table S2). In SILAM, a newer version of the emission data was used (IS4FIRES v2, Soares et al.,

25   2015), together with dynamic emission vertical profiles (Sofiev et al., 2012), while in other models the IS4FIRES v1 emission data was spread evenly to the first 1000m. Mainly due to the vertical profiles that release most of the smoke high aloft, the ground level concentrations of fire PM were substantially lower in SILAM and the fire PM did not negatively affect the model performance, demonstrating that the quality of the fire emission data is essential for simulating the particulate matter concentrations. The fires emit wide spectrum of pollutants and the observations rarely distinguish the fire-

30   originated aerosol from the rest of atmospheric PM. Specific tracers of combustion of organic materials, such as levoglucosan, are occasionally measured, but their relation to the total emitted PM is not fixed. Also, wood burning is common in many other sources, such as domestic heating, which cannot be told apart from large scale fires. As a result, evaluating the modelled fire smoke becomes possible only for episodes with strong domination of fire-induced pollution – and these were not common in Europe in 2005.

17

The spatial features of the compared data can also lead to uncertainties in model-measurement comparison. Regional models with grid-cell sizes of a few tens of kilometres are not designed to reproduce the concentration patterns with smaller spatial scales, e.g. in the vicinity of strong sources, in urban conditions or mountainous areas. For instance, the study by (Im et al., 2014) found a stronger underestimation of PM in urban stations than in rural ones, which, apart from emission underestimation, could also be explained by the limited representative area of these stations. Also (Vautard et al., (2007) found larger PM underestimation in the urban stations by the large scale models than by those with higher resolution. Even for stations of the EMEP network, whichwhose locations have been carefully selected to represent the regional background (EMEP, 2001), the effects of local topography and sources may still be noticeable. The models' performance was found to degrade in the higher stations - there is a strong negative correlation between the station altitude and the models' temporal correlation coefficients for both PM_{10} and $PM_{2.5}$. The bad model performance is caused not only by the altitude difference between the station and the model grid cell average, but also other inhomogeneities, such as strong emission sources in the area. Indications of wintertime overestimation are visible for some of the high stations, but not all the high stations are located at extreme points of the terrain, such as mountain summits, and not all of them have strong emission sources in the immediate vicinity. Opposite problems arise for sites located in narrow valleys, where the models cell-mean altitude is higher than the station and the models overspread the pollution that in reality can be trapped in the valley.

Wang et al., (2014) and Samset et al., (2014) demonstrate that shorter EC lifetimes are necessary for reproducing the EC vertical profiles and low concentrations in remote regions. This result contradicts with the current model intercomparison, where SILAM was found to best reproduce the observed EC concentrations, and longer EC lifetime due to slower deposition in that model was assumed as the main reason for the model-to-model differences. Also the temporal correlation with 2005 observations and spatial correlation between the models 2005 average EC and EC observed during the 2002-2003 EMEP campaign is no worse for SILAM than it is for the other models, and hence there is no clear indication that the slower deposition would not be consistent with the surface EC observations in European scale. However, as indications were found of strong underestimation of EC emission, the slower deposition in SILAM is likely to be compensating for the missing emissions. Observations of vertical profiles and concentrations in more remote locations would be necessary for investigating this issue; unfortunately such were not available in Europe in 2005.

4.2 Seasonality of model skills, relation to PM composition

Seasonal variations of secondary aerosols result from a wide range of processes. Firstly, the emissions of precursors vary seasonally and some of these depend on meteorology. For instance, NH_3 emission depends strongly on the seasonality and type of agricultural activities, as well as on the temperature. Secondly, formation of secondary pollutants from precursor gases is controlled by multiple factors with strong seasonal cycles: the abundance of oxidants and water, ambient temperature and solar radiation, etc. Thirdly, gas-particle partitioning of semi-volatile species depends on temperature and relative humidity. There are significant differences in the treatment of these processes in the models, leading to substantial variations between the modelled seasonal cycles of the secondary aerosol concentrations. Resulting from these variations,

18

the ability of the models to represent the observed $PM_{2.5}$ and PM_{10} concentrations also varies seasonally and largely depends on the completeness of PM chemical composition in each specific model. For instance, the models that do not include SOA have larger bias in summer. Missing the contribution of the desert dust and wild-land fires also leads to negative bias and strongly reduces spatial correlation during summer time.

Especially for NH_3 the timing of the emissions as used in the models (fixed temporal profiles) can deviate substantially from real world emission timing which is largely controlled by meteorology (Backes et al., 2016; Hamaoui-Laguel et al., 2014; Hendriks et al., 2016). Meteorology also influences the total amount of emitted NH_3 but the strongest influence is on the timing. The timing of agricultural activities, such as manure spreading has also a strong impact on the emissions (Hendriks et al., 2016). The inaccurate temporal emission profiles lead to models not reproducing the seasonal cycle of SIA (Figure 4) and PM.

The observed nss-Ca concentrations peak in spring and so do the modelled Saharan dust concentrations. Previous studies about Saharan dust confirm the emissions peaking at spring (Fiedler et al., 2013; Laurent et al., 2008). Additionally to Saharan emissions there are other reasons for elevated crustal aerosol concentration in spring, such as agricultural activities and vehicle caused erosion of roads - in colder regions where winter tires are used and the roads are sanded against slipperiness, high dust emissions occur when the road conditions get dry in spring. These emissions were not included in the model runs, which could be another reason why the models miss the spring peak in PM.

Another source of OC that has receieved very little attention is the primary biogenic particles, such as plant debris, fungal spores and pollen. While majority of these particles are larger than 10µm, the aerodynamic diameter of some common fungal spores is below 10µm and in some cases even below 2.5µm (Reponen et al., 2001), making them relevant to even $PM_{2.5}$. According to Hummel et al. (2014) and Winiwarter et al. (2009) the fungal spores could contribute noticeably to aerosol concentration in summer and autumn (up to a microgram m^{-3} in long term average and even more during specific episodes). The PM components mentioned above as the most uncertain and sometimes omitted in the models (wind-blown dust, wild-land fire smoke, biogenic primary and secondary particles), are all more common in summer time. The models mostly do underestimate PM by a larger fraction in summer. On the contrary, organic aerosol is underestimated by a larger fraction in winter. As noted by (Denier van der Gon et al., 2015; Lefebvre et al., 2016)(Denier van der Gon et al., 2015), the residential wood combustion emissions are severely underestimated in the current emission inventories and that would cause underestimation in carbonaceous particles during the cold seasons. According to Fountoukis et al., (2015) underestimation of the SOA formation rate in low light conditions could be another reason for the winter time OA underprediction.

4.3 Aerosol mass closure

Previous publications (Putaud et al., 2010; Sillanpää et al., 2006; Tsyro, 2005) have pointed out that a certain gap exists between the gravimetric total-PM observations and the sum of individual PM components (also seen in Figure 8). The main reason for this has been found to be aerosol-bound water contribution to the gravimetric observations, which can contribute ~20% of mass to annual average observations. Based on the modelled aerosol composition, the average water content at

laboratory conditions was estimated roughly between 5 and 20% for $PM_{2.5}$ and between 10 and 25% for PM_{10}, depending on whether the aerosol was assumed to be in stable or metastable state, the latter corresponding to situation, when the aerosol has been exposed to more humid conditions and crystallization has not occurred. Adding this contribution to the modelled PM reduced the model bias 25-70%, but also reduced both spatial and temporal correlations with the observations.

5   Several uncertainties exist estimating of the PM water content. Firstly, the water content depends on the outdoor humidity at the measurement location as well as the filter transportation and storage conditions, so it cannot be determined, whether the aerosol is in stable or metastable branch of the hysteresis cycle. Secondly, ISORROPIA2 computes the water content based on the inorganic part of aerosol – SIA, sea salt, calcium; it does not take into account the water related to the hydrophilic part of the organic aerosol, which could also influence the water uptake of the inorganic species (Jing et al., 2015). Thirdly, the

10   aerosols were assumed fully internally mixed, which lowers the deliquescence humidity compared to external mixtures and might lead to overestimation of water uptake. Overestimating hydrophilic compounds, such as sea salt can also lead to overestimation of the water content in PM. Also, ~~I~~in addition to the particle-bound water, the filters themselves can accumulate humidity and influence the measurement results (Brown et al., 2006). Taking into account all these uncertainties, ~~Hence, the observed concentrations will depend on the outdoor humidity as well as the filter transportation and storage~~

15   ~~conditions.~~the water content estimated based on the observed PM composition (Figure 8) assuming metastable state surprisingly well closes the budget for several stations (e.g. PM_{10} and $PM_{2.5}$ in Melpitz and $PM_{2.5}$ in Montesny).

~~In this study it is not possible to assess the importance of this issue as only four stations provided a sufficiently complete set of the PM components. However, it is reasonable to assume that this fraction would be similar to what has been found in the previous studies. If in the current evaluation we assume that dry PM mass of the soluble species reported by the models is~~

20   ~~increased by roughly 20% before comparing it with the PM~~$_{10}$~~ and PM~~$_{2.5}$~~ gravimetric observations, the under estimation visible in Figures S2 and S3 will become much smaller, essentially disappearing in several cases.~~

~~The above consideration has wide implications.~~ Even when non-gravimetric measurement methods are used, they often include processing steps to obtain similar values to the gravimetric method, which is defined as the reference for PM measurements by European Committee of Standardization. The reason for these corrections is that a substantial fraction of

25   secondary aerosols consists of components, such as ammonium nitrate and semivolatile organic species, whose partitioning between gaseous and particulate phase depends on the atmospheric conditions and concentrations of the compounds. Apart from water, also the semivolatile compounds can condense or evaporate during the measurement process. Loss of semivolatiles is an especially important issue for observation techniques that involve heated inlets, and ~~thus~~ dedicated methodologies have been developed to compensate for such losses and bring the results closer to the standard gravimetric

30   observations (Alastuey et al., 2012; Charron et al., 2004; Hauck et al., 2004). However, such corrections implicitly introduce the particle water related offset also to observations that should by their design avoid it. As various applications using the PM_{10} and $PM_{2.5}$ concentrations as an input (e.g. health impact assessment) are often calibrated using the total PM observations ~~exhibiting the aforementioned features~~, using the model-produced dry PM masses will introduce a bias to the impact analysis. ~~The most feasible way to handle this issue is to adjust the model output taking into account actual humidity~~

and corresponding amount of water in the particles. This correction, however, faces the difficulty because 50% RH is inside the hysteresis loop for some hygroscopic compounds and therefore the actual amount of water in the particles depends on RH history. But even taken on average such correction would improve the consistency between the observed and modelled PM total mass.

5   **5 Conclusions**

The currently available chemical transport models commonly under-predict the PM mass concentrations, however the previous multi-model studies have not thoroughly investigated how this underprediction is reflected in the PM chemical composition. The current study was conducted to quantify the model deficiencies in terms of the aerosol chemical constituents, source categories, seasonal variations, and geographical distribution.

10 The aerosol predictions of four widely used chemical transport models (CMAQ, EMEP, LOTOS-EUROS and SILAM) were compared to the chemically-speciated PM observations by the EMEP monitoring network. All models showed comparable scores in reproducing the PM observations, generally underestimating the total PM mass by 10-60%, depending on the season of the year and the model. The PM components for which the modelling and monitoring experience is longer, such as nitrates, sulphates and ammonia were reproduced fairly well by all the models, whereas there were major underestimations

15 for carbonaceous and mineral aerosols. The benzo(a)pyrene concentrations were overestimated by all models, probably owing to missing processes and inaccuracies in emission data.

The study highlighted the importance of the contribution of ~~specific~~ commonly omitted aerosol components, such as SOA, mineral dust and wildfire smoke~~, which are not always included in the computations~~. Neglecting the desert dust contribution to the PM budget substantially worsened the correlation of model predictions with PM observations in summer, which

20 indicates that accounting for the inflow of Saharan dust is important in PM simulations, especially for southern Europe - for central and northern parts, agricultural and road dust are more important on an annual basis. The impact of wild-land fires was also significant in summer of 2005 in the western and southern parts of the domain. Including SOA in the modelled PM also substantially reduced the model bias in summer. Providing that all major PM components are included, the particle-bound water in gravimetric PM observations can explain a major fraction of the remaining bias.

25 The ensemble median showed better correlation with the observations than the individual models. However, the bias demonstrated by all models propagated also into the median results. This effect can be reduced by computing the median for each of the PM components separately with subsequent summation to the total-PM concentration. This procedure reduces the effect of the components that have been omitted by some of the models within the ensemble.

Appendix A: Global models

EMAC-MADE

EMAC is a numerical chemistry and climate simulation system describing tropospheric and stratospheric processes (Jöckel et al., 2006). It is based on the 5th generation European Centre HAMburg general circulation model (ECHAM5, Roeckner et al., 2006) and uses the Modular Earth Submodel System (MESSy) as an interface to couple various sub-models to the core model. Aerosol microphysics is simulated with the sub-model MADE (Lauer et al., 2005, 2007), which describes the aerosol population by means of three log-normal size modes, taking into account nucleation of new particles, condensation of sulphuric acid vapour and condensable organic compounds, and coagulation. MADE considers eight aerosol species: black carbon, particulate organic matter, sulphate, nitrate, ammonium, mineral dust, sea-salt, and aerosol water. Basic tropospheric gas-phase chemistry (NO_x-HO_x-CH_4-CO-O_3) and the sulphur cycle are simulated by the MECCA submodel (Sander et al., 2005). Additional processes include liquid phase chemistry (SCAV submodel, (Tost et al., 2006), gas/particle partitioning (Metzger et al., 2002), wet and dry deposition (SCAV and DRYDEP submodels, Kerkweg et al., 2006), aerosol activation during cloud formation (Abdul-Razzak and Ghan, 2000) and cloud microphysical processes simulated by the two-moment cloud scheme by Lohmann et al. (1999) and Lohmann, (2002). The EMAC-MADE model system has been evaluated by Lauer et al. (2005, 2007), Aquila et al. (2011) and Righi et al. (2013).

The emission setup considers biomass burning emission from the GFED dataset (van der Werf et al., 2010), anthropogenic emissions according to the RCP 8.5 scenario (Lamarque et al., 2010; van Vuuren et al., 2011) for the year 2005, and natural sources (volcanic SO_2, DMS, secondary organic aerosol). Wind-dependent number and mass emission fluxes are calculated on-line based on the parameterization of Guelle et al.,(2001) for sea salt and Balkanski et al. (2003) for desert dust. Dust is emitted in two log-normal modes with the size distribution parameters from (Dentener et al., 2006).

The EMAC simulations for this study were performed with a T42L19 resolution, i.e., with a horizontal spectral resolution with a triangular cut-off at great circle wave number 42, corresponding to a Gaussian grid of about 2.8° resolution and 19 vertical hybrid σ-pressure layers with the top layer centred at 10 hPa. The model dynamics were nudged to the operational analysis data of the European Centre for Medium-range Weather Forecasts (ECMWF).

MATCH-MPIC

Boundary conditions for gas phase chemical species were provided from the global chemical transport model MATCH-MPIC (Model for Atmospheric CHemistry and Transport, Max Planck Institute for Chemistry version, Lawrence et al. (1999) and von Kuhlmann et al. (2003)). The model was operated with input meteorological fields of the NCEP GFS (National Center for Environmental Prediction Global Forecast System). Tracer transport by advection, vertical diffusion and deep convection, as well as the tropospheric hydrological cycle (water vapour transport, cloud condensate formation and precipitation) are computed within the model. Chemical reactions of anthropogenic and biogenic NMVOCs are included, along with background tropospheric chemical reactions. More details on the simulations can be found in Butler et al. (2012).

Appendix B: Regional models

CMAQ

The Community Multi-scale Air Quality (CMAQ) modelling system applied in the study is the CMAQ version 4.7.1 with carbon bond chemical mechanism version 5 (Foley et al., 2010). The model grid was in Lambert conformal Projection (LCP) centred at (54°, 0°) with standard parallel latitudes 30° and 60°, respectively. CMAQ was applied on horizontal grid dimension with 18 km resolution. The study domain encompassed entire Europe with Atlantic Ocean as its western boundary. The CMAQ model consisted of 34 vertical layers extending from the surface up to ~20 km height. The meteorological inputs for the chemical transport model were generated from the meteorological modelling simulations of the Weather Research and Forecast (WRF) model version 3.2.1 (Skamarock et al., 2008). The WRF simulation was performed using 18km x 18km horizontal grid resolution with 52 vertical layers. The simulations used NOAA soil vegetation model applied as the land surface scheme, RRTMG as the long wave radiation scheme, Morrison scheme for microphysics parameterization, Grell and Devenyi scheme for cumulus parameterization, and YSU scheme for boundary layer parameterization. Meteorological initial and lateral boundary conditions were derived from the ECMWF analysis. In order to constrain the meteorological model towards the analyses a grid nudging technique was employed every 6 hours of WRF simulation. The results from WRF simulations were pre-processed for CMAQ using Meteorology-Chemistry Interface Process (MCIP) version 3.6 (Otte et al., 2005). In MCIP, 52 layers of the WRF model simulations were collapsed to 34 layers used in the CMAQ simulation.

The primary particulate matter such as $PM_{2.5}$, PM_{10}, elemental carbon, and sea salt as well as secondary inorganic aerosol species (SO_4^{2-}, NO_3^- and NH_4^+) were included for the model comparison. The sea salt production in the marine boundary layer included the heterogeneous chemistry of sea salt aerosols (Spicer et al., 1998).

EMEP/MSC-W

The EMEP/MSC-W model (Simpson et al., 2012) is a chemical transport model developed at the Meteorological Synthesizing Centre West of EMEP (http://www.emep.int), hosted by Norwegian Meteorological institute. At the same website, the model code (Open Source) and a suite of input data for a full year run are available. The model performance is regularly evaluated with EMEP routine monitoring and intensive measurement campaigns, as well as with other observational data (AirBase, satellite, sun-photometer, LIDAR measurements).

The calculations were performed using ECMWF-IFS meteorology, on $0.2° \times 0.2°$ grid, and the results were interpolated to the unified $0.3° \times 0.2°$ grid. The vertical distribution was resolved with 20 layers, reaching 100 hPa, with the lowest layer being approximately 90 m thick. Calculated concentrations were interpolated between the model layers to provide data at the requested levels, i.e. 100, 500, 1000, 3000 m), in addition the concentrations at a height of 3 m were derived from the results in the lowest layer for comparison with observations. The emission data, including forest fires, and boundary conditions were harmonized with the other participating models as described in sections 3.1 and 3.2 but the temporal emission profiles

followed (Simpson et al., 2012). The model included all main aerosol components from anthropogenic and natural sources, namely SO_4^{2-}, NO_3^-, NH_4^+, elemental and organic (both primary and secondary) carbon, sea salt and mineral dust (here only from the boundary conditions). SO_4^{2-} is formed through SO_2 homogeneous and heterogeneous oxidation; NO_3^- and NH_4^+ are calculated through aerosol-gas partitioning using thermodynamic equilibrium model MARS. In addition, the formation of

5   coarse NO_3^- is included in a simplified way. Describing dry and wet deposition, the model treats separately fine and coarse aerosols.

LOTOS-EUROS

In this study we used LOTOS-EUROS v1.8, a 3-D regional CTM that simulates air pollution in the lower troposphere (Schaap et al., 2008, Wichink Kruit et al., 2012). The calculations were performed with longitude–latitude 0.3˚×0.2˚ grid.

10   The model vertical spans up to 3.5 km above sea level and consists of three dynamical layers: a mixing layer and two reservoir layers above it. The height of the mixing layer at each time and position is extracted from ECMWF meteorological data used to drive the model. The height of the reservoir layers is set to the difference between ceiling (3.5 km) and mixing layer height. Both layers are equally thick with a minimum of 50 m. If the mixing layer is near or above 3500 m high, the top of the model exceeds 3500 m. A surface layer with a fixed depth of 25 m is included to monitor ground-level concentrations.

15   Advection in all directions is handled with the monotonic advection scheme developed by Walcek, (2000). Gas phase chemistry is described using the TNO CBM-IV scheme (Schaap et al., 2009), which is a condensed version of the original scheme by Whitten et al. (1980). Hydrolysis of N_2O_5 is described following Schaap et al. (2004a). Aerosol chemistry is represented with ISORROPIA2 (Fountoukis and Nenes, 2007). The pH dependent cloud chemistry scheme follows Banzhaf et al. (2012). Formation of coarse-mode nitrate is included in a dynamical approach (Wichink Kruit et al., 2012). Dry

20   deposition for gases is modelled using the DEPAC3.11 module, which includes canopy compensation points for ammonia deposition (Van Zanten et al., 2010). Deposition of particles is represented following Zhang et al. (2001). Stomatal resistance is described by the parameterization of (Emberson et al., 2000a, 2000b) and the aerodynamic resistance is calculated for all land use types separately. Wet deposition of trace gases and aerosols are treated using simple scavenging coefficients for gases (Schaap et al., 2004b) and particles (Simpson et al., 2003). Biogenic VOC emissions (Schaap et al., 2009) are derived

25   from a dataset with the distributions of 115 tree species as obtained from Koeble and Seufert, (2001). Emissions of sea salt particulates (following Mårtensson et al., 2003; Monahan et al., 1986) are taken into account. The temporal variation of anthropogenic emissions is represented by monthly, daily and hourly time factors for each source category (Builtjes et al., 2003). The model set-up used here does not contain secondary organic aerosol formation.

SILAM

30   The System for Integrated modeLling of Atmospheric coMposition (SILAM; http://silam.fmi.fi, Sofiev et al., 2015) is a global-to-meso-scale chemical transport model developed at FMI and used in research and operational applications related to air quality and emergency. SILAM uses a transport algorithm based on the Eulerian advection scheme of (Sofiev et al.,

2015), and the adaptive vertical diffusion algorithm of (Sofiev, 2002). The model includes a meteorological pre-processor for diagnosing the basic features of the boundary layer and the free troposphere (such as diffusivities, similarity scales, and latent and sensible heat fluxes) from meteorological fields provided by various meteorological models (Sofiev et al., 2010). For secondary inorganic aerosol formation, the updated chemistry scheme from DMAT model (Sofiev, 2000) was extended

5   with the coarse-nitrate formation. The dry deposition scheme is described in (Kouznetsov and Sofiev, 2012). Sea-salt was emitted according to (Sofiev et al., 2011), the size distribution being represented by 5 bins from 0.01 to 30 μm. Wild land fire emissions of IS4FIRES v.2 (Soares et al., 2015) were used.

The SILAM model has been extensively evaluated against air quality observations over Europe and the globe (Huijnen et al., 2010), http://www.gmes-atmoshpere.eu, http://www.myair.eu (Solazzo et al., 2012a, 2012b). The model has recently been

10   applied to evaluate the dispersion of primary PM$_{2.5}$ emissions across Europe and in more detail over Finland, and to assess the resulting adverse health impacts (Karvosenoja et al., 2011; Tainio et al., 2009, 2010).

For TRANSPHORM, the computations were made using meteorological fields from ECMWF operational forecasts from 2005. The computational grid covered the domain with spatial resolution of 0.3° × 0.2°, vertical grid consisting of 8 unevenly spaced layers stacked up to ~8km. The aerosol components included secondary inorganic species SO_4^{2-}, NO_3^- and

15   NH_4^+; primary particulate matter PM$_{2.5}$ and PM$_{10}$, elemental carbon, dust, and sea salt.

20   **References**

Abdul-Razzak, H. and Ghan, S. J.: A parameterization of aerosol activation: 2. Multiple aerosol types, J. Geophys. Res. Atmos., 105(D5), 6837–6844, 2000.

Aiken, A. C., DeCarlo, P. F., Kroll, J. H., Worsnop, D. R., Huffman, J. A., Docherty, K. S., Ulbrich, I. M., Mohr, C., Kimmel, J. R., Sueper, D., Sun, Y., Zhang, Q., Trimborn, A., Northway, M., Ziemann, P. J., Canagaratna, M. R., Onasch, T.

25   B., Alfarra, M. R., Prevot, A. S. H., Dommen, J., Duplissy, J., Metzger, A., Baltensperger, U. and Jimenez, J. L.: O/C and OM/OC ratios of primary, secondary, and ambient organic aerosols with high-resolution time-of-flight aerosol mass spectrometry, Environ. Sci. Technol., 42(12), 4478–4485, doi:doi:10.1021/es703009q, 2008.

Akagi, S. K., Yokelson, R. J., Wiedinmyer, C., Alvarado, M. J., Reid, J. S., Karl, T., Crounse, J. D. and Wennberg, P. O.: Emission factors for open and domestic biomass burning for use in atmospheric models, Atmos. Chem. Phys. Discuss., 11,

30   4039–4072, doi:10.5194/acp-11-4039-2011, 2011.

Alastuey, A., Minguillón, M. C., Pérez, N., Querol, X., Viana, M. and Leeuw, F. De: PM 10 measurement methods and correction factors: 2009 status report. [online] Available from: http://acm.eionet.europa.eu/reports/ETCACM_TP_2011_21_PM10Equivalence, 2012.

Andreae, M. O. and Merlet, P.: Emission of trace gases and aerosols from biomass burning, Global Biogeochem. Cycles, 15(4), 955–966, 2001.

Aquila, V., Hendricks, J., Lauer, A., Riemer, N., Vogel, H., Baumgardner, D., Minikin, A., Petzold, A., Schwarz, J. P., Spackman, J. R., Weinzierl, B., Righi, M. and Dall'Amico, M.: MADE-in: a new aerosol microphysics submodel for global simulation of insoluble particles and their mixing state, Geosci. Model Dev., 4(2), 325–355, doi:10.5194/gmd-4-325-2011, 2011.

Arneth, A., Monson, R. K., Schurgers, G., Niinemets, Ü. and Palmer, P. I.: Why are estimates of global terrestrial isoprene emissions so similar (and why is this not so for monoterpenes)?, Atmos. Chem. Phys., 8(16), 4605–4620, doi:10.5194/acp-8-4605-2008, 2008.

Avila, A., Alarcón, M. and Queralt, I.: The chemical composition of dust transported in red rains—its contribution to the biogeochemical cycle of a holm oak forest in Catalonia (Spain), Atmos. Environ., 32(2), 179–191, doi:10.1016/S1352-2310(97)00286-0, 1998.

Backes, A. M., Aulinger, A., Bieser, J., Matthias, V. and Quante, M.: Ammonia emissions in Europe, part II: How ammonia emission abatement strategies affect secondary aerosols, Atmos. Environ., 126(x), 153–161, doi:10.1016/j.atmosenv.2015.11.039, 2016.

Balkanski, Y., Schulz, M., Claquin, T., Moulin, C. and Ginoux, P.: Global emissions of mineral aerosol: formulation and validation using satellite imagery, in Emissions of Atmospheric Trace Compounds, pp. 253–282, Springer, Kluwer Acad., Norwell, Mass., 2003.

Banzhaf, S., Schaap, M., Kerschbaumer, A., Reimer, E., Stern, R., van der Swaluw, E. and Builtjes, P.: Implementation and evaluation of pH-dependent cloud chemistry and wet deposition in the chemical transport model REM-Calgrid, Atmos. Environ., 49, 378–390, doi:10.1016/j.atmosenv.2011.10.069, 2012.

Belis, C. a., Karagulian, F., Larsen, B. R. and Hopke, P. K.: Critical review and meta-analysis of ambient particulate matter source apportionment using receptor models in Europe, Atmos. Environ., 69, 94–108, doi:10.1016/j.atmosenv.2012.11.009, 2013.

Bergström, R., Denier van der Gon, H. a. C., Prévôt, a. S. H., Yttri, K. E. and Simpson, D.: Modelling of organic aerosols over Europe (2002–2007) using a volatility basis set (VBS) framework: application of different assumptions regarding the formation of secondary organic aerosol, Atmos. Chem. Phys., 12(18), 8499–8527, doi:10.5194/acp-12-8499-2012, 2012.

Bessagnet, B., Colette, A., Meleux, F., Rouïl, L., Ung, A., Favez, O., Cuvelier, K., Thunis, P., Tsyro, S., Stern, R., Manders, A., Kranenburg, R., Aulinger, A., Bieser, J., Mircea, M., Briganti, G., Cappelletti, A., Calori, G., Finardi, S., Silibello, C., Ciarelli, G., Aksoyoglu, S., Prévot, A., Pay, M. T., Baldasano, M., García Vivanco, M., Garrido, J. L., Palomino, I., Martín, F., Pirovano, G., Roberts, P., Gonzalez, L., White, L., Menut, L., Dupont, J.-C., Carnevale, C. and Pederzoli, A.: The EURODELTA III exercise – Model evaluation with observations issued from the 2009 EMEP intensive period and standard measurements in Feb / Mar 2009, Geneva. [online] Available from: http://emep.int/publ/reports/2014/MSCW_technical_1_2014., 2014.

Bessagnet, B., Pirovano, G., Mircea, M., Cuvelier, C., Aulinger, A., Calori, G., Ciarelli, G., Manders, A., Stern, R., Tsyro, S., García Vivanco, M., Thunis, P., Pay, M.-T., Colette, A., Couvidat, F., Meleux, F., Rouïl, L., Ung, A., Aksoyoglu, S., Baldasano, J. M., Bieser, J., Briganti, G., Cappelletti, A., D'Isodoro, M., Finardi, S., Kranenburg, R., Silibello, C., Carnevale, C., Aas, W., Dupont, J.-C., Fagerli, H., Gonzalez, L., Menut, L., Prévôt, A. S. H., Roberts, P. and White, L.: Presentation of the EURODELTA III inter-comparison exercise &ndash; Evaluation of the chemistry transport models performance on criteria pollutants and joint analysis with meteorology, Atmos. Chem. Phys. Discuss., (January), 1–61, doi:10.5194/acp-2015-736, 2016.

Bieser, J., Aulinger, a., Matthias, V., Quante, M. and Denier Van Der Gon, H. a C.: Vertical emission profiles for Europe based on plume rise calculations, Environ. Pollut., 159(10), 2935–2946, doi:10.1016/j.envpol.2011.04.030, 2011.

Briggs, G. A.: Some Recent Analyses of Plume Rise Observation, in Proceedings of the Second International Clean Air

Congress, edited by H. M. Englun and W. T. Beery, pp. 1029–1032, Academic Press, New York., 1971.

Brown, A., Yardley, R., Quincey, P. and Butterfield, D.: Studies of the effect of humidity and other factors on some different filter materials used for gravimetric measurements of ambient particulate matter, Atmos. Environ., 40(25), 4670–4678, doi:10.1016/j.atmosenv.2006.04.028, 2006.

5 Builtjes, P. J. H. J. H., van Loon, M., Schaap, M., Teeuwisse, S., Visschedijk, A. J. H., Bloos, J. P. P., Visschedijnk, A. J. H. and Bloos, J. P. P.: Project on the Modelling and Verification of Ozone Reduction Strategies: Contribution of TNO-MEP, Apeldoorn, The Netherlands., 2003.

Butler, T. M., Stock, Z. S., Russo, M. R., Denier van der Gon, H. A. C. and Lawrence, M. G.: Megacity ozone air quality under four alternative future scenarios, Atmos. Chem. Phys., 12(10), 4413–4428, doi:10.5194/acp-12-4413-2012, 2012.

10 Chang, K., Lu, C., Bai, H. and Fang, G. C.: A theoretical evaluation on the HNO_3 artifact of the annular denuder system due to evaporation and diffusional deposition of NH_4NO_3-containing aerosols, Atmos. Environ., 36(27), 4357–4366, doi:10.1016/S1352-2310(02)00352-7, 2002.

Charron, A., Harrison, R. M., Moorcroft, S. and Booker, J.: Quantitative interpretation of divergence between PM10 and PM2.5 mass measurement by TEOM and gravimetric (Partisol) instruments, Atmos. Environ., 38(3), 415–423, 15 doi:10.1016/j.atmosenv.2003.09.072, 2004.

Curci, G., Ferrero, L., Tuccella, P., Barnaba, F., Angelini, F., Bolzacchini, E., Carbone, C., Denier Van Der Gon, H. A. C., Facchini, M. C., Gobbi, G. P., Kuenen, J. P. P., Landi, T. C., Perrino, C., Perrone, M. G., Sangiorgi, G. and Stocchi, P.: How much is particulate matter near the ground influenced by upper-level processes within and above the PBL? A summertime case study in Milan (Italy) evidences the distinctive role of nitrate, Atmos. Chem. Phys., 15(5), 2629–2649, doi:10.5194/acp-20 15-2629-2015, 2015.

Cuvelier, C., Thunis, P., Vautard, R., Amann, M., Bessagnet, B., Bedogni, M., Berkowicz, R., Brandt, J., Brocheton, F., Builtjes, P., Coppalle, A., Denby, B., Douros, G., Graf, A., Hellmuth, O., Honor´e, C., Hodzic, A., Jonson, J., Kerschbaumer, A., Leeuw, F. de, Minguzzi, E., Wind, P. and Zuber, A.: CityDelta: a model intercomparison study to explore the impact of emission reductions in European cities in 2010, Atmos. Env., 41, 189–2007, 2007.

25 Denier van der Gon, H. a. C., Bergström, R., Fountoukis, C., Johansson, C., Pandis, S. N., Simpson, D. and Visschedijk, a. J. H.: Particulate emissions from residential wood combustion in Europe – revised estimates and an evaluation, Atmos. Chem. Phys., 15(11), 6503–6519, doi:10.5194/acp-15-6503-2015, 2015.

Denier van der Gon, H. A. C., Visschedijk, A., Kuenen, J., R van Gijlswijk, C. Schieberle, U. K., Theloke, J. and Friedrich, R.: European Emission baseline (final dataset) for 2005 incl. specific transport emission grids and projection to 2020/30 30 dataset, Deliverable Report D1.3.5; EU FP7 TRANSPHORM (ENV.2009.1.2.2.1 Transport related air pollution and health impacts); revised vers., 2014.

Dentener, F., Kinne, S., Bond, T., Boucher, O., Cofala, J., Generoso, S., Ginoux, P., Gong, S., Hoelzemann, J. J., Ito, A., Marelli, L., Penner, J. E., Putaud, J.-P., Textor, C., Schultz, M. G., van der Werf, G. R. and Wilson, J.: Emissions of primary aerosol and precursor gases in the years 2000 and 1750 prescribed data-sets for AeroCom, Atmos. Chem. Phys., 6, 4321–35 4344 [online] Available from: www.atmos-chem-phys.net/6/4321/2006/, 2006.

Donahue, N. M., Robinson, a. L., Stanier, C. O. and Pandis, S. N.: Coupled partitioning, dilution, and chemical aging of semivolatile organics, Environ. Sci. Technol., 40(8), 2635–2643, doi:10.1021/es052297c, 2006.

Emberson, L. D., Ashmore, M. R., Cambridge, H. M., Simpson, D. and Tuovinen, J.-P.: Modelling stomatal ozone flux across Europe, Environ. Pollut., 109(3), 403–413, doi:10.1016/S0269-7491(00)00043-9, 2000a.

40 Emberson, L. D., Simpson, D., Tuovinen, J., Ashmore, M. R. and Cambridge, H. M.: Towards a model of ozone deposition and stomatal uptake over Europe., 2000b.

EMEP, C.: Manual for Sampling and Chemical Analysis., 2001.

Fiedler, S., Schepanski, K., Heinold, B., Knippertz, P. and Tegen, I.: Climatology of nocturnal low-level jets over North

Africa and implications for modeling mineral dust emission, J. Geophys. Res. Atmos., 118(12), 6100–6121, doi:10.1002/jgrd.50394, 2013.

Foley, K. M., Roselle, S. J., Appel, K. W., Bhave, P. V, Pleim, J. E., Otte, T. L., Mathur, R., Sarwar, G., Young, J. O., Gilliam, R. C. and others: Incremental testing of the Community Multiscale Air Quality (CMAQ) modeling system version 4.7, Geosci. Model Dev., 3(1), 205–226, 2010.

Formenti, P., Schütz, L., Balkanski, Y., Desboeufs, K., Ebert, M., Kandler, K., Petzold, A., Scheuvens, D., Weinbruch, S. and Zhang, D.: Recent progress in understanding physical and chemical properties of African and Asian mineral dust, Atmos. Chem. Phys., 11(16), 8231–8256, doi:10.5194/acp-11-8231-2011, 2011.

Fountoukis, C., Megaritis, A. G., Skyllakou, K., Charalampidis, P. E., Denier van der Gon, H. A. C., Crippa, M., Prévôt, A. S. H., Freutel, F., Wiedensohler, A., Pilinis, C. and Pandis, S. N.: Simulating the formation of carbonaceous aerosol in a European Megacity (Paris) during the MEGAPOLI summer and winter campaigns, Atmos. Chem. Phys. Discuss., 15(18), 25547–25582, doi:10.5194/acpd-15-25547-2015, 2015.

Fountoukis, C. and Nenes, A.: ISORROPIA II : a computationally efficient thermodynamic equilibrium model for K+-Ca2+-Mg2+-NH4+-Na+-SO42--NO3--Cl--H2O aerosols, Atmos. Chem. Phys., 7(17), 4639–4659, 2007.

Friedman, C. L. and Selin, N. E.: Long-range atmospheric transport of polycyclic aromatic hydrocarbons: a global 3-D model analysis including evaluation of Arctic sources., Environ. Sci. Technol., 46(17), 9501–10, doi:10.1021/es301904d, 2012.

Guelle, W., Schulz, M., Balkanski, Y. and Dentener, F.: Influence of the source formulation on modeling the atmospheric global distribution of sea salt aerosol, J. Geophys. Res. Atmos., 106(D21), 27509–27524, 2001.

Hamaoui-Laguel, L., Meleux, F., Beekmann, M., Bessagnet, B., Génermont, S., Cellier, P. and Létinois, L.: Improving ammonia emissions in air quality modelling for France, Atmos. Environ., 92(3), 584–595, doi:10.1016/j.atmosenv.2012.08.002, 2014.

Hass, H., van Loon, M., Kessler, C., Stern, R., Matthijsen, J., S., F. Zlatev, Z., Langner, J., Voltescu, V. and Schaap, M.: Aerosol modeling: results and intercomparison from European regional-scale modeling systems. A contribution to the EUROTRAC-2 subproject GLOREAM., , (JANUARY), 2003.

Hauck, H., Berner, A., Gomiscek, B., Stopper, S., Puxbaum, H., Kundi, M. and Preining, O.: On the equivalence of gravimetric PM data with TEOM and beta-attenuation measurements, J. Aerosol Sci., 35(9), 1135–1149, doi:10.1016/j.jaerosci.2004.04.004, 2004.

Hendriks, C., Kranenburg, R., Kuenen, J. J. P., Van den Bril, B., Verguts, V. and Schaap, M.: Ammonia emission time profiles based on manure transport data improve ammonia modelling across north western Europe, Atmos. Environ., 131, 83–96, doi:10.1016/j.atmosenv.2016.01.043, 2016.

Huijnen, V., Eskes, H. J., Poupkou, A., Elbern, H., Boersma, K. F., Foret, G., Sofiev, M., Valdebenito, A., Flemming, J., Stein, O., Gross, A., Robertson, L., D'Isidoro, M., Kioutsioukis, I., Friese, E., Amstrup, B., Bergstrom, R., Strunk, A., Vira, J., Zyryanov, D., Maurizi, A., Melas, D., Peuch, V.-H. and Zerefos, C.: Comparison of OMI NO2 tropospheric columns with an ensemble of global and European regional air quality models, Atmos. Chem. Phys., 10(7), 3273–3296, 2010.

Hummel, M., Hoose, C., Gallagher, M., Healy, D. a., Huffman, J. a., O'Connor, D., Pöschl, U., Pöhlker, C., Robinson, N. H., Schnaiter, M., Sodeau, J. R., Toprak, E. and Vogel, H.: Regional-scale simulations of fungal spore aerosols using an emission parameterization adapted to local measurements of fluorescent biological aerosol particles, Atmos. Chem. Phys. Discuss., 14(7), 9903–9950, doi:10.5194/acpd-14-9903-2014, 2014.

Im, U., Bianconi, R., Solazzo, E., Kioutsioukis, I., Badia, A., Balzarini, A., Baró, R., Bellasio, R., Brunner, D., Chemel, C., Curci, G., Denier van der Gon, H., Flemming, J., Forkel, R., Giordano, L., Jiménez-Guerrero, P., Hirtl, M., Hodzic, A., Honzak, L., Jorba, O., Knote, C., Makar, P. a., Manders-Groot, A., Neal, L., Pérez, J. L., Pirovano, G., Pouliot, G., San Jose, R., Savage, N., Schroder, W., Sokhi, R. S., Syrakov, D., Torian, A., Tuccella, P., Wang, K., Werhahn, J., Wolke, R., Zabkar, R., Zhang, Y., Zhang, J., Hogrefe, C. and Galmarini, S.: Evaluation of operational online-coupled regional air quality models

over Europe and North America in the context of AQMEII phase 2. Part II: Particulate matter, Atmos. Environ., doi:10.1016/j.atmosenv.2014.08.072, 2014.

IPCC: Climate Change 2013: The Physical Science Basis. Contribution of Working Group I to the Fifth Assessment Report of the Intergovernmental Panel on Climate Change [Stocker, T.F., D. Qin, G.-K. Plattner, M. Tignor, S.K. Allen, J.
5   Boschung, A. Nauels, Y. Xia, Cambridge University Press, Cambridge, United Kingdom and New York, NY, USA., 2013.

Jing, B., Tong, S. R., Liu, Q. F., Li, K., Wang, W. G., Zhang, Y. H. and Ge, M. F.: Hygroscopic behavior of multicomponent organic aerosols and their internal mixtures with ammonium sulfate, Atmos. Chem. Phys. Discuss., 15, 23357–23405, doi:10.5194/acpd-15-23357-2015, 2015.

Jöckel, P., Tost, H., Pozzer, A., Brühl, C., Buchholz, J., Ganzeveld, L., Hoor, P., Kerkweg, A., Lawrence, M. G., Sander, R.,
10   Steil, B., Stiller, G., Tanarhte, M., Taraborrelli, D., Van Aardenne, J. and Lelieveld, J.: The atmospheric chemistry general circulation model ECHAM5/MESSy1: consistent simulation of ozone from the surface to the mesosphere, Atmos. Chem. Phys. Discuss., 6(4), 6957–7050 [online] Available from: http://hal.archives-ouvertes.fr/hal-00302020 (Accessed 5 September 2014), 2006.

Karvosenoja, N., Kangas, L., Kupiainen, K., Kukkonen, J., Karppinen, A., Sofiev, M., Tainio, M., Paunu, V.-V., Ahtoniemi,
15   P., Tuomisto, J.-T. and Porvari, P.: Integrated modeling assessments of the population exposure in Finland to primary PM2.5 from traffic and domestic wood combustion on the resolutions of 1 and 10 km, Air Qual. Atmos. Heal., doi:DOI 10.1007/s11869-010-0100-9, 2011.

Kerkweg, A., Buchholz, J., Ganzeveld, L., Pozzer, A., Tost, H. and Jöckel, P.: Technical Note: an implementation of the dry removal processes DRY DEPosition and SEDImentation in the Modular Earth Submodel System (MESSy), Atmos. Chem.
20   Phys., 6(12), 4617–4632, 2006.

Kim, D., Chin, M., Yu, H., Diehl, T., Tan, Q., Kahn, R. a., Tsigaridis, K., Bauer, S. E., Takemura, T., Pozzoli, L., Bellouin, N., Schulz, M., Peyridieu, S., Chédin, A. and Koffi, B.: Sources, sinks, and transatlantic transport of North African dust aerosol: A multimodel analysis and comparison with remote sensing data, J. Geophys. Res. Atmos., n/a–n/a, doi:10.1002/2013JD021099, 2014.

25   Koeble, R. and Seufert, G.: Novel maps for forest tree species in Europe, in Proceedings of the 8th European Symposium on the Physico-Chemical Behaviour of Air Pollutants: "A Changing Atmosphere!", Sept 17-20, 2001, Torino, Italy., 2001.

Kouznetsov, R. and Sofiev, M.: A methodology for evaluation of vertical dispersion and dry deposition of atmospheric aerosols, J. Geophys. Res., 117(D01202), doi:doi:10.1029/2011JD016366, 2012.

Kuenen, J. J. P., Visschedijk, a. J. H., Jozwicka, M. and Denier van der Gon, H. a. C.: TNO-MACC_II emission inventory: a
30   multi-year (2003–2009) consistent high-resolution European emission inventory for air quality modelling, Atmos. Chem. Phys. Discuss., 14(5), 5837–5869, doi:10.5194/acpd-14-5837-2014, 2014.

von Kuhlmann, R., Lawrence, M. G., Crutzen, P. J. and Rasch, P. J.: A model for studies of tropospheric ozone and nonmethane hydrocarbons: Model evaluation of ozone-related species, J. Geophys. Res. Atmos., 108(D23), 2003.

Kukkonen, J., Olsson, T., Schultz, D. M., Baklanov, a., Klein, T., Miranda, a. I., Monteiro, a., Hirtl, M., Tarvainen, V.,
35   Boy, M., Peuch, V.-H., Poupkou, a., Kioutsioukis, I., Finardi, S., Sofiev, M., Sokhi, R., Lehtinen, K. E. J., Karatzas, K., San José, R., Astitha, M., Kallos, G., Schaap, M., Reimer, E., Jakobs, H. and Eben, K.: A review of operational, regional-scale, chemical weather forecasting models in Europe, Atmos. Chem. Phys., 12(1), 1–87, doi:10.5194/acp-12-1-2012, 2012.

Lamarque, J.-F., Bond, T. C., Eyring, V., Granier, C., Heil, A., Klimont, Z., Lee, D., Liousse, C., Mieville, A., Owen, B. and others: Historical (1850--2000) gridded anthropogenic and biomass burning emissions of reactive gases and aerosols:
40   methodology and application, Atmos. Chem. Phys., 10(15), 7017–7039, 2010.

Larson, T. . and Koenig, J. .: A summary of the emissions characterization and noncancer respiratory effects of wood smoke, EPA-453/R-93-036., 1993.

Lauer, A., Eyring, V., Hendricks, J., Jöckel, P. and Lohmann, U.: Global model simulations of the impact of ocean-going

ships on aerosols, clouds, and the radiation budget, Atmos. Chem. Phys., 7(19), 5061–5079, doi:10.5194/acp-7-5061-2007, 2007.

Lauer, A., Hendricks, J., Ackermann, I., Schell, B., Hass, H. and Metzger, S.: Simulating aerosol microphysics with the ECHAM/MADE GCM--Part I: Model description and comparison with observations, Atmos. Chem. Phys., 5(12), 3251–
3276, 2005.

Laurent, B., Marticorena, B., Bergametti, G., Leon, J. F. and Mahowald, N. M.: Modeling mineral dust emissions from the Sahara desert using new surface properties and soil database, J. Geophys. Res. Atmos., 113(14), 1–20, doi:10.1029/2007JD009484, 2008.

Lawrence, M. G., Crutzen, P. J., Rasch, P. J., Eaton, B. E. and Mahowald, N. M.: A model for studies of tropospheric photochemistry: Description, global distributions, and evaluation, J. Geophys. Res. Atmos., 104(D21), 26245–26277, 1999.

Lee, D. S. and Pacyna, J. M.: An industrial emissions inventory of calcium for Europe, Atmos. Environ., 33(11), 1687–1697, doi:10.1016/S1352-2310(98)00286-6, 1999.

Lefebvre, W., Fierens, F., Vanpoucke, C., Renders, N., Jespers, K., Vercauteren, J., Deutsch, F. and Janssen, S.: The Effect of Wood Burning on Particulate Matter Concentrations in Flanders, Belgium, in Air Pollution Modeling and its Application XXIV, edited by D. G. Steyn and N. Chaumerliac, pp. 459–464, Springer, Switzerland., 2016.

Lim, S. S., Vos, T., Flaxman, A. D., Danaei, G., Shibuya, K., Adair-Rohani, H., Amann, M., Anderson, H. R., Andrews, K. G., Aryee, M., Atkinson, C., Bacchus, L. J., Bahalim, A. N., Balakrishnan, K., Balmes, J., Barker-Collo, S., Baxter, A., Bell, M. L., Blore, J. D., Blyth, F., Bonner, C., Borges, G., Bourne, R., Boussinesq, M., Brauer, M., Brooks, P., Bruce, N. G., Brunekreef, B., Bryan-Hancock, C., Bucello, C., Buchbinder, R., Bull, F., Burnett, R. T., Byers, T. E., Calabria, B., Carapetis, J., Carnahan, E., Chafe, Z., Charlson, F., Chen, H., Chen, J. S., Cheng, A. T.-A., Child, J. C., Cohen, A., Colson, K. E., Cowie, B. C., Darby, S., Darling, S., Davis, A., Degenhardt, L., Dentener, F., Des Jarlais, D. C., Devries, K., Dherani, M., Ding, E. L., Dorsey, E. R., Driscoll, T., Edmond, K., Ali, S. E., Engell, R. E., Erwin, P. J., Fahimi, S., Falder, G., Farzadfar, F., Ferrari, A., Finucane, M. M., Flaxman, S., Fowkes, F. G. R., Freedman, G., Freeman, M. K., Gakidou, E., Ghosh, S., Giovannucci, E., Gmel, G., Graham, K., Grainger, R., Grant, B., Gunnell, D., Gutierrez, H. R., Hall, W., Hoek, H. W., Hogan, A., Hosgood, H. D., Hoy, D., Hu, H., Hubbell, B. J., Hutchings, S. J., Ibeanusi, S. E., Jacklyn, G. L., Jasrasaria, R., Jonas, J. B., Kan, H., Kanis, J. A., Kassebaum, N., Kawakami, N., Khang, Y.-H., Khatibzadeh, S., Khoo, J.-P., Kok, C., et al.: A comparative risk assessment of burden of disease and injury attributable to 67 risk factors and risk factor clusters in 21 regions, 1990-2010: a systematic analysis for the Global Burden of Disease Study 2010., Lancet, 380(9859), 2224–60, doi:10.1016/S0140-6736(12)61766-8, 2012.

Lohmann, U.: Possible Aerosol Effects on Ice Clouds via Contact Nucleation, J. Atmos. Sci., 59(3), 647–656, doi:10.1175/1520-0469(2001)059<0647:PAEOIC>2.0.CO;2, 2002.

Lohmann, U., Feichter, J., Chuang, C. C. and Penner, J. E.: Prediction of the number of cloud droplets in the ECHAM GCM, J. Geophys. Res. Atmos., 104(D8), 9169–9198, 1999.

Loomis, D., Grosse, Y., Lauby-Secretan, B., Ghissassi, F. El, Bouvard, V., Benbrahim-Tallaa, L., Guha, N., Baan, R., Mattock, H. and Straif, K.: The carcinogenicity of outdoor air pollution, Lancet Oncol., 14(13), 1262–1263, doi:10.1016/S1470-2045(13)70487-X, 2013.

van Loon, M., Tarrasson, L. and Posch, M.: Modelling Base Cations in Europe. [online] Available from: http://emep.int/publ/reports/2005/emep_technical_2_2005.pdf, 2005.

Marconi, M., Sferlazzo, D. M., Becagli, S., Bommarito, C., Calzolai, G., Chiari, M., Di Sarra, a., Ghedini, C., Gómez-Amo, J. L., Lucarelli, F., Meloni, D., Monteleone, F., Nava, S., Pace, G., Piacentino, S., Rugi, F., Severi, M., Traversi, R. and Udisti, R.: Saharan dust aerosol over the central Mediterranean Sea: PM10 chemical composition and concentration versus optical columnar measurements, Atmos. Chem. Phys., 14, 2039–2054, doi:10.5194/acp-14-2039-2014, 2014.

Mårtensson, E. M., Nilson, E. D., de Leeuw, G., Cohen, L. H. and Hansson, H.-C.: Laboratory simulations and parameterization of the primary marine aerosol production, J. Geophys. Res., 108(D9), 1–12, doi:10.1029/2002JD002263,

2003.

Martin, S. T.: Phase Transitions of Aqueous Atmospheric Particles, Chem. Rev., 100(9), 3403–3454, doi:10.1021/cr990034t, 2000.

Matthias, V., Aulinger, A. and Quante, M.: CMAQ simulations of the benzo(a)pyrene distribution over Europe for 2000 and 2001, Atmos. Environ., 43(26), 4078–4086, doi:10.1016/j.atmosenv.2009.04.058, 2009.

Metzger, S., Dentener, F., Pandis, S. and Lelieveld, J.: Gas/aerosol partitioning: 1. A computationally efficient model, J. Geophys. Res., 107(D16), 4312, doi:10.1029/2001JD001102, 2002.

Monahan, E. C., Spiel, D. E. and Davidson, K. L.: A model of marine aerosol generation via whitecaps and wave disruption, in Oceanic whitecaps, edited by E. C. Monahan and G. Mac Niocell, pp. 167–174, D. Reidel Publishing., 1986.

Ots, R., Young, D. E., Vieno, M., Xu, L., Dunmore, R. E., Allan, J. D., Coe, H., Williams, L. R., Herndon, S. C., Ng, N. L., Hamilton, J. F., Bergström, R., Di Marco, C., Nemitz, E., Mackenzie11, I. A., Kuenen, J. J. P., Green, D. C., Reis, S. and Heal, M. R.: Simulating secondary organic aerosol from missing diesel-related intermediate-volatility organic compound emissions during the Clean Air for London (ClearfLo) campaign, Atmos. Chem. Phys. Discuss., (in review), doi:10.5194/acp-2015-920, 2016.

Otte, T. L., Pouliot, G., Pleim, J. E., Young, J. O., Schere, K. L., Wong, D. C., Lee, P. C. S., Tsidulko, M., McQueen, J. T., Davidson, P., Mathur, R., Chuang, H.-Y., DiMego, G. and Seaman, N. L.: Linking the Eta Model with the Community Multiscale Air Quality (CMAQ) Modeling System to Build a National Air Quality Forecasting System, Weather Forecast., 20(3), 367–384, doi:10.1175/WAF855.1, 2005.

Perez, L., Tobias, A., Querol, X., Künzli, N., Pey, J., Alastuey, A., Viana, M., Valero, N., González-Cabré, M. and Sunyer, J.: Coarse particles from Saharan dust and daily mortality., Epidemiology, 19(6), 800–807, doi:10.1097/EDE.0b013e31818131cf, 2008.

Perez, L., Tobías, A., Querol, X., Pey, J., Alastuey, A., Díaz, J. and Sunyer, J.: Saharan dust, particulate matter and cause-specific mortality: a case-crossover study in Barcelona (Spain)., Environ. Int., 48, 150–5, doi:10.1016/j.envint.2012.07.001, 2012.

Putaud, J.-P., Van Dingenen, R., Alastuey, A., Bauer, H., Birmili, W., Cyrys, J., Flentje, H., Fuzzi, S., Gehrig, R., Hansson, H. C., Harrison, R. M., Herrmann, H., Hitzenberger, R., Hüglin, C., Jones, A. M., Kasper-Giebl, A., Kiss, G., Kousa, A., Kuhlbusch, T. a. J., Löschau, G., Maenhaut, W., Molnar, A., Moreno, T., Pekkanen, J., Perrino, C., Pitz, M., Puxbaum, H., Querol, X., Rodriguez, S., Salma, I., Schwarz, J., Smolik, J., Schneider, J., Spindler, G., ten Brink, H., Tursic, J., Viana, M., Wiedensohler, A. and Raes, F.: A European aerosol phenomenology – 3: Physical and chemical characteristics of particulate matter from 60 rural, urban, and kerbside sites across Europe, Atmos. Environ., 44(10), 1308–1320, doi:10.1016/j.atmosenv.2009.12.011, 2010.

Putaud, J.-P., Van Dingenen, R., Dell'Acqua, A., Raes, F., Matta, E., Decesari, S., Facchini, M. C. and Fuzzi, S.: Size-segregated aerosol mass closure and chemical composition in Monte Cimone (I) during MINATROC, Atmos. Chem. Phys., 4, 889–902, doi:10.5194/acpd-3-4097-2003, 2004a.

Putaud, J.-P., Raes, F., Van Dingenen, R., Brüggemann, E., Facchini, M.-C., Decesari, S., Fuzzi, S., Gehrig, R., Hüglin, C., Laj, P., Lorbeer, G., Maenhaut, W., Mihalopoulos, N., Müller, K., Querol, X., Rodriguez, S., Schneider, J., Spindler, G., Brink, H. Ten, Tørseth, K. and Wiedensohler, A.: A European aerosol phenomenology—2: chemical characteristics of particulate matter at kerbside, urban, rural and background sites in Europe, Atmos. Environ., 38(16), 2579–2595, doi:10.1016/j.atmosenv.2004.01.041, 2004b.

Querol, X., Alastuey, A., Ruiz, C. R., Artiñano, B., Hansson, H. C., Harrison, R. M., Buringh, E., ten Brink, H. M., Lutz, M., Bruckmann, P., Straehl, P. and Schneider, J.: Speciation and origin of PM10 and PM2.5 in selected European cities, Atmos. Environ., 38(38), 6547–6555, doi:10.1016/j.atmosenv.2004.08.037, 2004.

Reponen, T., Grinshpun, S. a., Conwell, K. L., Wiest, J. and Anderson, M.: Aerodynamic versus physical size of spores: Measurement and implication for respiratory deposition, Grana, 40(3), 119–125, doi:10.1080/00173130152625851, 2001.

Righi, M., Hendricks, J. and Sausen, R.: The global impact of the transport sectors on atmospheric aerosol: simulations for year 2000 emissions, Atmos. Chem. Phys., 13(19), 9939–9970, 2013.

Robinson, A. L., Donahue, N. M., Shrivastava, M. K., Weitkamp, E. a, Sage, A. M., Grieshop, A. P., Lane, T. E., Pierce, J. R. and Pandis, S. N.: Rethinking Organic Aerosols : Semivolatile Emissions and Photochemical Aging, Science (80-.)., 315, 1259–1262, doi:10.1126/science.1133061, 2007.

Roeckner, E., Brokopf, R., Esch, M., Giorgetta, M., Hagemann, S., Kornblueh, L., Manzini, E., Schlese, U. and Schulzweida, U.: Sensitivity of Simulated Climate to Horizontal and Vertical Resolution in the ECHAM5 Atmosphere Model, J. Clim., 19(16), 3771–3791, doi:10.1175/JCLI3824.1, 2006.

Samset, B. H., Myhre, G., Herber, A., Kondo, Y., Li, S. M., Moteki, N., Koike, M., Oshima, N., Schwarz, J. P., Balkanski, Y., Bauer, S. E., Bellouin, N., Berntsen, T. K., Bian, H., Chin, M., Diehl, T., Easter, R. C., Ghan, S. J., Iversen, T., Kirkevag, A., Lamarque, J. F., Lin, G., Liu, X., Penner, J. E., Schulz, M., Seland, Skeie, R. B., Stier, P., Takemura, T., Tsigaridis, K. and Zhang, K.: Modelled black carbon radiative forcing and atmospheric lifetime in AeroCom Phase II constrained by aircraft observations, Atmos. Chem. Phys., 14(22), 12465–12477, doi:10.5194/acp-14-12465-2014, 2014.

Sander, R., Kerkweg, A., Jöckel, P. and Lelieveld, J.: Technical note: The new comprehensive atmospheric chemistry module MECCA, Atmos. Chem. Phys., 5(2), 445–450, 2005.

Schaap, M., Denier Van Der Gon, H. A. C., Dentener, F. J., Visschedijk, A. J. H., Van Loon, M., Ten Brink, H. M., Putaud, J.-P., Guillaume, B., C., L. and Builtjes, P. J. .: Anthropogenic black carbon and fine aerosol distribution over Europe, J. Geophys. Res., 109(D18), D18207, doi:10.1029/2003JD004330, 2004a.

Schaap, M., Loon, M. Van, Brink, H. M., Dentener, F. J. and Builtjes, P. J. H.: Secondary inorganic aerosol simulations for Europe with special attention to nitrate, Atmos. Chem. Phys., 4, 857–874, 2004b.

Schaap, M., Manders, A. A. M., Hendriks, E. C. J., Cnossen, J. M., Segers, A. J. S., Denier van der Gon, H. A. C., Jozwicka, M., Sauter, F. J., Velders, G. J. M., Matthijsen, J. and Builtjes, P. J. H.: Regional Modelling of Particulate Matter for the Netherlands, Bilthoven, The Netherlands. [online] Available from: http://www.rivm.nl/bibliotheek/rapporten/500099008.pdf (Accessed 5 September 2014), 2009.

Schaap, M., Otjes, R. P. and Weijers, E. P.: Illustrating the benefit of using hourly monitoring data on secondary inorganic aerosol and its precursors for model evaluation, Atmos. Chem. Phys., 11(21), 11041–11053, doi:10.5194/acp-11-11041-2011, 2011.

Schaap, M., Timmermans, R. M. A., Roemer, M., Boersen, G. A. C., Builtjes, P. J. H., Sauter, F. J., Velders, G. J. M. and Beck, J. P.: The LOTOS-EUROS model: Description, validation and latest developments, Int. J. Environ. Pollut., 32, 270–290, 2008.

Seinfeld, J. H. and Pandis, S. N.: Atmospheric chemistry and physics. From air pollution to climate change, 2nd ed., John Wiley & sons, Inc, Hoboken, New Jersey., 2006.

Shrivastava, M., Fast, J., Easter, R., Gustafson, W. I., Zaveri, R. a., Jimenez, J. L., Saide, P. and Hodzic, a.: Modeling organic aerosols in a megacity: comparison of simple and complex representations of the volatility basis set approach, Atmos. Chem. Phys., 11(13), 6639–6662, doi:10.5194/acp-11-6639-2011, 2011.

Sillanpää, M., Hillamo, R., Saarikoski, S., Frey, A., Pennanen, A., Makkonen, U., Spolnik, Z., Van Grieken, R., Braniš, M. and Brunekreef, B.: Chemical composition and mass closure of particulate matter at six urban sites in Europe, Atmos. Environ., 40, 212–223, doi:10.1016/j.atmosenv.2006.01.063, 2006.

Simpson, D., Benedictow, a., Berge, H., Bergström, R., Emberson, L. D., Fagerli, H., Flechard, C. R., Hayman, G. D., Gauss, M., Jonson, J. E., Jenkin, M. E., Nyíri, a., Richter, C., Semeena, V. S., Tsyro, S., Tuovinen, J.-P., Valdebenito, Á. and Wind, P.: The EMEP MSC-W chemical transport model – technical description, Atmos. Chem. Phys., 12(16), 7825–7865, doi:10.5194/acp-12-7825-2012, 2012.

Simpson, D., Fagerli, H., Jonson, J. E., Tsyro, S., Wind, P. and Tuovinen, F. M. I. J.-P.: PART I Unified EMEP Model

Description., Oslo, Norway. [online] Available from: http://emep.int/publ/reports/2003/emep_report_1_part1_2003.pdf (Accessed 5 September 2014), 2003.

Simpson, D., Yttri, K. E., Klimont, Z., Kupiainen, K., Caseiro, A., Gelencsér, A., Pio, C., Puxbaum, H. and Legrand, M.: Modeling carbonaceous aerosol over Europe: Analysis of the CARBOSOL and EMEP EC/OC campaigns, J. Geophys. Res., 112(D23S14), doi:doi:10.1029/2006JD008158, 2007.

Skamarock, W. C., Klemp, J. B., Dudhia, J., Gill, D. O., Barker, D. M., Duda, M. G., Huang, X.-Y., Wang, W. and Powers, J. G.: A description of the advanced research WRF version 3, NCAR Tech. note, 113, 2008.

Soares, J., Sofiev, M. and Hakkarainen, J.: Uncertainties of wild-land fi res emission in AQMEII phase 2 case study, Atmos. Environ., doi:10.1016/j.atmosenv.2015.01.068, 2015.

Sofiev, M.: A model for the evaluation of long-term airborne pollution transport at regional and continental scales, Atmos. Environ., 34(15), 2481–2493, doi:10.1016/S1352-2310(99)00415-X, 2000.

Sofiev, M.: Extended resistance analogy for construction of the vertical diffusion scheme for dispersion models, J. Geophys. Res., 107(D12), doi:10.1029/2001JD001233, 2002.

Sofiev, M., Ermakova, T. and Vankevich, R.: Evaluation of the smoke-injection height from wild-land fires using remote-sensing data, Atmos. Chem. Phys., 12(4), 1995–2006, doi:10.5194/acp-12-1995-2012, 2012.

Sofiev, M., Genikhovich, E., Keronen, P. and Vesala, T.: Diagnosing the Surface Layer Parameters for Dispersion Models within the Meteorological-to-Dispersion Modeling Interface, J. Appl. Meteorol. Climatol., 49(2), 221–233, doi:10.1175/2009JAMC2210.1, 2010.

Sofiev, M., Soares, J., Prank, M., de Leeuw, G. and Kukkonen, J.: A regional-to-global model of emission and transport of sea salt particles in the atmosphere, J. Geophys. Res., 116(D21302), 25, doi:10.1029/2010JD014713, 2011.

Sofiev, M., Vankevich, R., Lotjonen, M., Prank, M., Petukhov, V., Ermakova, T., Koskinen, J. and Kukkonen, J.: An operational system for the assimilation of the satellite information on wild-land fires for the needs of air quality modelling and forecasting, Atmos. Chem. Phys., 9(18), 6833–6847, doi:10.5194/acpd-9-6483-2009, 2009.

Sofiev, M., Vira, J., Kouznetsov, R., Prank, M., Soares, J. and Genikhovich, E.: Construction of an Eulerian atmospheric dispersion model based on the advection algorithm of M. Galperin: dynamic cores v.4 and 5 of SILAM v.5.5, Geosci. Model Dev. Discuss., 8(1), 1–43, doi:10.5194/gmdd-8-1-2015, 2015.

Solazzo, E., Bianconi, R., Pirovano, G., Matthias, V., Vautard, R., Moran, M. D., Wyat Appel, K., Bessagnet, B., Brandt, J., Christensen, J. H., Chemel, C., Coll, I., Ferreira, J., Forkel, R., Francis, X. V., Grell, G., Grossi, P., Hansen, A. B., Miranda, A. I., Nopmongcol, U., Prank, M., Sartelet, K. N., Schaap, M., Silver, J. D., Sokhi, R. S., Vira, J., Werhahn, J., Wolke, R., Yarwood, G., Zhang, J., Rao, S. T. and Galmarini, S.: Operational model evaluation for particulate matter in Europe and North America in the context of AQMEII, Atmos. Environ., 53, 75–92, doi:10.1016/j.atmosenv.2012.02.045, 2012a.

Solazzo, E., Bianconi, R., Vautard, R., Appel, K. W., Moran, M. D., Hogrefe, C., Bessagnet, B., Brandt, J., Christensen, J. H., Chemel, C., Coll, I., Denier van der Gon, H., Ferreira, J., Forkel, R., Francis, X. V., Grell, G., Grossi, P., Hansen, A. B., Jeričević, A., Kraljević, L., Miranda, A. I., Nopmongcol, U., Pirovano, G., Prank, M., Riccio, A., Sartelet, K. N., Schaap, M., Silver, J. D., Sokhi, R. S., Vira, J., Werhahn, J., Wolke, R., Yarwood, G., Zhang, J., Rao, S. T. and Galmarini, S.: Model evaluation and ensemble modelling of surface-level ozone in Europe and North America in the context of AQMEII, Atmos. Environ., 53, 60–74, doi:10.1016/j.atmosenv.2012.01.003, 2012b.

Spicer, C. W., Chapman, E. G., Finlayson-Pitts, B. J., Plastridge, R. A., Hubbe, J. M., Fast, J. D. and Berkowitz, C. M.: Unexpectedly high concentrations of molecular chlorine in coastal air, , 394(6691), 353–356, doi:10.1038/28584, 1998.

Stanek, L. W., Sacks, J. D., Dutton, S. J. and Dubois, J.-J. B.: Attributing health effects to apportioned components and sources of particulate matter: An evaluation of collective results, Atmos. Environ., 45(32), 5655–5663, doi:10.1016/j.atmosenv.2011.07.023, 2011.

Stern, R., Builtjes, P., Schaap, M., Timmermans, R., Vautard, R., Hodzic, a., Memmesheimer, M., Feldmann, H., Renner, E.

and Wolke, R.: A model inter-comparison study focussing on episodes with elevated PM10 concentrations, Atmos. Environ., 42(19), 4567–4588, doi:10.1016/j.atmosenv.2008.01.068, 2008.

Tainio, M., Sofiev, M., Hujo, M., Tuomisto, J. T., Loh, M., Jantunen, M. J., Karppinen, A., Kangas, L., Karvosenoja, N., Kupiainen, K., Porvari, P. and Kukkonen, J.: Evaluation of the European population intake fractions for European and Finnish anthropogenic primary fine particulate matter emissions, Atmos. Environ., 43(19), 3052–3059, doi:10.1016/j.atmosenv.2009.03.030, 2009.

Tainio, M., Tuomisto, J. T., Pekkanen, J., Karvosenoja, N., Kupiainen, K., Porvari, P., Sofiev, M., Karppinen, A., Kangas, L. and Kukkonen, J.: Uncertainty in health risks due to anthropogenic primary fine particulate matter from different source types in Finland, Atmos. Environ., 44(17), 2125–2132, doi:10.1016/j.atmosenv.2010.02.036, 2010.

Tost, H., Jöckel, P., Kerkweg, A., Sander, R. and Lelieveld, J.: Technical note: A new comprehensive SCAVenging submodel for global atmospheric chemistry modelling, Atmos. Chem. Phys., 6(3), 565–574, doi:10.5194/acp-6-565-2006, 2006.

Tsyro, S.: To what extent can aerosol water explain the discrepancy between model calculated and gravimetric PM 10 and PM 2.5?, Atmos. Chem. Phys., 5, 515–532 [online] Available from: http://www.atmos-chem-phys.net/5/515/2005/acp-5-515-2005.html (Accessed 17 July 2014), 2005.

Tsyro, S., Aas, W., Soares, J., Sofiev, M., Berge, H. and Spindler, G.: Modelling of sea salt concentrations over Europe: Key uncertainties and comparison with observations, Atmos. Chem. Phys., 11(20), 10367–10388, doi:10.5194/acp-11-10367-2011, 2011.

Tsyro, S., Simpson, D., Tarrasón, L., Klimont, Z., Kupiainen, K., Pio, C. and Yttri, K. E.: Modeling of elemental carbon over Europe, J. Geophys. Res., 112(D23S19), doi:doi:10.1029/2006JD008164, 2007.

Turpin, B. J. and Lim, H.-J.: Species Contributions to PM2.5 Mass Concentrations: Revisiting Common Assumptions for Estimating Organic Mass, Aerosol Sci. Technol., 35(1), 602–610, doi:10.1080/02786820119445, 2001.

Vautard, R., Builtjes, P. H. J., Thunis, P., Cuvelier, C., Bedogni, M., Bessagnet, B., Honoré, C., Moussiopoulos, N., Pirovano, G., Schaap, M., Stern, R., Tarrason, L. and Wind, P.: Evaluation and intercomparison of Ozone and PM10 simulations by several chemistry transport models over four European cities within the CityDelta project, Atmos. Environ., 41(1), 173–188, doi:10.1016/j.atmosenv.2006.07.039, 2007.

van Vuuren, D. P., Edmonds, J., Kainuma, M., Riahi, K., Thomson, A., Hibbard, K., Hurtt, G. C., Kram, T., Krey, V., Lamarque, J.-F., Masui, T., Meinshausen, M., Nakicenovic, N., Smith, S. J. and Rose, S. K.: The representative concentration pathways: an overview, Clim. Change, 109(1-2), 5–31, doi:10.1007/s10584-011-0148-z, 2011.

Walcek, C. J.: Minor flux adjustment near mixing ratio extremes for simplified yet highly accurate monotonic calculation of tracer advection, J. Geophys. Res., 105(D7), 9335, doi:10.1029/1999JD901142, 2000.

Wang, X., Heald, C. L., Ridley, D. A., Schwarz, J. P., Spackman, J. R., Perring, A. E., Coe, H., Liu, D. and Clarke, A. D.: Exploiting simultaneous observational constraints on mass and absorption to estimate the global direct radiative forcing of black carbon and brown carbon, Atmos. Chem. Phys., 14(20), 10989–11010, doi:10.5194/acp-14-10989-2014, 2014.

van der Werf, G. R., Randerson, J. T., Giglio, L., Collatz, G. J., Mu, M., Kasibhatla, P. S., Morton, D. C., DeFries, R. S., Jin, Y. and van Leeuwen, T. T.: Global fire emissions and the contribution of deforestation, savanna, forest, agricultural, and peat fires (1997–2009), Atmos. Chem. Phys., 10(23), 11707–11735, doi:10.5194/acp-10-11707-2010, 2010.

Whitten, G. Z., Hogo, H. and Killus, J. P.: The carbon-bond mechanism: a condensed kinetic mechanism for photochemical smog., Environ. Sci. Technol., 14(6), 690–700, doi:10.1021/es60166a008, 1980.

Wichink Kruit, R., Schaap, M., Sauter, F., Van der Swaluw, E. and Weijers, E.: Improving the understanding of the secondary inorganic aerosol distribution over the Netherlands, Utrecht., 2012.

Winiwarter, W., Bauer, H., Caseiro, a. and Puxbaum, H.: Quantifying emissions of primary biological aerosol particle mass in Europe, Atmos. Environ., 43(7), 1403–1409, doi:10.1016/j.atmosenv.2008.01.037, 2009.

Young, D. E., Allan, J. D., Williams, P. I., Green, D. C., Flynn, M. J., Harrison, R. M., Yin, J., Gallagher, M. W. and Coe, H.: Investigating the annual behaviour of submicron secondary inorganic and organic aerosols in London, Atmos. Chem. Phys., 15, 6315–6366, doi:10.5194/acpd-14-18739-2014, 2015.

Yttri, K.-E., Aas, W., Tarrasón, L., Vestreng, V., Tsyro, S., Simpson, D., Putaud, J. P. and Cavalli, F.: Transboundary particulate matter in Europe. Status report 2007., 2007.

Van Zanten, M. C., Sauter, F. J., Wichink Kruit, R. J., Van Jaarsveld, J. A. and Van Pul, W. A. J.: Description of the DEPAC module: Dry deposition modelling with DEPAC_GCN2010, Bilthoven, the Netherlands., 2010.

Zhang, L., Gong, S., Padro, J. and Barrie, L.: A size-segregated particle dry deposition scheme for an atmospheric aerosol module, Atmos. Environ., 35(3), 549–560, doi:10.1016/S1352-2310(00)00326-5, 2001.

5

10

Table 1 Model setup

Model	CMAQ v4.7.1	EMEP/MSC-W rv. 4.4	LOTOS-EUROS v1.8	SILAM v5.3
Horizontal resolution	18 km	$0.2° \times 0.2°$	$0.3° \times 0.2°$	$0.3° \times 0.2°$
Vertical resolution	34 layers up to ~20 km; lowest layer ~20m	20 layers up to 100 hPa; lowest layer ~ 90m; 3m concentrations derived from the lowest layer values	3 layers up to 3.5 km; lowest the mixing layer; 25m surface layer for tracking surface concentrations	8 layers up to ~8km; lowest layer 20 m
Meteo driver	WRF v3.2.1	ECMWF	ECMWF	ECMWF
Chemistry scheme	CB05	EMEP EmChem09 (Simpson et al., 2012)	TNO CBM-IV	DMAT (Sofiev, 2000)
Aerosol scheme	aero5	EMEPMARS and VBS (Bergström et al., 2012)	ISORROPIA2	Extended DMAT (Sofiev, 2000)
Temporal emission profiles	(Builtjes et al., 2003)	(Simpson et al., 2012)	(Builtjes et al., 2003)	EuroDelta
Vertical emission profiles	SMOKE plume rise based on (Briggs, 1971)	(Simpson et al., 2012)	EURODELTA (Cuvelier et al., 2007)	(Bieser et al., 2011)
Sea salt emission	(Spicer et al., 1998).	(Tsyro et al., 2011)	Mårtensson et al., 2003; Monahan et al., 1986	(Sofiev et al., 2011)
Reference	(Foley et al., 2010)	(Simpson et al., 2012)	(Schaap et al., 2008, Wichink Kruit et al., 2012)	(Sofiev et al., 2015)

Table 2. The chemical components of PM ~~provided~~ computed by the different models, particle sizes, speciation and lumping used in the model simulations. The ~~plus and~~ minus signs ~~(+,)~~ indicate that the chemical component ~~has been~~was ~~included in or~~excluded from the computations~~, respectively~~.

Component	CMAQ	EMEP	LOTOS-EUROS	SILAM
SO_4^{2-}	Aitken, accumulation and coarse modes	$PM_{2.5}$	$PM_{2.5}$, $PM_{2.5-10}$	$PM_{2.5}$
NO_3^-	Aitken, accumulation and coarse	$PM_{2.5}$, $PM_{2.5-10}$	$PM_{2.5}$, $PM_{2.5-10}$	$PM_{2.5}$, $PM_{2.5-10}$
~~SIA (SO_4^{2-}, NO_3^-,~~ NH_4^+~~)~~	Aitken, accumulation and coarse+	$PM_{2.5}$+	$PM_{2.5}$+	$PM_{2.5}$+
EC	Aitken, accumulation +	$PM_{2.5}$+	$PM_{2.5}$+	$PM_{2.5}$+
P~~O~~A (primary organic aerosol)~~C~~	Aitken, accumulation as total organic mass +	$PM_{2.5}$ both carbon and total OA masses +	Anthropogenic primary OC included in other primary PM	Anthropogenic primary OC included in other primary PM
SOA (secondary organic aerosol)	Accumulation mode As total OA mass +	$PM_{2.5}$, both carbon and total OA masses +	-	-
Sea salt	Accumulation, coarse chemical components computed separately+	$PM_{2.5}$, $PM_{2.5-10}$, unspeciated+	$PM_{2.5}$, $PM_{2.5-10}$, as chemical components computed separately +	Five bins up to 30 μm size, unspeciated+
Mineral dust (from boundary conditions)	Lumped with ~~other~~ unspeciated primary PM	$PM_{2.5}$, $PM_{2.5-10}$+	-	$PM_{2.5}$, $PM_{2.5-10}$+
Fire originated aerosol	Fine fraction lumped with primary OC, coarse with ~~Lumped with~~ unspeciated primary PM~~other~~	$PM_{2.5}$, $PM_{2.5-10}$ Unspeciated, ~~P~~provided but not included in total PM field	$PM_{2.5}$, $PM_{2.5-10}$ Unspeciated, ~~P~~provided but not included in total PM field	$PM_{2.5}$, $PM_{2.5-10}$ Unspeciated,+

	~~primary PM~~			
B~~enzo[a]~~p~~P~~yrene	-	PM$_{2.5}$+	PM$_{2.5}$+	PM$_{2.5}$+

Table 3. The availability of concentration data for the relevant chemical species from for the EMEP network in 2005.

Species	PM$_{2.5}$	PM$_{10}$	Na$^+$	Ca^{2+}	NH$_4^+$	NH$_4^+$ + NH$_3$	NO$_3^-$	NO$_3^-$ + HNO$_3$	SO$_4^{2-}$	SO$_2$	EC/ OC	BaP
Particle size	PM$_{2.5}$	PM$_{10}$	TPM	TPM	TPM	Gas + TPM	TPM	Gas + TPM	TPM	Gas	PM$_{2.5}$ and PM$_{10}$	Gas + TPM
Number of stations	25	35	26	21	34	45	42	45	73	58	4	8

TPM – total PM without size limitations

Table 4. The chemical components of PM available from the four EMEP stations that included the EC/OC measurements.

Station	Temporal resolution	Observed species
Melpitz (DE0044R, 51.53N, 12.93E)	Daily	$PM_{2.5}$, PM_{10}; EC, OC, NH_4^+, NO_3^-, SO_4^{2-}, Na^+, Cl, Ca^{2+}, Mg, K in $PM_{2.5}$ and PM_{10}
Montseny (ES1778R, 41.77N, 2.35E)	One day per week	$PM_{2.5}$; EC, OC, NH_4^+, NO_3^-, SO_4^{2-}, Na^+, Cl, Ca^{2+}, Mg, K, Si, CO_3, Fe, Al in $PM_{2.5}$ and PM_{10}
Ispra (IT0004R, 45.8N, 8.63E)	Daily	$PM_{2.5}$, PM_{10}; EC, OC, NH_4^+, NO_3^-, SO_4^{2-} in $PM_{2.5}$ and PM_{10} (no EC observations until 01.05.2005)
Birkenes (NO0001R, 58.38N, 8.25E)	Weekly	EC, OC in $PM_{2.5}$ and PM_{10}
	Daily	$PM_{2.5}$, PM_{10}; NH_4^+, NO_3^-, SO_4^{2-}, Na^+, Cl, Ca^{2+}, Mg, K in aerosol, no size segregation.

Table 5. Model-measurement statistics <u>for dry PM </u>for the four models and the two ensemble median models. The colour scale emphasizes the range of values.

	$PM_{2.5}$ winter (djf)		obs ave 12.08		$PM_{2.5}$ summer (jja)		obs ave 10.78	
	Bias	tCor	sCor	Fac2	Bias	tCor	sCor	Fac2
CMAQ	-6.41	0.48	0.53	0.49	-6.15	0.54	0.68	0.30
EMEP	-4.48	0.68	0.79	0.67	-3.41	0.62	0.70	0.69
LOTOS-EUROS	-3.70	0.61	0.62	0.61	-6.36	0.37	0.26	0.30
SILAM	-2.10	0.65	0.86	0.66	-4.56	0.52	0.59	0.46
median	-4.41	0.70	0.77	0.67	-5.46	0.61	0.69	0.44
medianComp	-4.42	0.70	0.76	0.65	-2.96	0.59	0.58	0.54

	PM_{10} winter (djf)		obs ave 16.15		PM_{10} summer (jja)		obs ave 16.53	
	Bias	tCor	sCor	Fac2	Bias	tCor	sCor	Fac2
CMAQ	-7.79	0.36	0.30	0.56	-9.99	0.43	0.64	0.28
EMEP	-4.53	0.55	0.56	0.66	-5.55	0.59	0.77	0.7
LOTOS-EUROS	-5.47	0.48	0.54	0.6	-9.78	0.25	0.06	0.38
SILAM	-4.56	0.56	0.78	0.57	-7.24	0.43	0.76	0.44
median	-5.82	0.60	0.62	0.65	-8.69	0.51	0.70	0.45
medianComp	-5.86	0.59	0.64	0.64	-6.02	0.53	0.77	0.54

Notations:

Obs ave – average observed value, mean over all stations, µg/m^3.

Bias – absolute bias of the predicted concentrations, mean over all stations (model-measurement, non-scaled, in µg/m^3)

tCor – mean temporal correlation of the daily timeseries, mean over all stations

sCor – spatial correlation of the seasonal mean values for the stations

Fac2 – fraction of daily modelled values within a factor of two from the observations

medianComp – sum of the ensemble median fields of the aerosol components

Table 6 Annual statistics for the $PM_{2.5}$ and PM_{10}, dry mass, aerosol bound water added assuming stable state (lower curve of the hysteresis loop) and metastable state (higher curve of the hysteresis loop). ScaledBias - bias divided with the mean observed value, tCor - temporal correlation of the daily values, Fac2 – the fraction of daily values within factor of two from the observed ones. The shading emphasizes the range of the values

| Species | Model | Dry | | | 50% relative humidity, 20° C, stable | | | 50% relative humidity, 20° C, metastable | | |
		Scaled bias	tCor	Fac2	Scaled bias	tCor	Fac2	Scaled bias	tCor	Fac2
$PM_{2.5}$ *Ave obs: 11.78 µg/m³*	CMAQ	-0.47	0.50	0.47	-0.44	0.50	0.50	-0.34	0.49	0.58
	EMEP	-0.33	0.62	0.69	-0.30	0.62	0.71	-0.17	0.62	0.77
	LOTOS-EUROS	-0.40	0.46	0.51	-0.34	0.43	0.54	-0.26	0.45	0.58
	SILAM	-0.26	0.59	0.58	-0.18	0.57	0.61	-0.08	0.57	0.64
	median	-0.38	0.63	0.61	-0.35	0.63	0.63	-0.26	0.63	0.70
	medianComp	-0.30	0.60	0.62	-0.28	0.60	0.64	-0.17	0.60	0.71
PM_{10} *Ave obs: 17.09 µg/m³*	CMAQ	-0.49	0.46	0.49	-0.40	0.42	0.53	-0.29	0.41	0.59
	EMEP	-0.31	0.57	0.69	-0.21	0.51	0.70	-0.09	0.51	0.72
	LOTOS-EUROS	-0.44	0.40	0.53	-0.32	0.29	0.57	-0.25	0.32	0.61
	SILAM	-0.34	0.54	0.54	-0.24	0.50	0.58	-0.16	0.51	0.60
	median	-0.41	0.59	0.59	-0.33	0.53	0.63	-0.23	0.54	0.68
	medianComp	-0.35	0.57	0.63	-0.26	0.53	0.66	-0.17	0.54	0.70

5

10

Table 6. Annual statistics for the PM components: ScaledBias – bias divided with the mean observed value, tCor – temporal correlation of the daily values, Fac2 – the fraction of daily values within factor of two from the observed ones. The shading emphasizes the range of the values.

Table 7 Annual statistics for the PM components: ScaledBias - bias divided with the mean observed value, tCor - temporal correlation of the daily values, Fac2 – the fraction of daily values within factor of two from the observed ones. The shading emphasizes the range of the values.

Species	Model	Scaled bias	tCor	Fac2	Species	Model	Scaled bias	tCor	Fac2
NH₄	CMAQ	-0.08	0.55	0.49	**NO₃**	CMAQ	-0.12	0.35	0.47
Ave obs:	EMEP	-0.08	0.58	0.51	Ave obs:	EMEP	0.13	0.46	0.45
0.86 µg N/m³	LOTOS-EUROS	-0.06	0.56	0.47	0.52 µg N/m³	LOTOS-EUROS	0.06	0.44	0.42
	SILAM	-0.16	0.55	0.37		SILAM	0.06	0.44	0.39
	median	-0.13	0.61	0.5		median	0.00	0.49	0.49
NH₃+NH₄	CMAQ	0.00	0.38	0.44	**NO₃+HNO₃**	CMAQ	0.14	0.49	0.67
Ave obs:	EMEP	-0.06	0.45	0.59	Ave obs:	EMEP	0.24	0.49	0.56
1.54 µg N/m³	LOTOS-EUROS	0.12	0.39	0.59	0.58 µg N/m³	LOTOS-EUROS	0.12	0.47	0.6
	SILAM	0.10	0.44	0.54		SILAM	0.02	0.48	0.49
	median	0.01	0.47	0.6		median	0.10	0.54	0.65
NH₃	CMAQ	0.04	0.18	0.25	**HNO₃**	CMAQ	0.21	0.34	0.43
Ave obs:	EMEP	-0.07	0.30	0.36	Ave obs:	EMEP	-0.11	0.38	0.39
0.75 µg N/m³	LOTOS-EUROS	0.19	0.22	0.38	0.19 µg N/m³	LOTOS-EUROS	0.00	0.38	0.40
	SILAM	0.32	0.30	0.40		SILAM	-0.53	0.32	0.32
	median	0.05	0.31	0.39		median	-0.16	0.41	0.44
SO₄	CMAQ	-0.10	0.59	0.73	**SO₂**	CMAQ	0.25	0.53	0.49
Ave obs:	EMEP	-0.18	0.58	0.57	Ave obs:	EMEP	0.23	0.47	0.48
0.77 µg S /m³	LOTOS-EUROS	-0.38	0.56	0.45	0.79 µg S/m³	LOTOS-EUROS	0.05	0.49	0.54
	SILAM	-0.04	0.51	0.52		SILAM	-0.13	0.48	0.5
	median	-0.23	0.63	0.63		median	0.04	0.55	0.54
Sea salt	CMAQ	0.40	0.48	0.46	**Mineral dust**	EMEP	-0.75	0.29	0.29
Ave obs:	EMEP	0.38	0.54	0.49	Ave obs:	SILAM	-0.58	0.31	0.33
0.78 µg Na/m³	LOTOS-EUROS	-0.03	0.38	0.49	0.12 µg Ca/m³	median	-0.67	0.32	0.31
	SILAM	0.08	0.44	0.48					
	median	0.13	0.55	0.58					
EC in PM₂.₅	CMAQ	-0.61	0.51	0.35	**EC in PM₁₀**	CMAQ	-0.69	0.42	0.32
Ave obs:	EMEP	-0.56	0.53	0.4	Ave obs:	EMEP	-0.66	0.46	0.35
1.08 µg C/m³	LOTOS-EUROS	-0.34	0.51	0.44	1.32 µg C/m³	LOTOS-EUROS	-0.48	0.39	0.44
	SILAM	-0.17	0.61	0.4		SILAM	-0.35	0.45	0.38
	median	-0.45	0.6	0.38		median	-0.58	0.49	0.37
OC in PM₂.₅	CMAQ	-0.80	0.52	0.26	**OC in PM₁₀**	CMAQ	-0.85	0.36	0.18
Ave obs:	EMEP	-0.25	0.54	0.6	Ave obs:	EMEP	-0.37	0.46	0.52
3.61 µg C/m³	median	-0.52	0.54	0.61	4.78 µg C/m³	median	-0.61	0.46	0.48
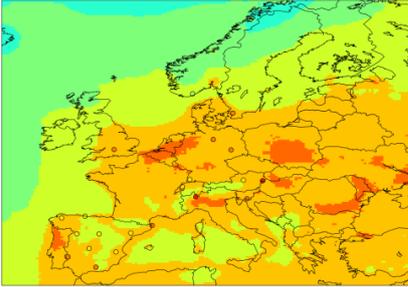
5
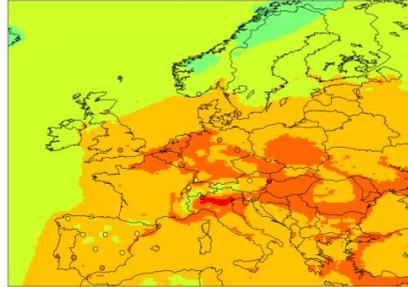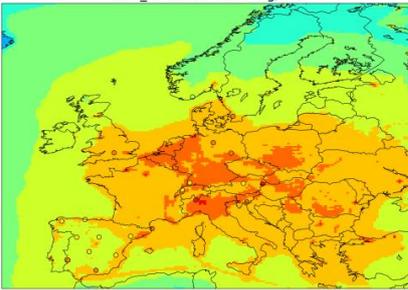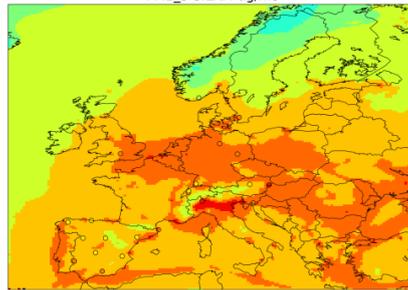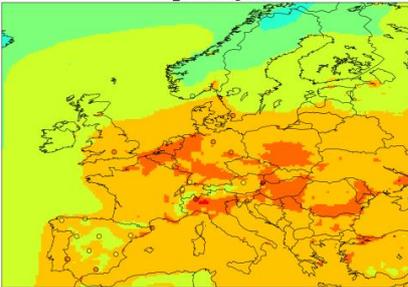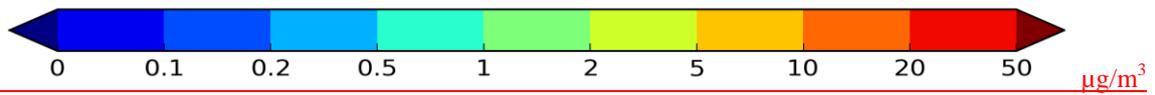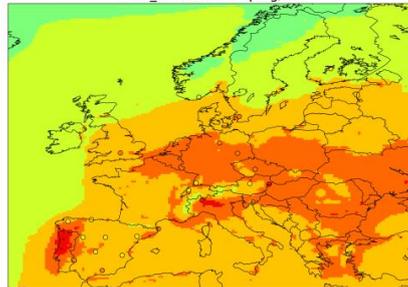
Figure 1. Annual mean dry PM$_{2.5}$ concentration predicted by the models, their median and medianComp [µg PM m^{-3}]. The dots show the annual mean observed values in EMEP stations (only the stations with observations available for at least 75% of the time are shown)
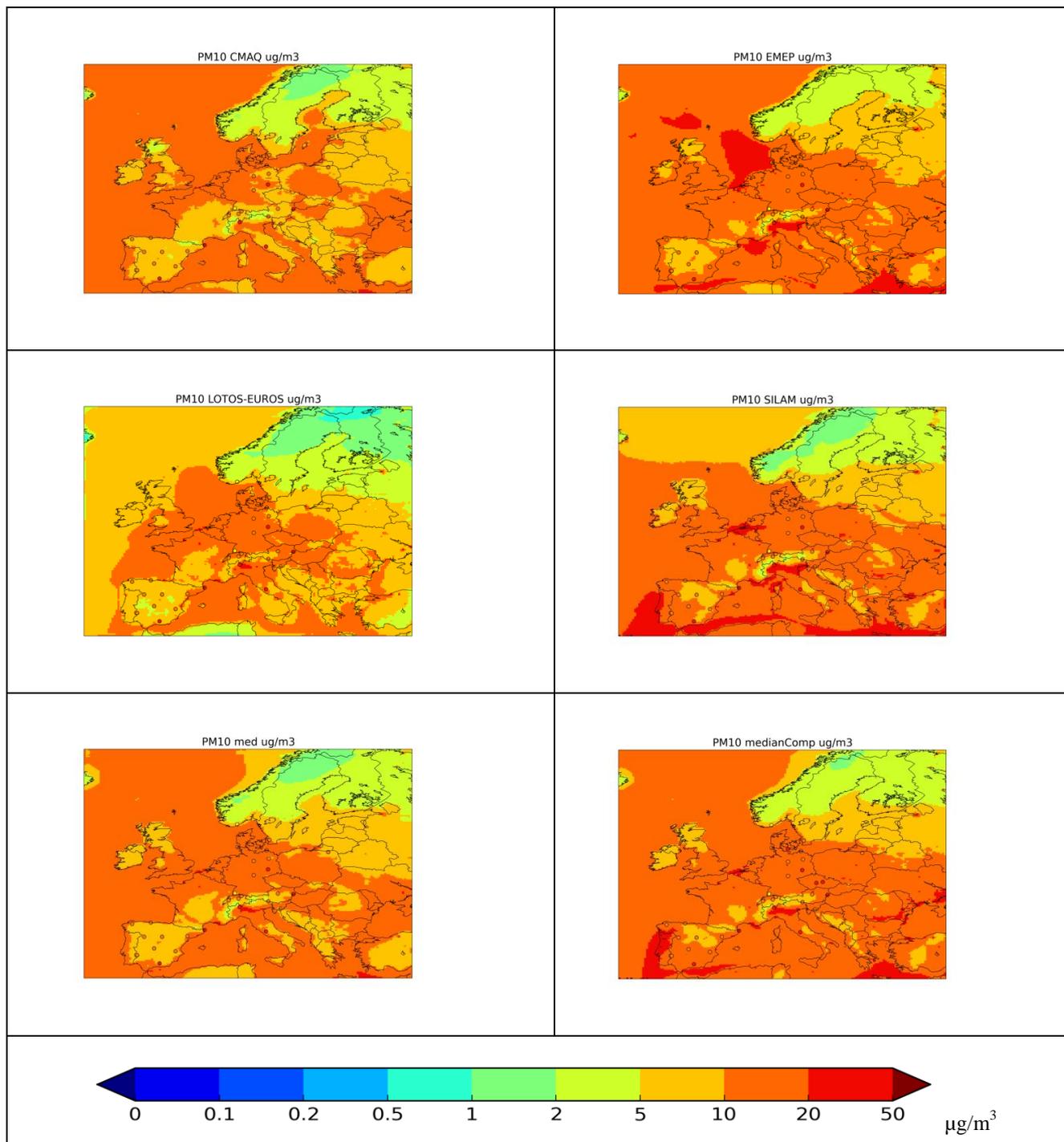
Figure 2. Annual mean dry PM$_{10}$ concentration predicted by the models, their median and medianComp [μg PM m^{-3}]. The dots show the annual mean observed values in EMEP stations (only the stations with observations available for at least 75% of the time are shown).
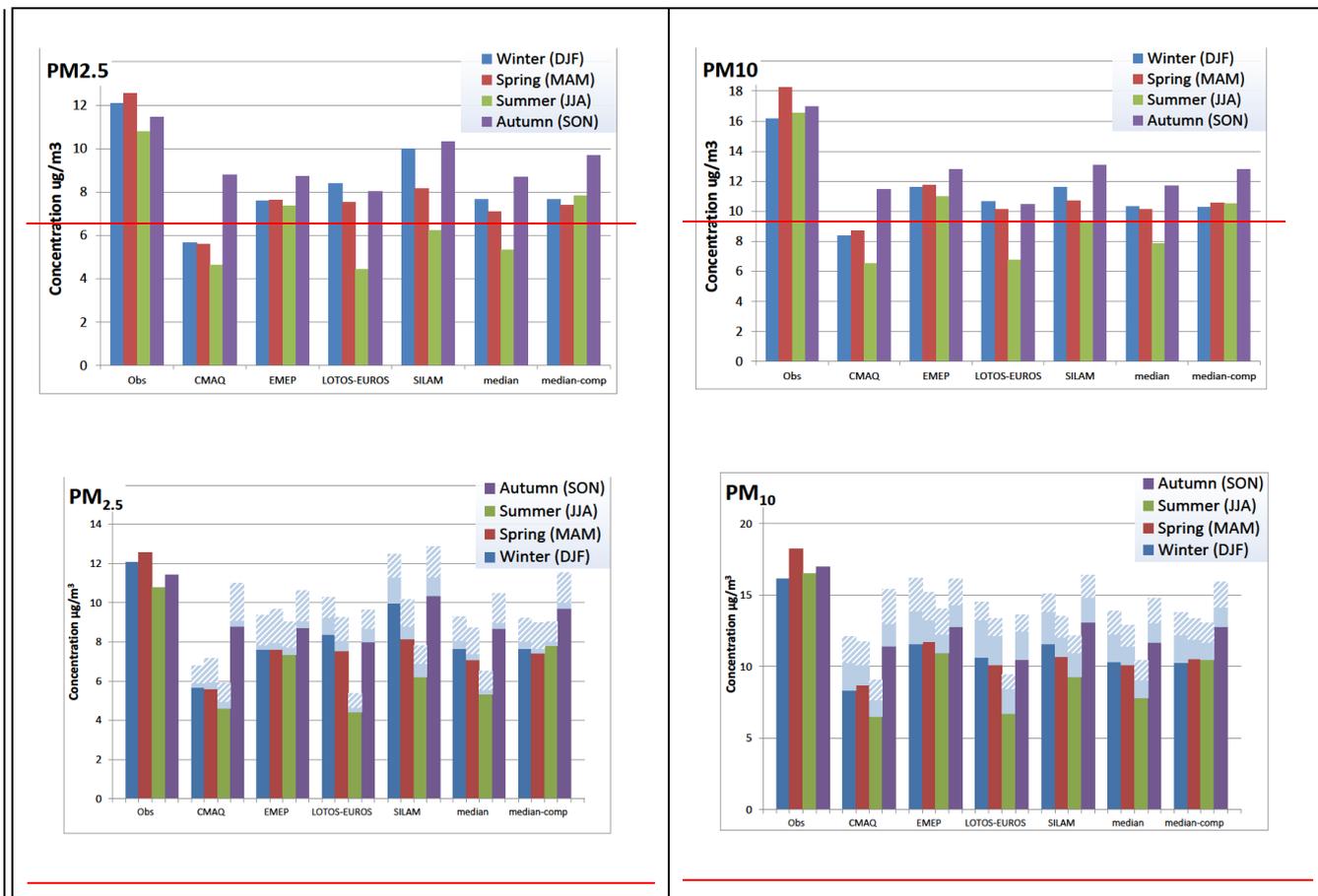
Figure 3. Observed and predicted seasonal concentrations of $PM_{2.5}$ (left) and PM_{10} (right), mean over the EMEP stations [µg PM m^{-3}]. The light blue part shows the aerosol-bound water amount at the filter weighting conditions (50% relative humidity, 20°C), estimated with ISORROPIA2 based on the modelled aerosol composition. The solid light blue shows the water content in stable case (the lower curve of the hysteresis loop) and the striped part in metastable case (the upper branch of the hysteresis loop), when the crystallization has not occurred to aerosol coming from more humid conditions.
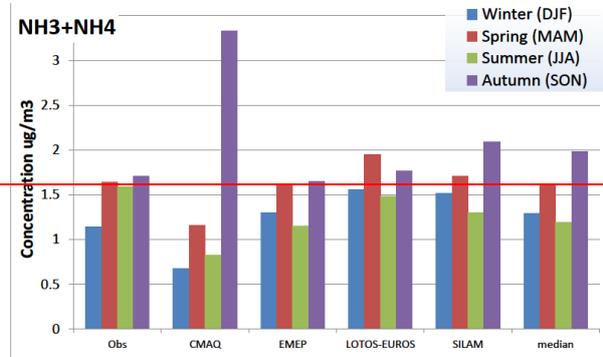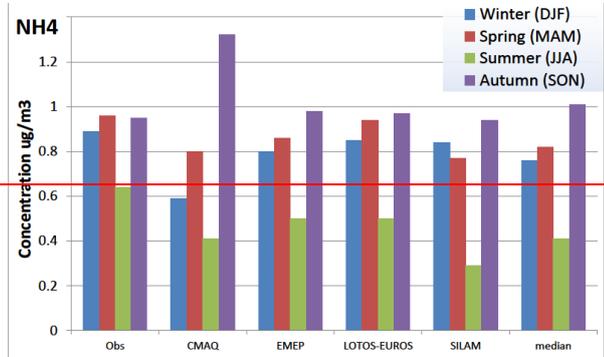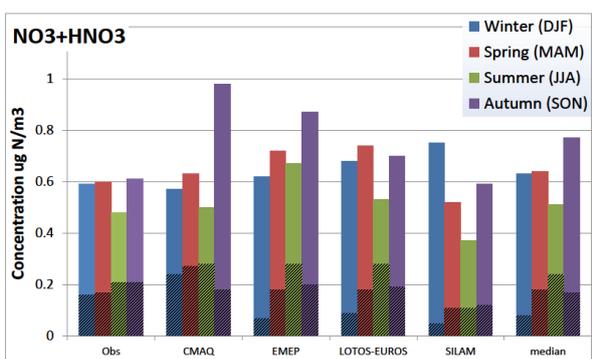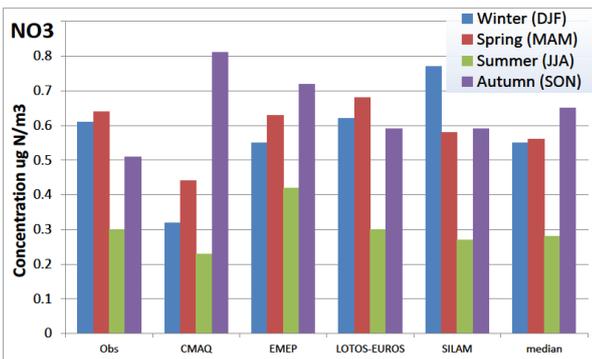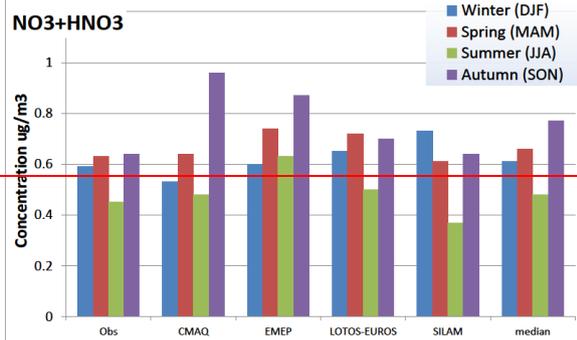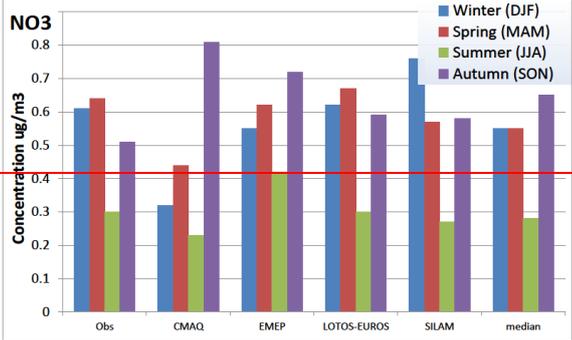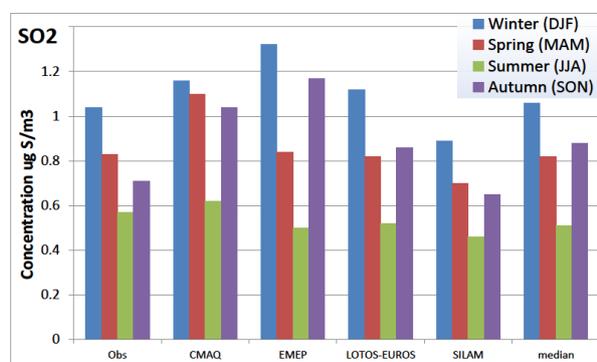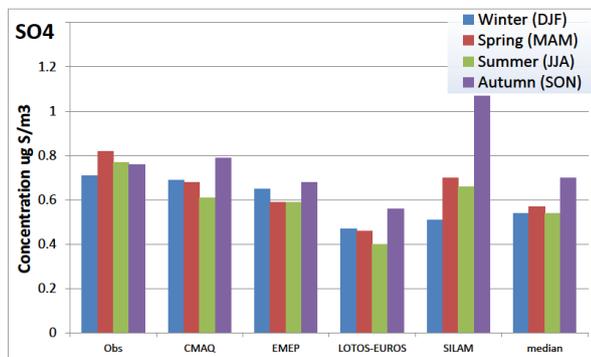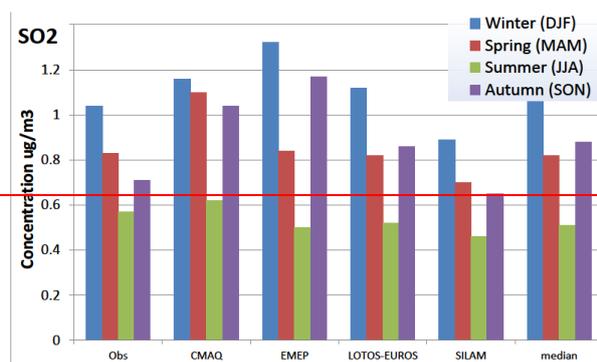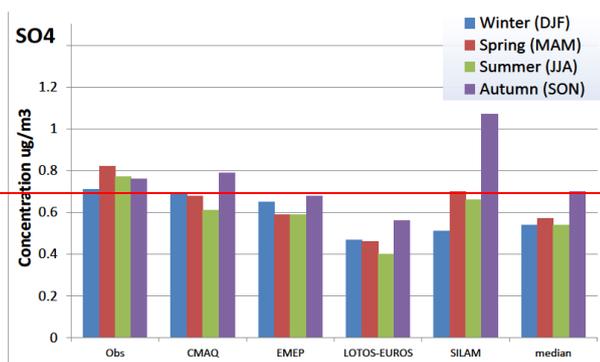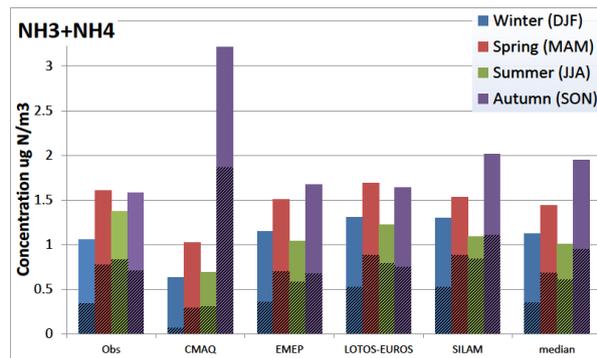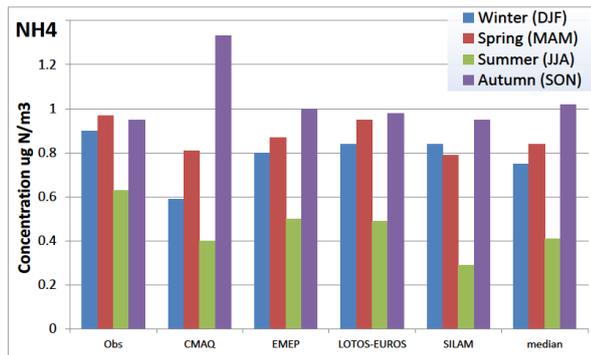
Figure 4. Observed and predicted seasonal concentrations of secondary inorganic aerosols and their precursors, mean over the EMEP stations [µg S/N m^{-3}]. Shaded part shows the concentration of the gas phase species HNO$_3$ and NH$_3$. Only the stations where at least two of the gas, aerosol and their sum were observed, so that the gas phase fraction could be estimated, are included in the averaging.
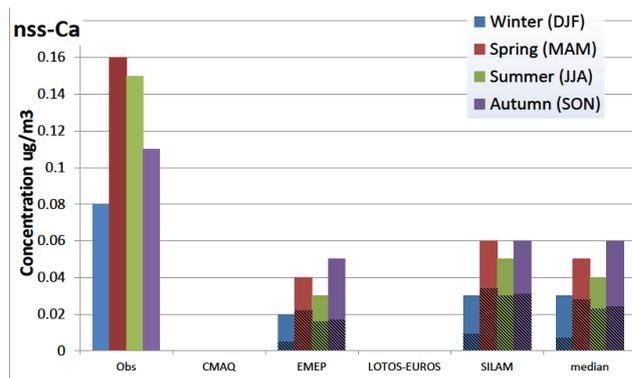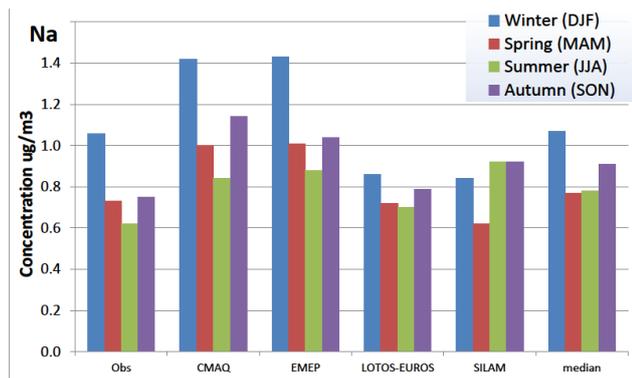
Figure 5. Observed and predicted seasonal concentrations of sodium and non-seasalt calcium in aerosol, mean over the EMEP stations [µg m^{-3}]. Modelled Na$^+$ concentrations are based on sea salt containing 30.8% Na$^+$. Model values of non-sea-salt calcium assume 10% Ca^{2+} content of desert dust (shaded bottom part of the columns) and 3.5% calcium content of non-carbonaceous primary anthropogenic PM (the non-shaded upper part).
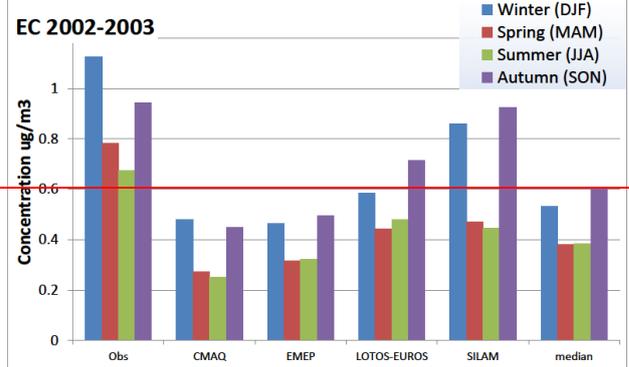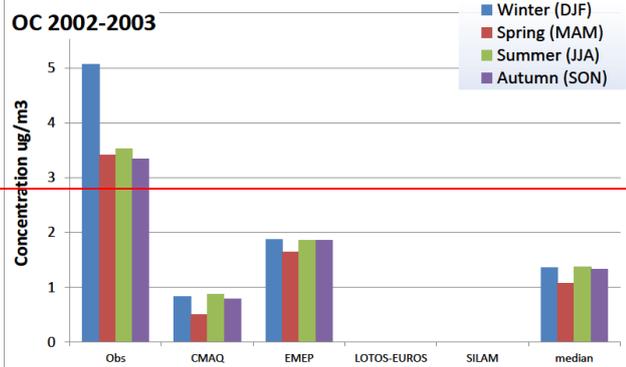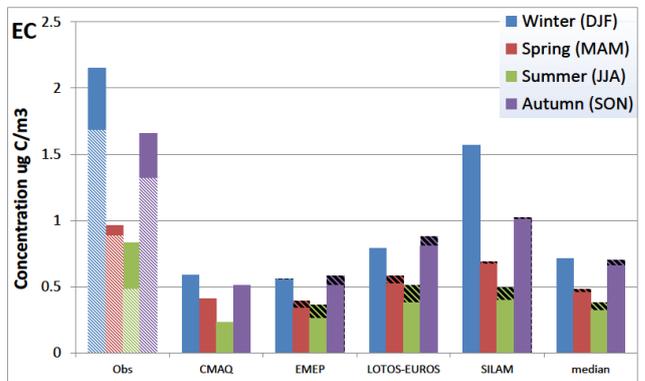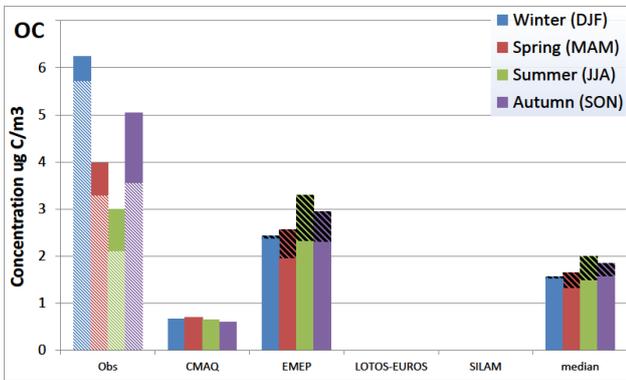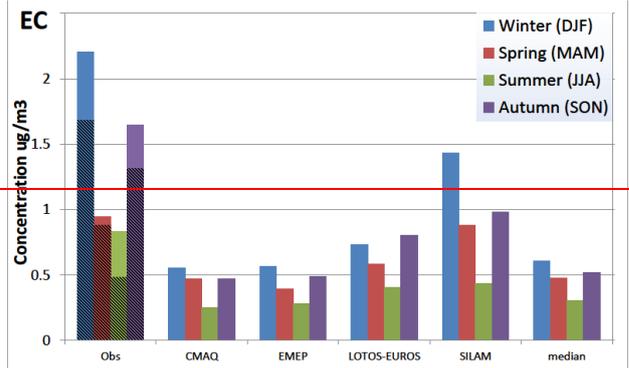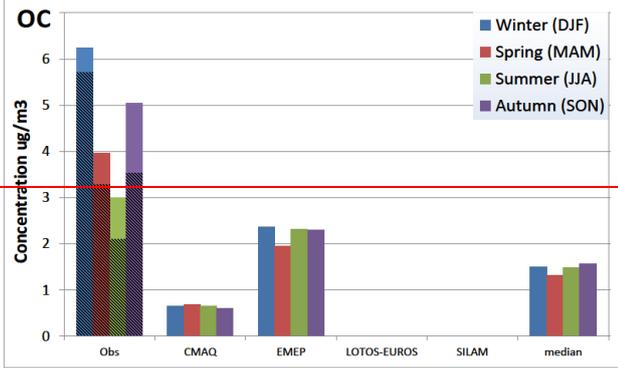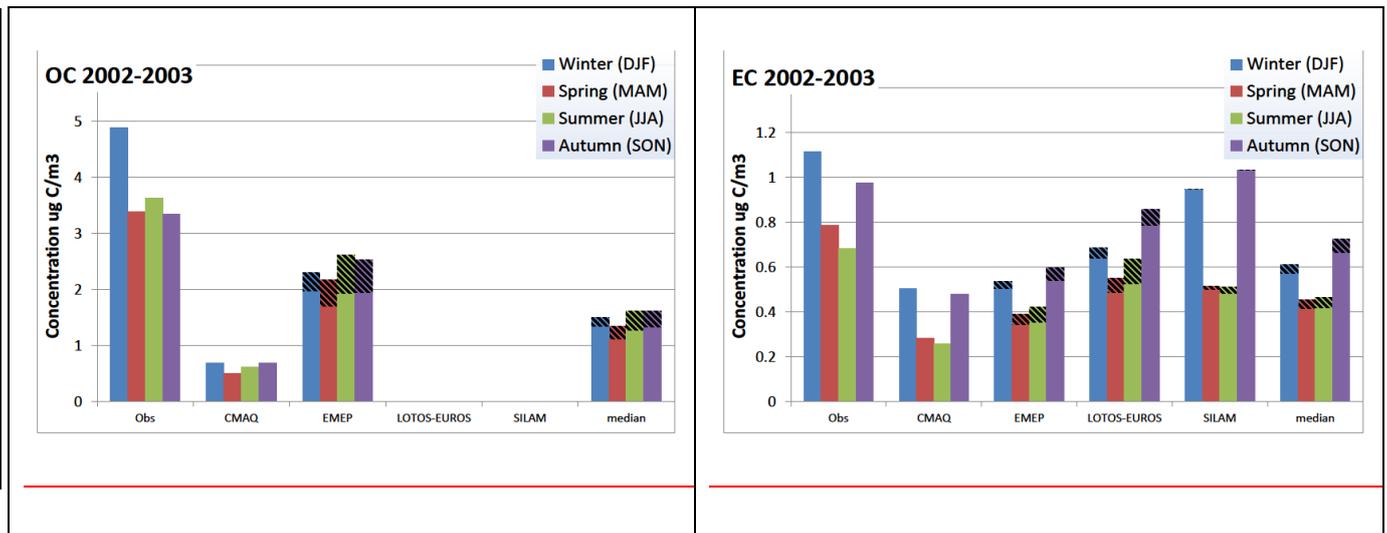
Figure 6. Observed and predicted seasonal concentrations of carbonaceous aerosols, mean over the EMEP stations [μg m-3]. The panels on the left-hand and right-hand sides represent OC and EC, respectively. The upper row: 2005, data from 4 stations, for the observations the lighter shading marks the concentration in PM2.5, whole column the concentration in PM10; the lower row: EMEP 2002-2003 campaign, observations of OC and EC in PM10. Dark shaded part shows the contribution from wild land fires (not separated for CMAQ OC, missing for CMAQ EC).~~Observed and predicted seasonal concentrations of carbonaceous aerosols, mean over the EMEP stations [μg m^{-3}]. The panels on the left-hand and right-hand sides represent OC and EC, respectively. The upper row: 2005, data from 4 stations, for the observations the darker shading marks the concentration in PM$_{2.5}$, whole column the concentration in PM$_{10}$; the lower row: EMEP 2002-2003 campaign, observations of OC and EC in PM$_{10}$.~~

53

Figure 7 Observed and predicted seasonal concentrations of benso(a)pyrene, mean over the EMEP stations in 2005 [ng/m³]
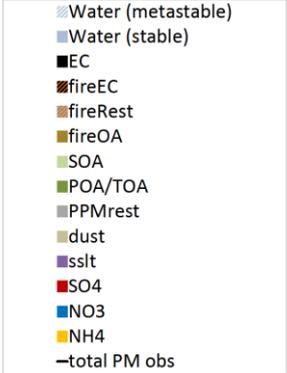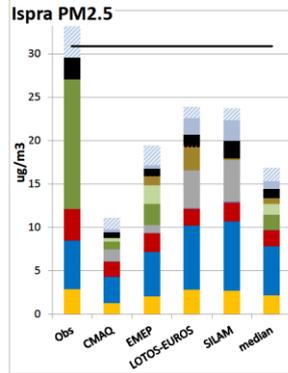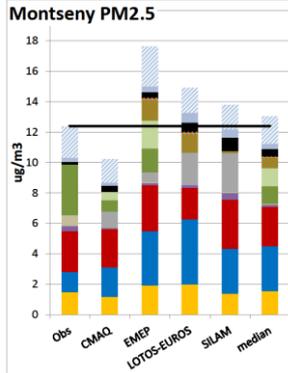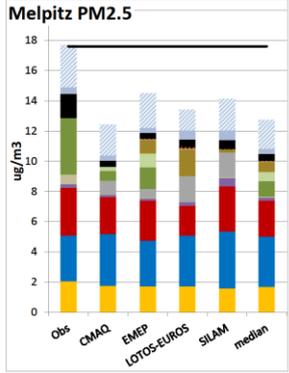
Figure 7. Observed and predicted seasonal concentrations of Benzo(a)pyrene, mean over the EMEP stations [ng m⁻³] in 2005.
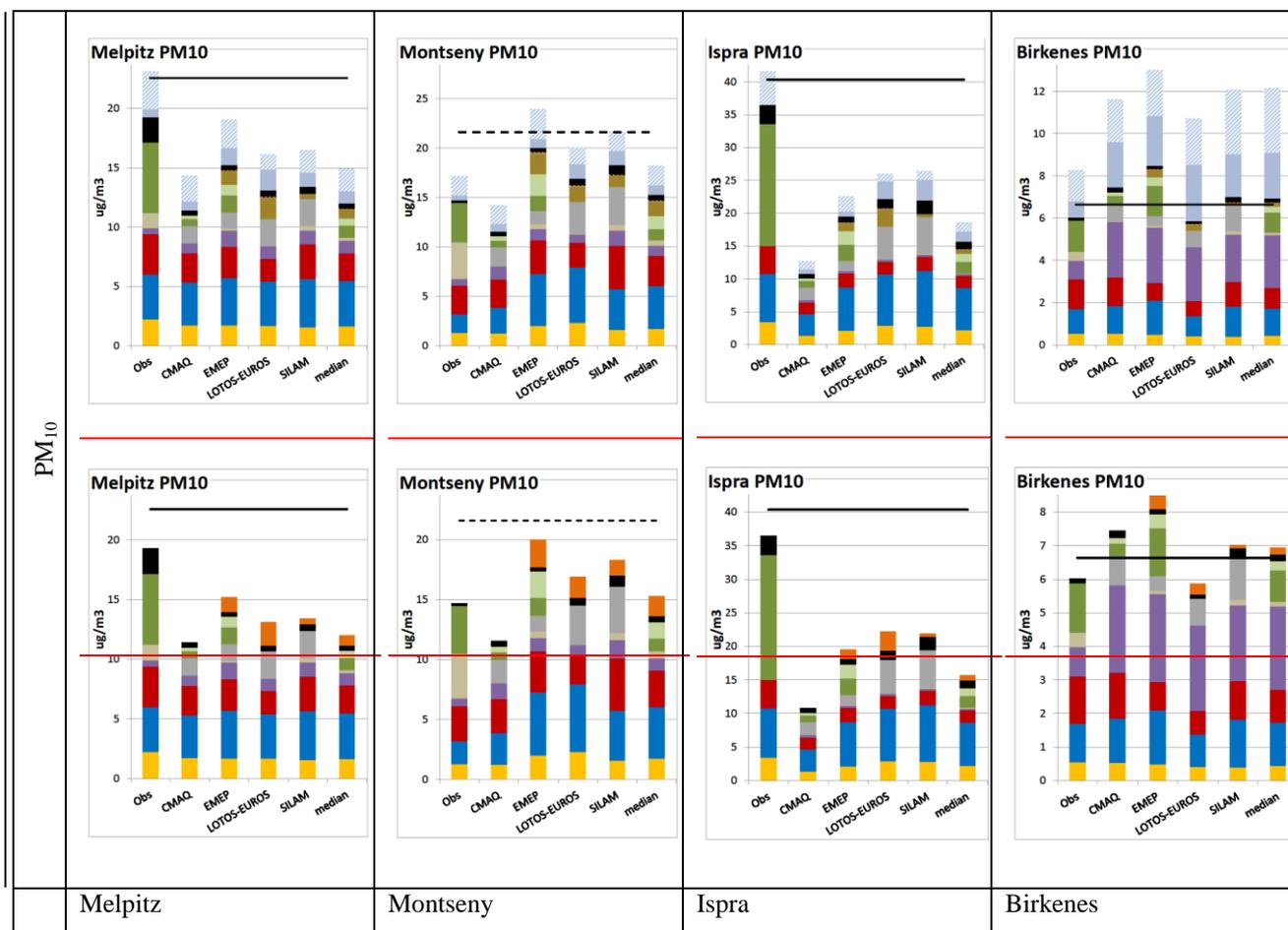
PM₂.₅
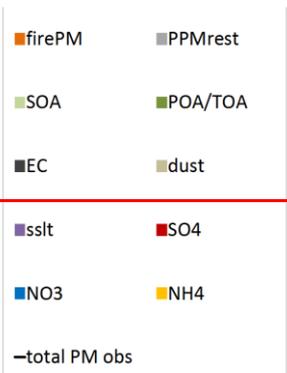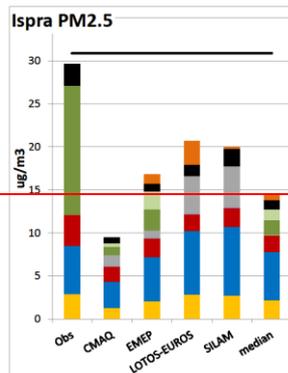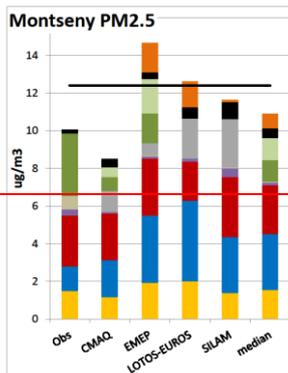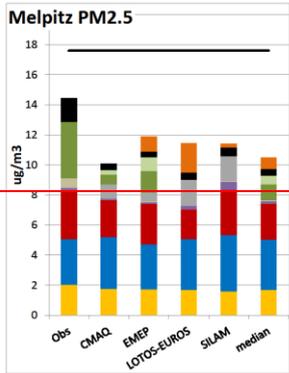
Figure 8. Aerosol chemical composition measured and modelled at four stations. Upper row – PM$_{2.5}$, lower row – PM$_{10}$

Water – aerosol water content at 50%RH and 20°C, computed with ISORROPIA2 based on observed or modelled aerosol composition.
metastable – particle is assumed to be in supersaturated liquid state if the relative humidity is below its deliquescence point
stable – particle is assumed solid if the relative humidity is below its deliquescence point
EC – elemental carbon from anthropogenic emissions
fireEC - elemental carbon from wild-land fire emissions, 5% of fire emitted PM
fireRest – mineral PM from wild-land fire emissions, 5% of fire emitted PM
fireOA– organic aerosol from wild-land fire emissions, 90% of fire emitted PM
SOA – secondary organic aerosol
POA/TOA – the primary part of organic aerosol for the models, total organic aerosol for the observations (OC * 1.6)
PPMrest – the unspeciated part of the modelled primary anthropogenic PM
Dust – modelled desert dust, observed non-sea-salt Ca^{2+} x 10
Sslt – sea-salt, observed Na^{+} + Cl^{-}
SO4, NO3, NH4 – secondary inorganic aerosols
Total PM obs – observed total PM$_{2.5}$ and PM$_{10}$.
* PM$_{10}$ observations were not available for Montseny station. The dotted line marks an estimate calculated by averaging PM$_{10}$ observations from the nearest EMEP stations (ES0010R, ES0014R).
* Na observations were not available in Ispra and were excluded from ISORROPIA input. ~~PPMrest – the unspeciated part of the modelled primary anthropogenic PM~~
~~POA/TOA – the primary part of organic aerosol for the models, total organic aerosol for the observations~~
~~Sslt – sea-salt, observed Na^{+} + Cl^{-}~~
~~Dust – modelled desert dust, observed non-sea-salt Ca^{2+} x 10~~
~~firePM – PM originating from wild-land fires~~

PM$_{10}$ observations were not available for Montseny station. The dotted line marks an estimate calculated by averaging PM$_{10}$ observations from the nearest EMEP stations (ES0010R, ES0014R).